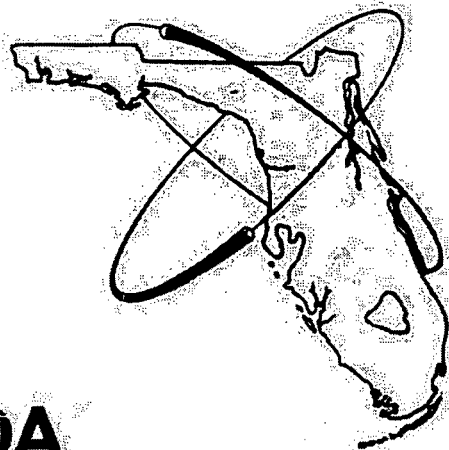
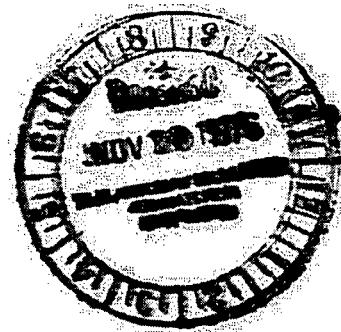


# CRYSTAL RIVER UNIT 3 NUCLEAR GENERATING PLANT REACTOR BUILDING DOME DELAMINATION

**FINAL REPORT**

December 10, 1976



12-30-76  
Docket #  
Control # 12459  
12-10-76

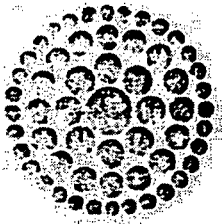
**FLORIDA**

**POWER**

**CORPORATION**

12459

P/224



Regulatory File Cy. 7



**Florida Power**  
CORPORATION

June 11, 1976

Mr. Norman C. Moseley, Director  
U. S. Nuclear Regulatory Commission  
Region II  
230 Peachtree Street, NW  
Suite 818  
Atlanta, Georgia 30303

Re: Docket No. 50-302

Dear Mr. Moseley:

Pursuant to 10CFR50.55(e), we wish to follow up our written notification of April 21, 1976 regarding a separation in the concrete of the Crystal River Unit #3 containment structure dome.

Attached is our interim report entitled, "CRYSTAL RIVER #3 DOME DELAMINATION REPORT", dated June 11, 1976. This report addresses:

1. Introduction
2. Original Structure
3. Problem Definition
4. Delamination Structure
5. Corrective Action
6. References
7. Quality Assurance

During the investigation and evaluation period, we have had benefit of informal staff discussions on two occasions and numerous exchanges of staff and ACRS Members reported concerns. This interim report addresses each of these concerns to the extent our present information and expertise allows at this time.

The included evaluation does not provide any reasonable direction as to why the delamination occurred.

Our report includes a proposed corrective action in Section 5. We feel that further theorizing as to "why" will be inconclusive and time consuming. We are, therefore, prepared to proceed with the corrective action as entirely adequate to assure that the containment structure, when so repaired, will be capable of meeting the original design criteria as demonstrated by calculation and the Structural Integrity Test (SIT).

5923

Mr. Norman C. Moseley  
June 11, 1976

2

We are very cognizant of staff concerns for the detensioning activity proposed and have incorporated in the report our response to these concerns. In this regard, development of detailed work procedures addressing the repair effort is ongoing and will be made available to I&E inspectors at the site or forwarded to the Commission directly as required.

It has been concluded by Florida Power Corporation from all evaluations available to us at this time, that the proposed corrective action is a correct and reasonably risk-free approach to an acceptable repair.

We, therefore, propose to begin work activities associated with the proposed corrective actions outlined on June 15, 1976 in accordance with the attached schedule. Assuming no adverse occurrences, we will proceed toward ultimate conclusion of this work on this schedule.

To allow you and ourselves the opportunity for continued cooperation, exchange of questions and our responses, we request an informal session in Bethesda on June 18, 1976. At the close of this session, we would solicit your concurrence with our corrective action and the proposed work schedule.

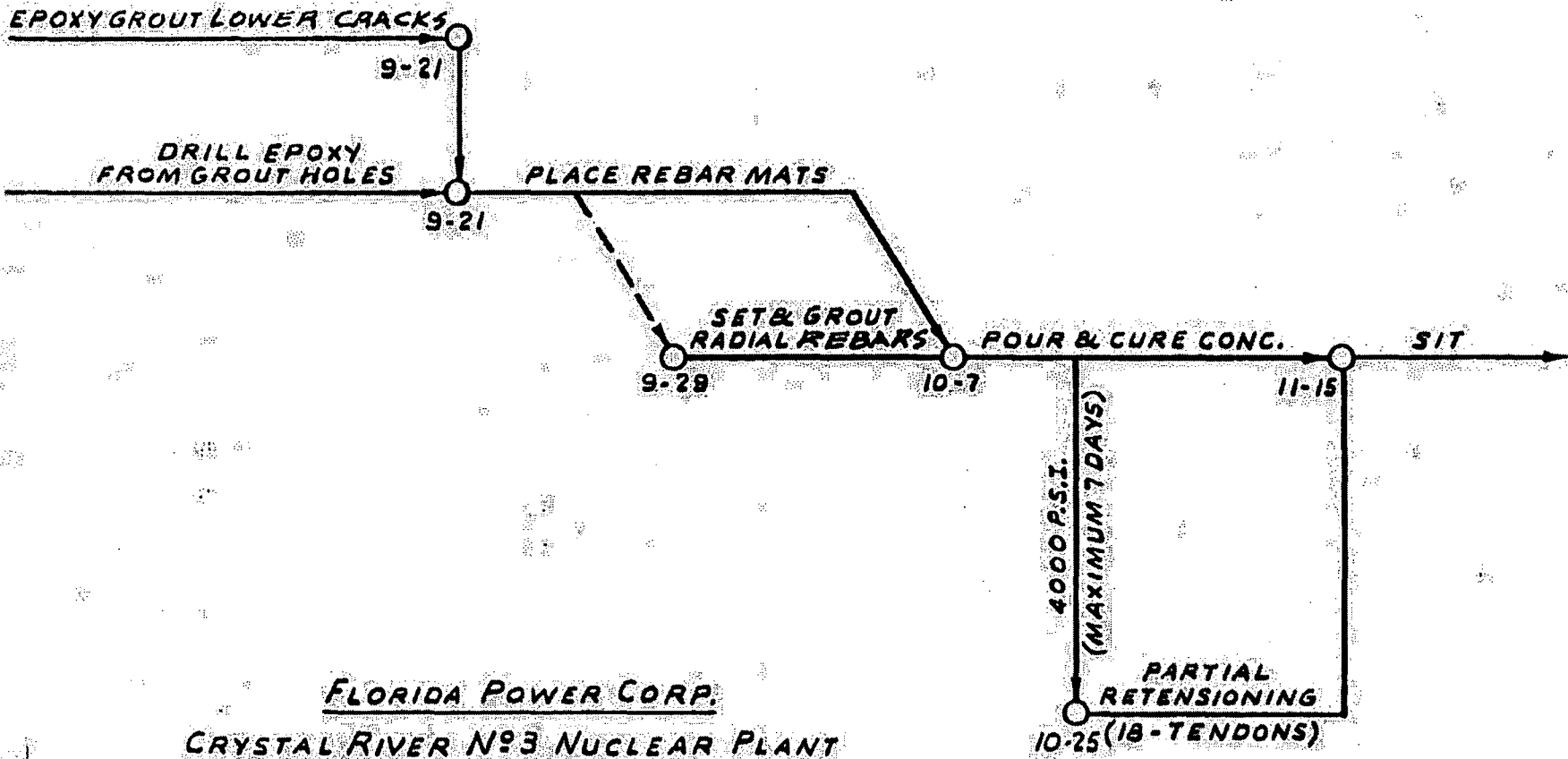
If you have any questions concerning our filing or the subsequent meetings with the Commission, please advise us.

Very truly yours,

  
J. T. Rodgers  
Asst. Vice President

JTR:pam

cc: E. Volganeau  
L. Engle CR-3 w/40 attach.



**FLORIDA POWER CORP.**  
**CRYSTAL RIVER N°3 NUCLEAR PLANT**  
**DOME REPAIR SCHEDULE**

Revised: 9-22-76

REACTOR BUILDING DOME DELAMINATION  
FLORIDA POWER CORPORATION  
CRYSTAL RIVER UNIT 3

TABLE OF CONTENTS

<u>Section</u>	<u>Title</u>	<u>Page</u>
	<u>TABLE OF CONTENTS</u>	i
	<u>LIST OF TABLES</u>	iv
	<u>LIST OF FIGURES</u>	v
1.0	<u>INTRODUCTION</u>	1-1
1.1	<u>PURPOSE</u>	1-1
1.2	<u>SUMMARY AND CONCLUSIONS</u>	1-1
2.0	<u>ORIGINAL STRUCTURE</u>	2-1
2.1	<u>PHYSICAL DESCRIPTION</u>	2-1
2.2	<u>APPLICABLE CODES AND STANDARDS</u>	2-2
2.3	<u>CRITERIA</u>	2-2
2.3.1	<u>Flexural and Membrane Tensile Stresses</u>	2-2
2.3.2	<u>Shear</u>	2-3
2.4	<u>SUMMARY OF ANALYTICAL RESULTS</u>	2-4
2.4.1	<u>Structure Prior to Operation</u>	2-6
2.4.2	<u>Normal Winter Operating Condition</u>	2-6
2.4.3	<u>Structural Integrity Test</u>	2-6a
2.4.4	<u>Accident Condition</u>	2-7
2.4.5	<u>Small Pipe Break</u>	2-7
2.4.6	<u>Summary</u>	2-7
3.0	<u>PROBLEM DEFINITION</u>	3-1
3.1	<u>INVESTIGATIONS</u>	3-1
3.1.1	<u>Original Indications</u>	3-1
3.1.2	<u>Preliminary Exploration</u>	3-1
3.1.3	<u>Additional Investigations</u>	3-2
3.1.4	<u>Other Events</u>	3-2b
3.2	<u>DELAMINATION GAP</u>	3-3
3.3	<u>POSSIBLE CAUSES OF THE DELAMINATION</u>	3-3
3.3.1	<u>Properties of Concrete and Constituents</u>	3-4
3.3.2	<u>Radial Tension Due to Prestress</u>	3-5
3.3.3	<u>Compression-Tension Interaction</u>	3-6a
3.3.4	<u>Thermal Effects</u>	3-7
3.3.5	<u>Tendon Alignment</u>	3-8
3.3.6	<u>Heavy Construction Loads</u>	3-9
3.3.7	<u>Coastal Location</u>	3-9
3.3.8	<u>Location Adjacent to Fossil Units</u>	3-9
3.3.9	<u>Construction Methods</u>	3-9
3.3.10	<u>Impact Loads</u>	3-10
3.3.11	<u>Shrinkage Effects</u>	3-10
3.4	<u>CONCLUSIONS</u>	3-11

TABLE OF CONTENTS (CONT'D)

<u>Section</u>	<u>Title</u>	<u>Page</u>
4.0	<u>DELAMINATED STRUCTURE</u>	4-1
4.1	<u>INTRODUCTION</u>	4-1
4.2	<u>APPLICABLE CODES AND STANDARDS</u>	4-1
4.3	<u>CRITERIA</u>	4-1
4.4	<u>EVALUATION</u>	4-1
4.4.1	<u>Structure Prior to Operation</u>	4-4
4.4.2	<u>Normal Winter Operating Condition</u>	4-4a
4.4.3	<u>Structural Integrity Test</u>	4-5
4.4.4	<u>Accident Condition</u>	4-5
4.5	<u>SUMMARY AND CONCLUSION</u>	4-7
5.0	<u>CORRECTIVE ACTION</u>	5-1
5.1	<u>INTRODUCTION</u>	5-1
5.2	<u>REPAIR METHOD</u>	5-1
5.2.1	<u>Instrumentation</u>	5-1
5.2.2	<u>Dome Retensioning</u>	5-3
5.2.3	<u>Drilling Radial Holes</u>	5-4
5.2.4	<u>Delaminated Cap Removal</u>	5-4
5.2.5	<u>Inspection of the 24" Structure</u>	5-4
5.2.6	<u>Lower Level Crack Grouting</u>	5-5
5.2.7	<u>New Reinforcement</u>	5-5
5.2.8	<u>New Cap</u>	5-5a
5.2.9	<u>Dome Retensioning</u>	5-6
5.2.10	<u>Structural Integrity Test (SIT)</u>	5-6
5.2.11	<u>Dome Surfacing</u>	5-6
6.0	<u>QUALITY ASSURANCE</u>	6-1
7.0	<u>REFERENCES</u>	7-1
	<u>FIGURES</u>	
	<u>APPENDICES</u>	
	Appendix A - Dome Concrete	A-1
	Appendix B - FPC Transmittal to NRC Dated July 11, 1974	B-1
	Appendix C - Progress Report of Concrete Quality Evaluation	C-1
	Appendix D - Computer Program Verification and Description	D-1
	Appendix E - Photographs of Existing Structure	E-1

TABLE OF CONTENTS (CONT'D)

<u>Section</u>	<u>Title</u>	<u>Page</u>
<u>APPENDICES (CONT'D)</u>		
	Appendix F - Discussion of Repair Method	F-1
	Appendix G - Comparison of Designs	G-1
	Appendix H - Cadwelding Requirements	H-1
	Appendix I - Radial Tension and Shear	I-1
	Appendix J - NRC Correspondence - SIT Instrumentation	J-1
	Appendix K - Discussion of Concrete and Aggregate Properties	K-1

TABLE OF CONTENTS (CONT'D)

<u>Section</u>	<u>Title</u>	<u>Page</u>
<b>SUPPLEMENT 1 - RESPONSES TO NRC COMMENTS TO THE CRYSTAL RIVER #3 REACTOR BUILDING DOME DELAMINATION REPORT</b>		S-1
GENERAL		S-1
SECTION 1.2		S-2
SECTION 2.3 AND TABLE 2-2 (Attachment 1 for answer to question 2.3(2) - 4 sheets)		S-3
SECTION 2.4 (Attachment 2 for answer to question 2.4(1) - 2 sheets) (Attachment 3 for answer to question 2.4(4) - 3 sheets)		S-4
SECTION 3.1		S-6
SECTION 3.3 (Attachment for answer to question 3.3(3) - 1 sheet) (Attachment for answer to question 3.3(6) - 1 sheet)		S-7
SECTION 4.4		S-9
SECTION 5.3 (Table 1 for answer to question 5.3(6b) - 1 sheet)		S-10
<b>SUPPLEMENT 2 - RESPONSES TO STRUCTURAL ENGINEERING BRANCH COMMENTS AND REQUEST FOR ADDITIONAL INFORMATION ON CR#3 DOME DELAMINATION INTERIM REPORT AND SUPPLEMENT NO. 1</b>		1
I GENERAL COMMENTS		1
II DOME REPAIR		3
III CAUSES OF DELAMINATION		6
ATTACHMENT 1		
J. T. Rodgers Letter (10-8-76) to Mr. John Stolz (1 sheet)		
Instrument Location (2 sheets)		
Displacement Acceptance Criteria (2 sheets)		
J. C. King Letter (9-23-76) to F. L. Moreadith, Epoxy Grouting (1 sheet)		

LIST OF FIGURES

<u>Figure</u>	<u>Title</u>	<u>Text Cross References</u>
2-1	REACTOR BUILDING DIMENSIONS	2-1
2-2*	NON-PRESTRESSED REINFORCEMENT	2-1, I-1
2-3	DOME CONCRETE PLACEMENT - PLAN	2-1, 2-8, 3-9
2-4	DOME CONCRETE PLACEMENT - SECTION	2-1
2-5	DETAIL "A"	2-1
2-6	SUPPORT DETAIL	2-1
2-7	DOME TENDON LOCATION PLAN	2-1
2-8	CONDUIT SPLICES LOCATION & DETAIL	2-1
2-9**	DOME DETAILS	2-1
2-10	36" DOME DEAD LOAD + PRESTRESS MERIDIONAL STRESSES	2-6, 3-6a
2-11	36" DOME DEAD LOAD + PRESTRESS HOOP STRESSES	2-6
2-12	36" DOME DEAD LOAD + PRESTRESS MEMBRANE STRESSES	2-6, I-1
2-13	36" DOME DEAD LOAD + PRESTRESS LINER STRAIN	2-6
2-14	36" DOME DEAD LOAD + PRESTRESS SHEAR-FSAR	2-6, I-1
2-15	DELETED	
2-16*	36" DOME NORMAL WINTER OPERATING MERIDIONAL STRESSES	2-6
2-17*	36" DOME NORMAL WINTER OPERATING HOOP STRESSES	2-6
2-18	36" DOME NORMAL WINTER OPERATING MEMBRANE STRESSES	2-6a
2-19	36" DOME NORMAL WINTER OPERATING LINER STRAIN	2-6a
2-20*	36" DOME NORMAL WINTER OPERATING SHEAR - FSAR	2-6a
2-21	DELETED	
2-22*	36" DOME STRUCTURAL INTEGRITY TEST MERIDIONAL STRESSES	2-6a

\*Revised: 8-10-76

\*\*Revised: 9-22-76

LIST OF FIGURES (CONT'D)

<u>Figure</u>	<u>Title</u>	<u>Text Cross References</u>
2-23	36" DOME STRUCTURAL INTEGRITY TEST HOOP STRESSES	2-6a
2-24	36" DOME STRUCTURAL INTEGRITY TEST MEMBRANE STRESSES	2-7
2-25	36" DOME STRUCTURAL INTEGRITY TEST LINER STRAIN	2-7
2-26	36" DOME STRUCTURAL INTEGRITY TEST SHEAR - FSAR	2-7
2-27	DELETED	
2-28*	36" DOME 1.0 D + 1.0 F + 1.5 P <sub>a</sub> + 1.0 T <sub>a</sub> MERIDIONAL STRESSES	2-7
2-29*	36" DOME 1.0 D + 1.0 F + 1.5 P <sub>a</sub> + 1.0 T <sub>a</sub> HOOP STRESSES	2-7
2-30*	36" DOME 1.0 D + 1.0 F + 1.5 P <sub>a</sub> + 1.0 T <sub>a</sub> MEMBRANE STRESSES	2-7
2-31	36" DOME 1.0 D + 1.0 F + 1.5 P <sub>a</sub> + 1.0 T <sub>a</sub> LINER STRAINS	2-7
2-32*	36" DOME 1.0 D + 1.0 F + 1.5 P <sub>a</sub> + 1.0 T <sub>a</sub> SHEAR - FSAR	2-7
2-33	DELETED	
2-34	36" DOME SMALL PIPE BREAK LINER STRAINS	2-7
3-1	INITIAL INVESTIGATION DETAILS	3-1
3-2	INITIAL INVESTIGATION CORE HOLE DETAILS	3-1
3-3	INITIAL INVESTIGATION - CORE HOLE DETAILS	3-1
3-4	LOCATION OF DEEP EXPLORATORY CORE HOLES	3-1
3-5	DEEP EXPLORATORY CORE HOLE DETAILS	3-1
3-6	DEEP EXPLORATORY CORE HOLE DETAILS	3-1
3-7	DEEP EXPLORATORY CORE HOLE DETAILS	3-1
3-8	CONSTRUCTION JOINT CORE HOLE DETAILS	3-2

\*Revised: 8-10-76

LIST OF FIGURES (CONT'D)

<u>Figure</u>	<u>Title</u>	<u>Text Cross References</u>
3-9	CONSTRUCTION JOINT CORE HOLE DETAILS	3-2
3-10	CONSTRUCTION JOINT CORE HOLE DETAILS	3-2
3-10A*	FEATHER EDGE CORE PLAN	3-2a
3-10B*	FEATHER EDGE CORE LOCATION IN "WINDOW" (TYPICAL)	3-2a
3-10C*	SECTION - RB DOME (SHEET 1)	3-2a
3-10C*	LOCATION OF MAJOR GAP (SHEET 2)	
3-10D*	LOWER LEVEL CRACK EXPLORATORY PROGRAM	3-2a, 3-18a
3-10E**	SEQUENCES 1-6, DETENSIONED TENDON LOCATION	3-2a
3-10F**	24" DOME DEFLECTIONS MEASURED AT LINER	3-2a
3-10G**	LINER STRAIN AT 30'-0" RADIUS, MEASURED HOOP (R119H)	3-2a
3-10H**	LINER STRAIN AT 30'-0" RADIUS, MEASURED MERID. (R119M)	3-2a
3-10I**	LINER STRAIN AT 30'-0" RADIUS, MEASURED HOOP (R121H)	3-2a
3-10J**	LINER STRAIN AT 30'-0" RADIUS, MEASURED MERID. (R121M)	3-2a
3-10K**	CONCRETE STRAIN AT TOP SURFACE OF 24" DOME, 30'-0" RADIUS, MEASURED HOOP (152H)	3-2a
3-10L**	CONCRETE STRAIN AT TOP SURFACE OF 24" DOME, 30'-0" RADIUS, MEASURED MERID. (153M)	3-2a
3-11	DOME CORE HOLE PLAN NORTHWEST QUADRANT	3-2, 3-2a
3-12	DOME CORE HOLE PLAN SOUTHWEST QUADRANT	3-2, 3-2a
3-13	DOME CORE HOLE PLAN SOUTHEAST QUADRANT	3-2, 3-2a
3-14	DOME CORE HOLE PLAN NORTHEAST QUADRANT	3-2a
3-15**	RADIAL TENSION DUE TO PRESTRESS - ORIGINAL STRUCTURE	3-5, I-1

\*Revised: 8-10-76

\*\*Revised: 9-22-76

LIST OF FIGURES (CONT'D)

<u>Figure</u>	<u>Title</u>	<u>Text Cross References</u>
3-16*	AXISYMMETRIC FINITE ELEMENT MODEL	3-5a, 5-7
3-17***	STRESS CONCENTRATION IN TWO DIMENSIONAL STATE OF STRESS	3-6,
3-18***	DELETED	
3-19***	COMPRESSION - TENSION INTERACTION	3-6a
3-20	SOLAR HEATING TRANSIENT TEMPERATURE PROFILE	3-7
3-21	THERMAL GRADIENT THROUGH THICKNESS AT CONSTRUCTION JOINT L-M DUE TO SOLAR RADIATION HEAT	3-7

\*Revised: 8-10-76

\*\*\*Revised: 12-10-76

LIST OF FIGURES (CONT'D)

<u>Figure</u>	<u>Title</u>	<u>Text Cross References</u>
3-22*	PLANE STRAIN FINITE ELEMENT MODEL	3-8, 3-11, S2-8
3-23	TEMPERATURE GRADIENTS DUE TO TENDON GREASING	3-8
3-24	DOME SECTION - 0° AZIMUTH	3-8, 3-10
3-25	DOME SECTION - 90° AZIMUTH	3-8, 3-10
3-26	DOME SECTION - 180° AZIMUTH	3-8, 3-10
3-27	DOME SECTION - 270° AZIMUTH	3-8, 3-10
3-27A***	TENDON D-118 (WEST SIDE) TOP OF CONDUIT PROFILE SHOWING RADIAL FORCE FROM TENDON MISALIGNMENT	3-8a
3-27B***	TENDON CONDUIT CURVATURE	3-8a
3-27C***	TENDON CONDUIT CURVATURE	3-8a
3-27D***	TENDON CONDUIT CURVATURE	3-8a
3-27E***	TENDON CONDUIT CURVATURE	3-8a
3-28	SEQUENCES 1-6 SPECIFIED PRESTRESSING SEQUENCE	3-9
3-29	SEQUENCES 1-10 SPECIFIED PRESTRESSING SEQUENCE	3-9
3-30	SEQUENCES 11-21 SPECIFIED PRESTRESSING SEQUENCE	3-9
3-31	SEQUENCES 22-31 SPECIFIED PRESTRESSING SEQUENCE	3-9
3-32	SEQUENCES 32-41 SPECIFIED PRESTRESSING SEQUENCE	3-9
3-33	DOME TENDONS STRESSED AS OF 11-4-74	3-10
3-34	DOME TENDONS STRESSED AS OF 11-8-74	3-10
3-35	DOME TENDONS STRESSED AS OF 11-12-74	3-10
3-36	DOME TENDONS STRESSED AS OF 11-18-74	3-10
3-37	DOME TENDONS STRESSED AS OF 11-20-74	3-10
3-38	DOME TENDONS STRESSED AS OF 11-26-74	3-10
3-39	DOME TENDONS STRESSED AS OF 12-2-74	3-10

\*Revised: 8-10-76  
 \*\*\*Revised: 12-10-76

LIST OF FIGURES (CONT'D)

<u>Figure</u>	<u>Title</u>	<u>Text Cross References</u>
3-40	DOMES TENDONS STRESSED AS OF 12-3-74	3-10
3-41	DOMES TENDONS STRESSED AS OF 12-4-74	3-10
3-42	DOMES TENDONS STRESSED AS OF 12-6-74 (DAY SHIFT)	3-10
3-43	DOMES TENDONS STRESSED AS OF 12-6-74 (NIGHT SHIFT)	3-10
3-44	ACTUAL STRESSING SEQUENCE SUMMATION OF VERTICAL FORCES	3-10

LIST OF FIGURES (CONT'D)

<u>Figure</u>	<u>Title</u>	<u>Text Cross References</u>
3-45	ACTUAL STRESSING SEQUENCE SUMMATION OF VERTICAL FORCES	3-10
3-46*	TANGENTIAL STRESS IN CONCRETE DUE TO SHRINKAGE	3-11
4-1*	DOME MODEL	4-1, 4-2
4-2*	24" DOME DEAD LOAD + PRESTRESS MERIDIONAL STRESSES	4-4
4-3*	24" DOME DEAD LOAD + PRESTRESS HOOP STRESSES	4-4
4-4*	24" DOME DEAD LOAD + PRESTRESS MEMBRANE STRESSES	4-4
4-5	24" DOME DEAD LOAD + PRESTRESS LINER STRAIN	4-4
4-6*	24" DOME DEAD LOAD + PRESTRESS SHEAR - FSAR	4-4, I-2
4-7	DELETED	
4-8*	24" DOME NORMAL WINTER OPERATING MERIDIONAL STRESSES	4-4a, 4-7
4-9*	24" DOME NORMAL WINTER OPERATING HOOP STRESSES	4-4a, 3-6a
4-10*	24" DOME NORMAL WINTER OPERATING MEMBRANE STRESSES	4-4a
4-11	24" DOME NORMAL WINTER OPERATING LINER STRAIN	4-4a
4-12*	24" DOME NORMAL WINTER OPERATING SHEAR - FSAR	4-5, I-2
4-13	DELETED	
4-14*	24" DOME STRUCTURAL INTEGRITY TEST MERIDIONAL STRESSES	4-5
4-15*	24" DOME STRUCTURAL INTEGRITY TEST HOOP STRESSES	4-5
4-16*	24" DOME STRUCTURAL INTEGRITY TEST MEMBRANE STRESSES	4-5
4-17	24" DOME STRUCTURAL INTEGRITY TEST LINER STRAIN	4-5
4-18*	24" DOME STRUCTURAL INTEGRITY TEST SHEAR - FSAR	4-5, I-2
4-19	DELETED	
4-20*	24" DOME D + F + 1.5P + T <sub>a</sub> (UNCRACKED ANALYSIS) MEMBRANE STRESSES	4-5, 5-5, Fig. 5-20 and 5-21

\*Revised: 8-10-76

LIST OF FIGURES (CONT'D)

<u>Figure</u>	<u>Title</u>	<u>Text Cross References</u>
4-21	24" DOME D + F + 1.5P + T <sub>a</sub> (UNCRACKED ANALYSIS) LINER STRAIN	4-5
4-22	24" DOME D + F + 1.5P + T <sub>a</sub> MEMBRANE STRESSES AT D + F + 1.15P + T <sub>a</sub> (ASSUMED CRACKING)	4-6
4-23	24" DOME D + F + 1.5P + T <sub>a</sub> MERIDIONAL LINER STRAINS	4-6
4-24	24" DOME D + F + 1.5P <sub>a</sub> + T <sub>a</sub> HOOP LINER STRAINS	4-6
4-25	24" DOME D + F + P <sub>a</sub> + T <sub>a</sub> MEMBRANE STRESSES	4-6
4-26	24" DOME D + F + P <sub>a</sub> + T <sub>a</sub> (MAX. PREDICTED COMP. STRAINS) LINER STRAIN	4-6
4-27*	24" DOME 1.0D + 1.0F + 1.5P <sub>a</sub> + 1.0T <sub>a</sub> SHEAR - FSAR	4-6, I-2
4-28	DELETED	
5-1**	RADIAL HOLE LOCATION PLAN (NORTH HALF)	5-1, 5-4,
5-2**	RADIAL HOLE LOCATION PLAN (SOUTH HALF)	5-1, 5-4
5-3*	PLAN - NEW STRAIN GAGE GROUP LOCATION ON LINER	5-1, 5-3
5-4*	CONCRETE STRAIN GAGE LOCATION PLAN	5-1, 5-3
5-5*	CONCRETE STRAIN GAGE LOCATION PLAN	5-1, 5-3
5-6*	TYPICAL SECTION AT INSTRUMENTATION LOCATION	5-1, 5-3
5-7*	PLAN - EXISTING STRAIN GAGES ON OUTSIDE FACE REBAR IN DOME	5-1, 5-3
5-8*	LINEAR POTENTIOMETERS FOR GAP MOVEMENT	5-1, 5-3
5-9**	EXTENSOMETERS ON LINER FOR DISPLACEMENT MEASUREMENT	5-1, 5-3
5-10*	TEMPERATURE MONITORING	5-1, 5-3
5-11**	TYPICAL SECTION AT INSTRUMENTATION LOCATION (FOR SIT)	5-3

\*Revised: 8-10-76

\*\*Revised: 9-22-76

LIST OF FIGURES (CONT'D)

<u>Figure</u>	<u>Title</u>	<u>Text Cross References</u>
5-12**	TENDON LOCATION PLAN	5-4
5-13**	TENDON LOCATION (ORIGINAL STRUCTURE)	5-4
5-14*	TYPICAL SECTION - NEW CONCRETE	5-4, 5-5a
5-15**	EDGE DETAIL	5-4, 5-5a
5-16**	GROUTING PACKER	5-5
5-17**	PARTIAL PLAN	5-5
5-18**	PARTIAL PLAN - SUPPLEMENTARY DOME REINFORCING	5-5, Fig. 5-19
5-19**	SECTION AA	5-5, Fig. 5-18, S2-4
5-20**	CAP REINFORCEMENT - MERIDIONAL DIRECTION PROVIDED VS REQUIRED	5-5, G-8, S2-4
5-21**	CAP REINFORCEMENT - HOOP DIRECTION PROVIDED VS REQUIRED	5-5, G-8
5-22***	RADIAL STRESSES DUE TO PRESTRESS - DELAMINATED STRUCTURE	5-5a, S2-3, S2-6
5-23**	RADIAL STRESSES DUE TO CREEP AND PRESTRESS - REPAIRED STRUCTURE	5-5a, S2-3
5-24**	NEW CONCRETE POUR SEQUENCE	5-5a
5-25***	DOMES REPAIR SEQUENCE	5-1
5-26***	NO. 6 RADIAL REINFORCEMENT TEST	5-5

\*Revised: 8-10-76  
 \*\*Revised: 9-22-76  
 \*\*\*Revised: 12-10-76

1.0

INTRODUCTION

1.1

PURPOSE

This report describes a delaminated condition of the dome of the Reactor Building of Crystal River Unit No. 3, the subsequent structural evaluation of the condition and the repair of the dome.

1.2

SUMMARY AND CONCLUSIONS

The condition was first discovered on April 14, 1976. Soundings, core borings and cutting investigations indicated that the dome had delaminated. The approximate maximum thickness of the delaminated concrete was found to be 15 inches with a maximum gap of approximately 2 inches between the two layers. The plan area of delaminated concrete was approximately circular in shape with a 105 foot diameter. The condition was not apparent via visual inspection of the dome surface.

Analyses of the delaminated structure were performed (see Section 4.0) and field investigations carried out (see Section 3.0) to determine its safety and its capacity to sustain the design loads. Based on the analytical and field investigations, it was concluded that the structure in its delaminated condition did not represent a hazard to personnel. Furthermore, those investigations provided the basis for the repair method described in Section 5.0.

The repair of the dome was completed on October 30, 1976. The subsequent Structural Integrity Test (SIT) of the reactor containment building was successfully completed on November 3, 1976, the preliminary SIT report was filed with the USNRC Nov. 5, 1976 and the final SIT report on Dec. 7, 1976. The investigations and analyses presented herein and the SIT provide an adequate demonstration of the serviceability of the reactor containment building.

Potential contributing factors have been investigated in an attempt to determine the cause or causes of the delaminated condition. Several effects which may have contributed to the problem have been identified. These include compression-tension interaction; tensile capacity of the concrete; misalignment of tendons; concentrated stresses generated by shrinkage, greasing and construction delays and stress concentrations associated with embedded conduit.

The calculated values of radial tension associated with several of the effects are as follows:

Radial Tension due to Prestress (See Section 3.3.2)	41 psi (nominal)
Thermal Effects - (See Section 3.3.4)	
a. Sudden cool down	9 psi (nominal)
b. Tendon greasing	80 psi (peak)

Tendon Alignment (See Section 3.3.5) 56 psi (nominal)

Shrinkage (See Section 3.3.11) 36 psi (peak)

In addition to the above, two local effects could have occurred at the construction joint between pours L and M due to construction delay (See Sections 3.3.4 and 3.3.11). The radial tensions associated with the delay were predicted to be:

from Solar Radiation 280 psi (peak)

from Shrinkage 360 psi (peak)

It has been concluded that radial tension stresses combined with biaxial compression to initiate the laminar cracking in a concrete having lower than normal direct tensile capacity and limited crack arresting capability.

The procedures used in the investigations and results obtained are discussed in Section 3.0.

## 2.0 ORIGINAL STRUCTURE

### 2.1 PHYSICAL DESCRIPTION

The torispherical dome of the Reactor Building has a major inside radius of 110 ft - 0 in., a minor inside radius of 20 ft - 6 in. and a design concrete thickness of 3 ft - 0 in. Lining the inside face of the dome is a continuous 3/8 in. thick carbon steel liner which acts as a vapor barrier. Figure 2-1 shows the basic configuration of the Reactor Building including the dome. The dome is prestressed by means of tendons forming a three way system. Non prestressed reinforcement as shown in Figure 2-2 is provided near the top surface in circumferential and radial directions. Also, shear and bottom reinforcement is provided adjacent to the supporting ring girder.

Concrete placement was symmetrical in the form of full depth concentric rings as shown in Figures 2-3 and 2-4, and Table 2-1. The construction specification required that concrete be placed in a maximum of 1 ft - 6 in. layers with the upper layers being vibrated into the lower layer to form a homogeneous full depth pour. An application of epoxy bonding compound was specified to be applied at each construction joint prior to placement of the next pour of concrete. Support of the wet concrete was by means of ties from the dome tendon conduit to the angle anchors on the concrete side of the liner. The dome tendon conduits were tied together and carried the load back to previous concrete placements. See Figures 2-5 and 2-6 for details. Concrete was specified to have a minimum 28 day compressive strength of 5000 psi.

Prestressing for the dome was 123 tendons arranged in a three way (layer) system anchored at the ring girder. The 41 tendons in each layer were spaced at a horizontal distance of 2 ft 6 in., center to center. Refer to Figure 2-7. The conduit for each tendon was a 5 inch diameter schedule 40 galvanized pipe. Sections of conduit were joined together by means of a sleeve coupling welded to each section of conduit to form a grease tight system. The desired location of splices as shown on drawings and a typical splice detail are shown on Figure 2-8. Each tendon has a guaranteed ultimate strength of 2.335 million pounds and was made of 163, 7mm diameter, low relaxation wires. After the tendons were installed, the air space in the conduit was filled (bulk filled) with Visconorust 2090 P2 corrosion protection grease. The grease was heated in a tank, and then pumped as a fluid via hoses, into the conduit. Based on information from the constructor, the temperature of the grease at the tank outlet was approximately 160°F.

The carbon steel liner plate, made from ASTM A 283 Grade C steel, lines the inside surface of the dome. The liner also acted as the inside form for the concrete. Attached to the concrete side of the liner are steel angles which serve as anchors.

Figure 2-9 illustrates the basic dome details.

## 2.2

### APPLICABLE CODES AND STANDARDS

Codes and standards used in the design of the dome were given in the Crystal River Unit 3 FSAR (Docket No. 50-302), Chapter 5. The design predated the establishment of a concrete pressure vessel code. Therefore the codes and standards used in the design and specified for the construction were:

- a. Building Code Requirements for Reinforced Concrete, American Concrete Institute (ACI) 318-63.
- b. Specifications for Structural Concrete for Buildings, ACI 301-66 with modifications as noted in the FSAR.
- c. Specification for the Design and Erection of Structural Steel for Buildings, 1963, AISC.
- d. ASME Boiler and Pressure Vessel Code, Section III, Nuclear Vessels, Section VIII, Unfired Pressure Vessels; Section IX, Welding Qualifications (applicable portions).
- e. Specification for the Design and Construction of Reinforced Concrete Chimneys, ACI 505-54.
- f. AEC Publication TID-7024, "Nuclear Reactors and Earthquake," as amplified in the FSAR.

## 2.3

### CRITERIA

Table 2-2 lists the basic criteria applicable to the original design of the dome and Table 2-3 gives the controlling load combinations.

The design complied with the following additional requirements as stated in the FSAR.

### 2.3.1

#### Flexural and Membrane Tensile Stresses

The allowable tensile capacity of concrete for membrane stresses (i.e., excluding all flexural and thermal stresses) due to the factored loads was  $3\sqrt{f'_c}$ . The allowable tensile capacity of concrete for maximum fiber stresses due to the factored loads including the thermal load plus other secondary effects was  $6\sqrt{f'_c}$ . Where tensile fiber stresses exceeded the allowable, mild steel reinforcement was added on the basis of cracked section design. The amount of additional mild steel reinforcement and the increase in steel stresses due to temperature effects were determined in a manner similar to that contained in ACI 505-54. The minimum steel on the exposed face of the concrete was 0.15 percent of the cross-sectional area of the concrete.

The concrete shell was prestressed sufficiently to eliminate tensile stresses due to membrane forces from design loads. Membrane tension due to factored loads was permitted to the limits described above. On those elements carrying primarily tensile membrane forces, any secondary tensile stresses due to bending could cause partial cracking. Mild steel reinforcing was provided to control this cracking by limiting crack width, spacing, and depth. The capacity reduction factor " $\phi$ " for tensile membrane stresses was taken as 0.95. The coefficient " $\phi$ " for flexure, shear, and compression is in accordance with ACI 318-63, Section 1504.

### 2.3.2

#### Shear

In computing the shear capacity of the concrete the effects of membrane forces were accounted for as follows:

- a. When membrane tension exists or when membrane compression less than 100 psi, the section was designed to the ultimate shear provisions of Chapter 17 of ACI 318-63.
- b. When membrane compression of greater than 100 psi existed, the shear capacity was determined by the ultimate shear provision of Chapter 26 of ACI 318-63.

The acceptability of the dome for shear is evaluated by the following procedures:

The minimum capacity of the concrete,  $\phi V_c$ , is compared with the ultimate shear,  $V_u$ , that exists on the section. If a case results where this minimum concrete capacity is less than the ultimate shear, then the actual section capacity is computed using the FSAR criteria.

The shear capacities described above represent ultimate capacities. For assessing the section adequacy in shear, the ultimate shear  $V_u$ , is calculated by applying a load factor of 1.5 to the net shears resulting from load combination a, b, and c in Table 2-3. A load factor of 1.0 is applied to the net shears for load combination d.

When membrane compression greater than 100 psi exists, the shear stress limits and shear reinforcing for radial shear used in the design were in accordance with Chapter 26, "Prestressed Concrete" of ACI 318-63, except as follows:

In equation (26-12) of ACI 318, the shear increment between flexural and diagonal tension cracking ( $0.6b'd\sqrt{f'_c}$ ) was modified based upon the results of testing under the direction of Professor A. H. Mattock of the University of Washington. The resulting equation is:

$$V_{ci} = K_{\Delta v} b'd \sqrt{f'_c} + \frac{M_{cr}}{v} \frac{d}{2} + V_d$$

$$\text{where } K_{\Delta v} = 1.75 - \frac{0.036}{np} + 4.0 np.$$

In accordance with ACI 318, the factor  $K_{\Delta v}$  is not considered to be greater than 0.6.

Requirements for minimum shear reinforcement as called for in Equation (26-11) of ACI 318 were provided only at discontinuities.

## 2.4 SUMMARY OF ANALYTICAL RESULTS

A summary of analytical results for the original structure is presented in the PSAR. For purposes of comparison with the analytical results of the delaminated structure, results for the original structure are presented in this section. The format is consistent with that used in Section 4.4 for the delaminated structure. The original acceptance criteria used in the design is given in Table 2-2.

The controlling load combinations are given in Table 2-3.

The structural analysis of the containment was performed using KALNIN'S Static Computer Program described in Appendix D. The individual loads which comprise the load combinations were input separately, and their results were combined internally in the program where possible. This was not possible for the Structural Integrity Test and Accident Condition load combinations due to the different Young's Modulus (E) values for the concrete under the sustained loads (D, F, and T<sub>0</sub>) and the rapidly applied loads (P<sub>a</sub> and T<sub>a</sub>). In these cases, stresses for each of the two types of loads were combined externally. The effects of shrinkage and creep were considered as discussed below.

### a. Shrinkage

The effect of concrete shrinkage on the overall structural response (stress resultants) is insignificant due to the large volume to surface ratios of the cylindrical wall, ring girder, and dome.

In the prestress loss calculations, a conservative value for long term shrinkage strain of 100 micro in/in is used to be consistent with the original design. This is the value recommended in Reference (12) for calculating prestress losses in  $f'_c = 5000$  psi concrete. Actually, use of the shrinkage equation appearing in this reference for time = 40 yr. and volume to surface ratio = 24" results in a shrinkage strain of 10 micro in/in at end of plant life.

b. Creep

The effect of concrete creep under the prestress loads was included in the prestress loss calculations and in the structural analysis. The creep curves appearing in Reference (12) allow specific creep strains to be determined considering both concrete age at loading and duration of load. Actual creep strains were calculated from these specific creep strains for use in determining prestress losses. Also, the reduction in concrete stresses, which results in an increase in liner stresses, caused by concrete creep under sustained loads was taken into account in the structural analysis by using an effective Young's Modulus,  $E'_c$ . This modulus is expressed in terms of specific creep as

$$E'_c = \frac{E_c}{1 + sc E_c}$$

where:

$E_c$  = instantaneous concrete Young's Modulus =  $4 \times 10^6$  psi,

sc = specific creep (micro in/in/psi)

Analysis of the containment for load combinations a, b, and c (Table 2-3) is based on calculated prestress losses and a sustained load (D, F,  $T_0$ )  $E'_c = 2.7 \times 10^6$  psi corresponding to the present time. In load combination c (SIT), the results for  $1.15P_a$  are based on  $E_c = 4.0 \times 10^6$  psi.

For investigation of the containment under load combination d(LOCA), 40 year calculated values of prestress losses and  $E'_c = 1.8 \times 10^6$  psi are used. The  $1.5P_a$  and  $T_a$  part are based on  $E_c = 4 \times 10^6$  psi.

c. Prestress Losses

The calculated prestress losses (ksi) and effective prestress (ksi) are given below:

	<u>Elastic Shortening</u>	<u>Creep</u>	<u>Steel Relaxation</u>	<u>Shrinkage</u>	<u>Total Losses</u>	<u>Effective Prestress</u>
<u>Present</u>						
Vertical	3.6	3.9	2.2	2.9	12.6	155.4
Hoop	6.4	7.0	2.2	2.9	18.5	146.25
Dome	6.9	7.6	2.2	2.9	19.6	148.4
<u>40 yr.</u>						
Vertical	3.6	9.1	3.4	2.9	19.0	149.0
Hoop	6.4	16.2	3.3	2.9	28.8	135.95
Dome	6.9	17.6	3.4	2.9	30.8	137.2

The membrane and extreme fiber stress results presented in this section are those obtained directly from the KALNIN'S Static Computer Program analyses (i.e. linear, elastic, uncracked). At locations in the dome where tensile stresses exceed the allowable values given in Table 2-2, the concrete is assumed to be cracked. Cracked section investigations are performed to calculate concrete compressive and rebar tensile stresses. In the cracking investigation, the axial force (P) and moment (M) stress resultants applied on the section are computed from the uncracked stresses (plotted). The only exception to this is for the Normal Winter Operating Condition load combination. In this case, the cracked section will reduce the effect of the through thickness gradient ( $\Delta T$ ) part of the  $T_o$  term in the load combination. Therefore, the uncracked stresses due to  $\Delta T$  are subtracted from the plotted stresses prior to computing P and M. Then, the effect of  $\Delta T$  applied to the section with P and M is considered in a manner similar to that described in ACI 505-54. Cracked section stresses, calculated as described above, are shown at selected locations in some of the figures for this section. Where allowable stresses are not exceeded, existing compression reinforcement is not included in the cracking analysis.

#### 2.4.1 Structure Prior to Operation

For this load combination, the allowable extreme fiber stress according to the FSAR requirements was  $0.6 f'_c = 0.6 \times 5000 = 3000$  psi compression and 0 psi in tension. Results shown in Figures 2-10 and 2-11 give compression throughout the dome with a peak stress of 2666 psi in the meridional direction.

The maximum allowable membrane stress using the FSAR requirements was  $0.45 f'_c = 0.45 \times 5000 = 2250$  psi compression and 0 psi tension. Results shown in Figure 2-12 indicate a maximum membrane compression stress of 1836 psi. No membrane tension exists.

With reference to liner strains the limits are shown in Table 2-2. Figure 2-13 shows a maximum compressive strain of 0.000948 in the meridional direction. For this load combination, the analysis indicates no liner tensile strains.

The shear stress limits noted in Section 2.3.2 were used in the original design. Figure 2-14 shows that the available shear capacity exceeds the required shear capacity using FSAR criteria.

#### 2.4.2 Normal Winter Operating Condition

The allowable extreme fiber stresses for this load combination according to the FSAR as given in Table 2-2 were 3000 psi in compression and 0 psi in tension. For an uncracked section, the results indicate that the stresses near the ring girder are tensile. Thus, a cracked section investigation was required. This results in the peak compressive stress of 3038 psi shown in Figure 2-16 and 1022 psi shown in Figure 2-17. The rebar stresses indicated in these figures are considerably less than their 20 ksi allowable values.

Membrane stress limits as stated in the FSAR were  $0.45 f'_c = 0.45 \times 5000 = 2250$  psi compression and 0 psi tension. The analytical results shown in Figure 2-18 indicate a peak compressive stress of 1759 psi in the meridional direction, which is less than the allowable values. No membrane tensile stress exists.

Figure 2-19 shows the peak compressive strain to be 0.00124. For this condition the analysis indicates no liner tensile strain.

For this load combination the shear capacity of the section is greater than the required capacity for the FSAR criteria. Refer to Figures 2-20.

#### 2.4.3 Structural Integrity Test

The extreme fiber stress allowable values noted in the FSAR are  $0.6 f'_c = 0.6 \times 5000 = 3000$  psi compression and 0 psi tension. The uncracked results shown in Figures 2-22 and 2-23 are a peak compressive stress of 1895 psi and a peak tensile stress of 227 psi. Based on a cracked section investigation, a concrete compressive stress of 1930 psi exists in the outside face. The rebar stress on the inside face is not tensile, since the crack does not extend far enough into the section to reach the inside face rebar.

For the condition of membrane stress, the FSAR limit was  $0.45 f'_c = 0.45 \times 5000 = 2250$  psi compression and 0 psi tension. Figure 2-24 indicated the peak membrane compressive stress to be 834 psi, which is well below these values. No membrane tension exists.

Figure 2-25 shows a peak liner compressive strain of 0.00051.

Using FSAR criteria, Figure 2-26 shows that the shear capacity of the section exceeds the required capacity.

#### 2.4.4 Accident Condition

The allowable extreme fiber stresses according to the FSAR as given in Table 2-2 were 3000 psi in compression and  $6\sqrt{f'_c} = 424$  psi in tension. Results shown in Figures 2-28 and 2-29 based on uncracked analysis indicates a maximum fiber compression stress of 1241 psi in the meridional direction. In accordance with the Design Criteria Table 2-2, rebar limited to a 36 ksi design stress is provided where  $6\sqrt{f'_c}$  is exceeded.

According to the FSAR requirements, the maximum allowable membrane stress was  $0.45 f'_c = 0.45 \times 5000 = 2250$  psi compression and  $3\sqrt{f'_c} = 212$  psi tension. Results shown in Figure 2-30 indicate a maximum concrete tensile stress of 148 psi. Therefore, no rebar was required to resist these membrane stresses.

Figure 2-31 shows a maximum compressive strain of .002057. For this load combination the analysis indicates no liner tensile strains.

Using FSAR criteria, Figure 2-32 shows that the available shear capacity exceeds the required capacity.

#### 2.4.5 Small Pipe Break

Although not addressed in the FSAR, NRC personnel informally requested that the maximum liner strain be calculated for a small pipe break producing a liner temperature ( $T_a$ ) of 320°F. This load combination is defined in Table 2-3. Analysis of this accident situation assumed to occur at the end of plant life indicates in Figure 2-34 a maximum compressive liner strain of 0.0029.

#### 2.4.6 Summary

The original design met the requirements set forth in the FSAR. It should be noted that the 90 day concrete strength equaled approximately 6000 psi thus resulting in further margin.

**TABLE 2-1**  
**DOME POUR LOG**

<u>Pour No.</u>	<u>Date</u>	<u>Location*</u>
G1	2-18-74	45° - 135°
G1	2-20-74	225° - 315°
G2	2-25-74	135° - 225°
G2	2-25-74	315° - 45°
H3	3-1-74	180° - 270°
H3	3-4-74	0° - 90°
H4	3-6-74	90° - 180°
H4	3-7-74	270° - 360°
J5	3-12-74	45° - 225°
J6	3-14-74	225° - 45°
K7	3-20-74	135° - 315°
K8	3-26-74	315° - 135°
L9	4-4-74	0° - 360°
M10	7-8-74	0° - 360°
N11	7-12-74	0° - 360°
P12	7-17-74	0° - 360°
Q13	7-22-74	0° - 360°

\*Refer to Figure 2-3 for plan location.

TABLE 2-2

DESIGN CRITERIA

<u>Criteria</u>	<u>Original Dome</u>	<u>Delaminated Dome</u>
Design accident pressure	55 psig	55 psig
Design accident temperature	281 <sup>o</sup> F	281 <sup>o</sup> F
Concrete compressive strength ( $f'_c$ )	5000 psi	6000 psi
Allowable membrane compression stress	$0.45f'_c = 2250$ psi	$0.45f'_c = 2700$ psi
Allowable extreme fiber compression stress	$0.6f'_c = 3000$ psi	$0.6f'_c = 3600$ psi
<b>Service Loads*</b>		
Allowable membrane tension stress	0	0
Allowable extreme fiber tension stress	0	0
<b>Factored Loads*</b>		
Allowable membrane tension stress	$3\sqrt{f'_c} = 212$ psi	0**
Allowable extreme fiber tension stress	$6\sqrt{f'_c} = 424$ psi	0**
<b>Liner ***</b>		
Compression strain	.005 in/in	ASME Section III
Tension stress	$f_y$	Division 2

\* Mild steel reinforcement (Grade 40) is provided where the allowable stresses are exceeded. The stress in this reinforcement is not to exceed 20 ksi for Service Loads and 36 ksi for Factored Loads.

\*\* The concrete tensile capacity is conservatively assumed to be zero for factored loads in the delaminated dome evaluation.

\*\*\* The design utilized  $0.84 f_y$  for both compression and tensile stresses during construction.

TABLE 2-3

CONTROLLING LOAD COMBINATIONS

a. Structure Prior to Operation

$$1.0D + 1.0F$$

b. Normal Winter Operating Condition

$$1.0D + 1.0F + 1.0T_o$$

c. Structural Integrity Test

$$1.0D + 1.0F + 1.15P_a + 1.0T_t$$

d. Accident Condition

$$1.0D + 1.0F + 1.5P_a + 1.0T_a$$

e. Small Pipe Break Accident

$$1.0D + 1.0F + 1.0T_a$$

Symbols used in the equations are:

D = dead load of structure

F = prestress force

T<sub>o</sub> = operating temperature

T<sub>t</sub> = test temperature

P<sub>a</sub> = accident pressure

T<sub>a</sub> = accident temperature including T<sub>o</sub>

### 3.0 PROBLEM DEFINITION

#### 3.1 INVESTIGATIONS

##### 3.1.1 Original Indications

On April 14, 1976 electricians were attempting to secure drilled-in anchors to the top surface of the dome and certain anchors would not hold. On the west side of the dome, 52 ft - 6 in. from the apex, further investigation revealed an area of the dome surface which sounded hollow when hit with a hammer. The size of the area was approximately 30 feet long by 3 feet wide. The area was curved slightly as it appeared to follow the circumferential construction joint between pours G and H. This area is shown in Figure 3-1.

In order to better define the hollow area concrete soundings were employed. The results of this examination indicated that a hollow sounding zone encircled the dome. No cracks appeared on the dome surface. The plan of the outer boundary of the affected area as determined by concrete soundings is shown in Figure 3-1.

##### 3.1.2 Preliminary Exploration

To determine the extent of the condition, it was decided to examine a portion of the initially discovered area. The examination consisted of saw cutting a 2 ft-6 in. long by 10 in. wide by 3-1/2 in. (maximum) deep section of concrete. Inspection of the removed pieces of concrete as well as the lower surface revealed a clean fracture (100% fracture of coarse aggregate) with little or no powder or rubble in the joint. The exposed surface revealed a gap running up into the dome towards the apex. A three foot length of wire could be probed into the gap without resistance. This gap, coupled with the results from the concrete soundings, appeared to indicate that the top of the dome had delaminated. The saw cut examination area is shown in Figure 3-1.

To confirm that the dome was delaminated, seven exploratory core holes were drilled. The location of each core hole was carefully selected to ensure that the stressed tendons were not damaged while achieving sufficient coverage of the dome to establish the extent of the condition. The location of these core holes is shown in Figure 3-1, with details shown in Figures 3-2 and 3-3. The results of the exploration, summarized in Table 3-1, shows that the dome had delaminated. The thickness of the delaminated concrete was found to be approximately 15 in. in the area of the apex. The dimension of the gap in the same area was approximately 1-3/4 inches. See Section 3.2 for a discussion of calculated gap versus measured gap.

The seven exploratory core holes were shallow holes confined to the thickness of the delaminated cap. By maintaining a shallow depth, contact with tendon conduit was avoided. To determine if there was deeper cracking, eight core holes were drilled to an average depth of 29-1/2 inches. The location of these core holes is shown in Figure 3-4, with details shown in Figures 3-5, 3-6 and 3-7. Care was taken to avoid the tendon conduit and to not penetrate the liner. Two

diameters of core hole were used, the first 12 to 14 inches of each core being 4 inches in diameter, and the remainder 1-3/4 inches in diameter. A borescope was then used to examine the surface of the 1-3/4 in. diameter hole. In five of the eight holes, additional cracks were found. The maximum width of these cracks at the exposed surface ranged from approximately 0.01 inches to 0.03 inches, with the orientation of the cracks being parallel to the surface of the dome. During core drilling, the drill water did not run out, indicating that the cracks might not be continuous.

With the knowledge that the dome had delaminated, further investigation was directed to determine the safety of the dome. A dimensional monitoring program measuring gap depth, dome cap displacement and ambient temperature was established. As results became available, they indicated that the gap increased and decreased in delayed response to ambient temperature changes. Results of the monitoring program, together with analytical results for the delaminated condition indicated that the structure was safe.

To provide the basis for determining the in-place strength of the dome concrete, cores were taken from the dome cap. For compressive testing, two cores per pour were tested which represented one set per 100 cubic yards or lesser quantity placed per day. In addition, a third core per pour was taken and either saved or used for a split tensile test. This program required a total of 51 cores. Table 3-2 lists these cores and their strength test results and Table 3-3 includes the location of these cores.

### 3.1.3 Additional Investigations

In order to further investigate the condition of the existing structure, the following programs were undertaken:

- a. Construction joint adequacy.
- b. Location of tendons.
- c. Direct tensile tests of concrete.
- d. Location and definition of the perimeter of the main delamination.
- e. Location and details of lower level cracks.
- f. Tendon forces, i.e., lift-off tests.
- g. 15% detensioning strains and deformations.

To establish that construction joints were sound, a series of cores were made and examined. These cores (I, VIA, IIIA, IIIB, VB and IV in Figures 3-11 and 3-13) indicate that the epoxy joint material had effectively bonded the joint together and that an acceptable bearing condition exists through the joints. Figures 3-8, 3-9 and 3-10 indicate details of these cores.

In order to provide a definition of the existing structure in the vicinity of the perimeter of the main delamination, a series of core holes were made in pours J, H and G to determine the elevation of the main delamination as well as the existence of any lower level cracks in pours (G and H) which contain radial reinforcing. Figures 3-10A and 3-10B indicate the location of these cores. Deep cores were also made in the region of the construction joint between pours H and J to locate any lower cracks or concrete crushing that might have existed in this high compressive stress area. A description of the cores is contained in Figure 3-10C.

The cores indicate that the main delamination did not penetrate the reinforced areas of pour G and H and that lower level cracking also did not occur there. The observed condition of the concrete material in the deeper cores did not indicate any crushing.

An additional set of deep cores was drilled in each of the original pours to supplement the original data on deep cracks. Figure 3-10D and Table 3-3A indicate the location of the cores and cracks. The plan extent of the cracks appeared to be rather extensive, at a relatively few levels. The levels appeared to correspond with the location of the tendon groups.

A sample group of 21 tendons were selected for lift-off readings in order to determine the level of prestress on the dome and to establish the accuracy of the predicted losses.

In addition to these lift-off tests, 18 other tendons (6 in each group) were detensioned and lift-off readings obtained. See Figure 3-10E. The detensioning of these tendons represents a symmetrical and uniform removal of 14.6% of the dome prestress. The associated stresses and deformations for this loading were compared with predicted values. Figures 3-10F thru 3-10L show these values. These figures indicate that the structure responded as a full 24 in. deep structure since actual response was less than predicted response. The 14.6% removal of dome prestress was equivalent to applying an internal pressure of approximately 14 psig.

Table 3-3B indicates the average lift-off values and the predicted design value for the 39 tendons. These results indicated that the in-place dome prestress was 9% in excess of the predicted.

Details of the location of all cores in the general gap study are given in Table 3-3 and in Figures 3-11, 3-12, 3-13 and 3-14.

At no time during the investigation was there any evidence of grease leakage from the tendon conduit.

#### 3.1.4

#### Other Events

Examination of construction records revealed that at 7:20 a.m. on December 4, 1974 a loud noise or boom occurred on the site. The noise reportedly appeared to come from the Reactor Building and was heard by certain construction workers in their construction change areas. One worker was in the Reactor Building personnel lock at the time, felt vibrations and saw dust falling. Since subsequent visual inspection by construction personnel of the Reactor Building interior and exterior including the dome did not reveal any damage, the incident was not reported to the NRC or the Engineer.

### 3.2

#### DELAMINATION GAP

Calculations were made to determine the apex displacement of the delaminated dome. The purpose of the calculations was to determine if correlation with the actual condition could be obtained. After allowance for concrete age of approximately 700 days and creep of the concrete, the delamination gap was calculated to be approximately 1-1/2 inches. The actual gap averages 1-3/4 inches. The calculated displacement is for a 2 foot thick dome. The correlation between actual and theoretical gap depths was considered satisfactory.

### 3.3

#### POSSIBLE CAUSES OF THE DELAMINATION

The engineering investigations took into consideration all factors which were believed to be potentially contributory to the delaminated condition. The source of much of the information was the constructors records. Factors considered in the investigation were:

1. Properties of concrete and constituents.
2. Radial tension due to prestress.
3. Compression - tension interaction.
4. Thermal effects.
5. Tendon alignment.
6. Heavy construction loads.
7. Coastal location.
8. Location adjacent to fossil units.
9. Construction methods.
10. Impact loads.
11. Shrinkage effects.

The following sections present discussions of these factors.

### 3.3.1 Properties of Concrete and Constituents

Sources of information on the properties of the concrete and its constituents include the results of tests performed for the original mix qualification and supplemental tests, during construction and subsequent to discovery of the delaminated condition.

#### a. Original Tests

At the beginning of the project, special tests were conducted on a mix to determine such properties as creep, shrinkage and thermal conductivity. In addition, concrete cylinders were tested in compression and splitting tension. The average compressive strength of two sets of cylinders (three per set) tested at 28 and 56 days was 7040 psi and 7610 psi, respectively. Split tensile tests for two sets of cylinders (three per set) gave an average of 585 psi and 600 psi when tested at 28 and 90 days, respectively. Test results are contained in Appendix A.

Requirements for concrete materials and available qualification test results are also contained or referenced in Appendix A.

The mix proportions for the dome concrete are described in Appendix A.

#### b. Construction Testing

During concrete placement of the dome, test cylinders were made. The compressive strength of the cylinders was assessed in accordance with the requirements of Section 4.3.3 of ACI 318-71 and resulted in a 90 day design strength of 5930 psi. Table 3-4 summarizes the results for both concrete and the epoxy bonding compound.

On April 4, 1974 concrete was placed in pour L-9 of the reactor building dome. The concrete was to have a design strength of 5000 psi at 28 days. Seven day test cylinder breaks indicated that the concrete would not achieve the design strength level. The 28 day cylinder test results averaged 4570 psi. A review of the dome design was made to determine a minimum acceptable concrete strength for this particular area of the structure. The results of the review indicated that 4500 psi was an acceptable minimum design strength. Refer to Appendix B for further details. The 90 day cylinder test results averaged 5820 psi.

#### c. Subsequent Tests

Subsequent to the discovery of the delamination, cores with a 3-3/4 in. diameter were obtained to establish in-place compressive strength. Locations of the cores are described in Section 3.1. The compressive strength of the cores was assessed in accordance with the requirements of Section 4.3.3 of ACI 318-71 and resulted in a design strength of 6130 psi. Results are summarized in Table 3-2. Cores were also obtained

for testing by the split cylinder method. Locations of the cores are described in Section 3.1. Testing by this method indicated an average split tensile strength of 708 psi. Results are summarized in Table 3-2. The age of the concrete at the time the cores were tested ranged from approximately 630 days to 790 days with a weighted average age of 720 days.

Cores were also obtained for testing in direct tension to establish correlation between the standard tests, i.e., compressive and split tensile strength, and the direct tensile strength. The average direct tensile strength of 420 psi when compared to the average compressive strength of 6177 psi for the pours from which tensile specimens were obtained and an average split tensile strength of 708 psi is low using standard ratios. The ratio of the split tensile strength to the compressive strength does not appear abnormal. When the range of tensile values is considered, 230 to 505 psi, depending on the amount of soft aggregate, the variation from the normal ratio of strengths is pronounced.

Based on the average compressive cylinder tests a design  $f'_c$  of 6000 psi is justified.

Concrete specimens were also petrographically examined.

Results of the foregoing tests are presented in Appendix C.

### 3.3.2 Radial Tension Due to Prestress

Any change in tendon direction produces radial stresses when the tendon is tensioned. Since the tendons are not at the outside surface of the dome the radial forces are tensile for the concrete above the tendon groups and compressive for concrete below the tendon groups. Subsections a, b and c address design criteria, material properties and stress concentrations in relation to radial tension due to prestress.

#### a. Design Criteria

At the time of the structural design of the CR3 containment, there were no code criteria for allowable radial tension stresses. Based on calculations, the average radial tensile stress at the centerline of the top tendon group (i.e., at the level of the delamination) for the theoretical geometry is approximately 41 psi based on the gross area (see Figure 3-15). The minimum direct tensile strength of the dome concrete, based on testing of cores (see pg. C-15), was 230 psi.

Delamination of the dome would not have been expected based on this comparison.

b. Variation of Material Properties

In order to evaluate the effects of material properties on radial tension stresses, the axisymmetric element in the SAP IV computer program was used to perform a parametric study. The basic model as shown in Figure 3-16 divided the through thickness shell into layers with the following properties. The concrete above and below the tendon groups was assumed to have a Young's modulus  $E = 4 \times 10^6$  psi and a Poisson's ratio  $\nu = 0.2$ . For the middle layer containing concrete and tendon conduit the assumptions were  $E = 3.17 \times 10^6$  psi and  $\nu = 0.2$ . The Young's modulus,  $E = 3.17 \times 10^6$  psi, was estimated on the basis of the ratio of net concrete volume to gross concrete volume. Values of  $E = 30 \times 10^6$  psi and  $\nu = 0.3$  were assumed for the steel liner. In order to simulate the effect of rebar near the top surface, the equivalent Young's Modulus based on transformed area was used for the concrete near the top surface. To simulate the effect of conduit on Poisson's ratio,  $\nu = 0.3$  was used for the middle layer. A lower bound value of  $E = 2.5 \times 10^6$  psi was also used for the middle layer to check the sensitivity of the structure to an assumed soft layer. The Poisson's ratio of concrete varies

between 0.15 and 0.2 for stress below 40% of ultimate strength<sup>(3)</sup>. Another reference gives test results which indicate an average value of  $\nu = 0.2$ <sup>(4)</sup>. In order to simulate the effect of a concrete stress higher than  $0.4 f'_c$   $\nu = 0.3$  was assumed.

A summary of the parametric study is shown in the following Table:

Case	Basic Case	Temperature Rebar Case	Poisson's Ratio Effect	Young's Modulus Effect	Poisson's Ratio Effect
E (concrete)	$4 \times 10^6$	$4 \times 10^6$	$4 \times 10^6$	$4 \times 10^6$	$4 \times 10^6$
E (concrete & conduit)	$3.17 \times 10^6$	$3.17 \times 10^6$	$3.17 \times 10^6$	$2.5 \times 10^6$	$3.17 \times 10^6$
$\nu$ (concrete & conduit)	0.2	0.2	0.3	0.2	0.3
$\nu$ (concrete)	0.2	0.2	0.2	0.2	0.3
Rebar Effect	No	Yes	No	No	No
Resulting Max. Radial tension	42.5	43.5	41.0	44.6	42.8

These calculations indicate that the radial tension stress is low and not sensitive to variations in these parameters.

### c. Stress Concentrations

The geometry of the tendons in the CR3 dome suggests that stress concentrations around the conduit might be a contributing factor to the delamination. Consequently, investigation of the potential for stress concentrations was undertaken.

Referring to Figure 3-17, a model is shown which represents a simplistic simulation of the conduit effect. If the hole were unlined (i.e., no Schedule 40 pipe), a theory of elasticity solution for the model shown, subject to a uniform uniaxial compression,  $\sigma_c$ , would result in a transverse tension at the face of the hole of  $\sigma_t = \sigma_c$ . That is, an applied compression of 1000 psi would result in transverse tension of 1000 psi.

In addition to the above, a detailed finite element analysis of the model subject to  $\sigma_c$  with a Schedule 40 pipe embedded as shown was also investigated. Assuming linear elastic behavior and that the pipe and concrete remained bonded together, the results were somewhat different. The location and magnitude of maximum tensile stress was changed. The location and orientation of  $\sigma_t$  is as shown in Figure 3-17. The magnitude of  $\sigma_t$  was found to be approximately  $0.5 \sigma_c$ .

Available literature (e.g. References 13 and 14) and test results presented in Reference 15 indicate elastic stress concentration calculations do not accurately predict the failure stress for concrete structures. The effect of stress concentrations in the CR3 dome, however, may have been greater than would have been expected in normal concrete as a result of aggregate quality (see Appendix K).

### 3.3.3 Compression-Tension Interaction

The state of stress at the top tendon layer is triaxial, two membrane compressive stresses and one radial tensile stress. It is conservative to consider the interaction of one compressive stress with the radial tensile stress (Ref. 4, 8, 9, & 10). Before discussing compression-tension interaction in the CR3 dome at the time of stressing the tendons, it is necessary to establish applicable stresses and material strengths.

The initial membrane compression stresses would have been higher than those defined in Section 2.0, since the time dependent losses assumed in the calculations of Section 2.0 would not have occurred. The maximum meridional compressive stress for a fully prestressed dome (Figure 2-10) of 2,275 psi on the outside face would have been approximately 2,500 psi due to initial prestress forces. The radial tension stress could have been as high as 55 psi.

At the time of stressing the tendons, concrete compressive strength ( $f'_c$ ) was approximately 6,000 psi (based on 90-day strengths, see Table 3-4). The splitting tensile strength of the material was in the neighborhood of 500 to 600 psi (based on trial mix data, see page A-3-2). The direct tensile strength based on recent tests (see page C-15) could have been as low as 230 psi for some of the dome concrete.

Using the interaction lines suggested in Reference 15 (Figure 4-9), the straight line failure envelope shown in Figure 3-19 was constructed as follows:

1. A tensile strength of 160 psi was calculated using the minimum CR3 tensile test result of 230 psi with an approximate 30% reduction due to the presence of holes (see Reference 15, page 4-10).
2. A compression strength of 4800 psi was calculated using  $f'_c = 6000$  psi and a 20% reduction for size effects (see Reference 15, page 4-10). The compressive strength was not reduced for the effect of holes since the transformed area of the pipe effectively fills the holes for compressive stresses.

The interaction line used is more conservative than other possible representations of the failure envelope.

The plotted state of stress for the dome (55 psi, 2500 psi) corresponding to full initial prestress indicates a nominal safety factor against delamination. However, the 55 psi radial tension stress due to prestress could have been increased in local regions of the dome due to other effects discussed in Section 3.3 and could have resulted in delamination.

A compression-tension interaction of the stresses in the concrete would explain the appearance of the main delamination surfaces, the delamination of the upper cap and the presence of some cracking in levels below the top tendon group. It would also explain the fact that the structure retained its load carrying capacity subsequent to the delamination.

### 3.3.4

#### Thermal Effects

Two types of thermal effects considered were solar radiation (environmental) and tendon greasing (bulk filling).

##### a. Solar Radiation

The effect of solar radiation on the surface concrete temperature was calculated. In performing this calculation the initial condition assumed was 60°F throughout the dome thickness. The effect of solar radiation was calculated to heat the dome surface to 152°F. Subsequent to a six hour heat up period, the 6.0 hour gradient shown in Figure 3-20 was calculated. To determine if a thermal shock could have had a significant effect on the stress state in the dome, a sudden cool down due to a thunderstorm was postulated. Therefore, a step function of a six hour quench using a surface temperature of 50°F was assumed.

Figure 3-20 shows the gradients after the initial heat up (0.5 hr), just prior to quench (6.0 hr), after quenching (6.5 hr), and two points along the cooling period (8.0 hr and 12.0 hr).

Using the analytical model described in Section 3.3.2, and the gradients shown in Figure 3-20, the maximum tensile stress at the level of the centerline of the top tendon group was calculated to be 8 psi.

The solar radiational heat also had an affect at construction joint L-M during the three month construction delay. The conduit protruding from the joint had a different temperature than the surrounding concrete. This causes hoop tension around the conduit in the same way as that due to hot grease injection. The temperature gradient is as shown in Figure 3-21 and the maximum tension as calculated by plane strain element of computer program SAP IV (see Appendix D) is 280 psi.

Based upon these studies it is unlikely that the solar effect by itself could have produced other than very limited cracking at the construction joint interface.

##### b. Tendon Greasing

The field records show that tendon greasing took place in two stages. Eight unstressed tendons were greased prior to stressing the tendons (with the exception of three). The remainder were

greased about four months later, after all tendons had been stressed. The second greasing operation was completed in a period of eight days.

The grease was heated prior to injection to reduce its viscosity. According to available field records, the temperature of the grease at the tank outlet was in the range of 150-170°F. It was then pumped via a rubber hose into one tendon conduit at a time. After all the air had been purged from the conduit, pumping ceased and the conduit was sealed at 0 psig.

During hot grease injection, the conduit heated more rapidly than the concrete due to the lower thermal conductivity of concrete. For a step change of temperature from conduit to concrete, the tensile stress in the concrete surrounding the conduit can be calculated from the theory of elasticity. Using the compatibility of radial displacements at the conduit-concrete interface, (11) the tensile stress is determined to be 11 psi/°F. The plane strain element of the SAP IV program as shown in Figure 3-22 yields a tensile stress of 15 psi/°F for the identical condition.

Based upon an averaging of field records of grease temperature in the storage tank and at the conduit outlet, a heat transfer analysis was performed to establish the temperature gradients within the structure due to the greasing operation. The resulting gradients at a point approximately midway between ring girder and dome apex are shown in Figure 3-23. Using the plane strain element in the SAP IV computer program, shown in Figure 3-22, the maximum tension stress is approximately 80 psi, which occurs at the location where the thermal gradient drops to zero. It is recognized that variations in the greasing operation could produce more severe gradients and consequently higher concrete tensile stresses.

The injection pressure of hot grease can also cause tension around the conduit. With the same kind of radial displacement compatibility calculation, the maximum grease pressure reported by the constructor of 85 psi causes 40 psi tension in the concrete by compatibility calculation (11).

The cases studied indicate stresses of sufficient magnitude to cause the delamination only when considered in conjunction with other effects.

### 3.3.5 Tendon Alignment

To establish the accuracy of the positioning of the tendons within the dome, a survey was conducted to determine the actual dome thickness and the depth from the dome exterior surface to the top of the upper tendon group conduit. The results of the survey are shown in Figures 3-24 through 3-27. This shows that the conduit are high near the periphery and low at the apex and suggests that an increased curvature might exist.

Subsequent to the removal of the delaminated cap (see Section 5.2.4) and prior to placing a new cap (see Section 5.2.8), a more extensive survey was conducted. Elevations were obtained at 2.5' horizontal intervals along the exposed outer conduit. Figure 3-27A is a plot of the elevations for the West portion of tendon D-118. The elevations obtained and plotted are for the outer surface of the conduit. The prestress wires, of course, bear against the structure and induce the prestressing force on the inside bottom of the conduit. Assuming the profile of the conduit inner surface is the same as the profile of the top outer surface, tendon D-118 would tend to bear on the conduit at the high points and would tend to be straight between them. In the case of tendon D-118, the concentrated load at one of the bearing points based on an initial magnitude of the prestress force (1650 kips) would be approximately 180 kips. Although this value would be distributed along a finite length, it would result in a change in local load due to prestress for tendon D-118 from 41 psi to approximately 100 psi.

The survey data was also evaluated by fitting a circular curve to each data point using the adjacent points on either side of the point being considered. Average radii of all the outer conduit was computed to be 111.4' compared to the specified theoretical average radius of 110'. However, the individual variations from the theoretical radii were significant. Figures 3-27B through 3-27E present the calculated radii for the outer tendon group.

The significance of the increase in radial tendon pressure due to either concentrated loads or decrease in tendon radius was analyzed using two approaches. The first studied the effect on radial tension of a ring load 4' wide, 40 feet from the apex and the second the effect of a 4' diameter uniform load at the apex. This increase of load in local areas resulted in the following: four (4) psi increase in load results in one (1) psi increase in radial tension stress at the level of the outer conduit. For the survey example discussed previously the 100 psi local pressure results in a nominal radial tension stress of 56 psi.

The survey and analysis results indicate that conditions that would have increased loads in local areas existed in the CR3 dome. This would have resulted in increased radial tension stresses in local regions of the dome.

### 3.3.6 Heavy Construction Loads

The construction of the dome did not require heavy construction loads to be placed on the dome. A small mobile crane was located on the ring girder for use in tendon installation and stressing, but no heavy equipment was located on the dome surface.

### 3.3.7 Coastal Location

It was postulated that the coastal environment might have had a detrimental effect on the material in the structure. Subsequent investigation did not reveal detrimental effects due to coastal location.

### 3.3.8 Location Adjacent to Fossil Units

There was a period of time when tendon conduits were exposed to the atmosphere prior to concreting. Although a potential for damage due to the presence of sodium, calcium, and magnesium sulfates from the stacks of the adjacent fossil units exists, (2) there is no evidence that reactions occurred.

### 3.3.9 Construction Methods

Concrete construction joints were located as shown in Figure 2-3 and the concrete placed in the sequence and on the dates indicated in Table 3-5. The field coring investigation program did not indicate unsatisfactory conditions such as honeycombing, voids or cold joints.

During construction a deficiency in concrete cylinder compressive strength in pour "L" was observed. However, the concrete attained approximately 5800 psi at 90 days which was satisfactory (see Appendix B).

The specified prestressing sequence is shown in Figure 3-28 through 3-32 and given in Table 3-6. Three tendons, one from each layer or group, were to be stressed at a time (a sequence). Each tendon was to be stressed from both ends. The concept of the sequences was to put balanced loads into the dome.

The stressing sequence log developed from constructor's records is given in Table 3-7. Table 3-8 shows the daily cumulative totals of tendons stressed. The stages of the stressing are shown in Figures 3-33 through 3-43. Figures 3-44 and 3-45 show a relative vertical force imbalance on the dome. The Tables and Figures indicate that at certain times the sequence of stressing gave unbalanced forces as high as 16.9%. Immediately prior to the boom or loud noise on the morning of December 4, 1974, 72% of the dome tendons had been stressed. It is extremely difficult to accurately assess the consequences of any given sequence but, the stressing sequence used did create unbalanced forces.

A field investigation was conducted by coring through the delaminated cap and using survey methods to establish thicknesses of the dome and the delaminated cap and the location of the top of tendon conduit. The results are shown in Figures 3-24 through 3-27, and reflect concrete thickness variations between 33-1/4 in. and 39 in. and top of conduit location from exterior concrete surface which varies between 6-1/2 in. and 13-1/2 in.

The effect of these variations is not considered significant. However, small force imbalances might have significance if coupled with tendon misalignment as discussed in Section 3.3.5.

#### 3.3.10 Impact Loads

The boom heard by the workers at the site at 7:20 a.m. on December 4, 1974 was discussed in Section 3.1. This boom might have been caused by the breakage of tendon wires or by a kink in a tendon adjusting itself to the proper position. In either case, this boom could have represented an impact load applied to the dome causing initial cracks.

End caps were removed from each end of the tendons which were detensioned or used for lift off tests (see Section 3.1.3). Inspection of the anchorage assemblies did not reveal any conditions which might be associated with sudden breakage.

#### 3.3.11 Shrinkage Effects

Because of the presence of the steel liner on the inner surface of the dome, the exterior surface concrete will shrink more rapidly than the balance of the concrete. The in-plane dimensional changes due to shrinkage produce meridional and hoop tension in top surface of the dome and meridional and hoop compression in the bottom surface. This effect should not produce radial tension near the top surface.

During the three-month construction delay between April 4, 1974 and July 8, 1974 at construction joint L-M, shrinkage could have also affected the concrete. Since the concrete on the top surface and at the construction joint shrinks and the conduits protruding from the joint do not shrink, micro-cracks could be produced in the concrete surrounding the conduits. This is similar to the case of micro-cracks in the mortar surrounding coarse aggregates due to shrinkage<sup>(1)</sup>. Figure 9 of Reference 1 indicates that when the distance between coarse aggregates is greater than 0.45 times the radius of the aggregates, shrinkage will cause radial compression, hence, hoop tension surrounding the coarse aggregates.

In order to evaluate the amount of radial tension due to shrinkage for the three month construction delay, the amount of shrinkage has to be estimated first. The average final shrinkage of concrete (i.e. at 40 years) with volume/surface ratio of 24 in. has been estimated to be  $1 \times 10^{-5}$  in/in. However, based on the ASTM C 157 test of the design mix by the Pittsburgh Testing Laboratory, the shrinkage strain at 12 weeks is  $4.5 \times 10^{-4}$  in/in. Taking into account the difference between testing specimen and in-place concrete, it is reasonable to assume that shrinkage strain at the construction joint surface at the end of 12 weeks is  $2.25 \times 10^{-4}$  in/in. Assuming thermal expansion coefficient of concrete to be  $5.5 \times 10^{-6}$  in/in/ $^{\circ}$ F, the shrinkage strain is equivalent to  $41^{\circ}$ F temperature drop.

A 20" x 20" plane stress concrete analytical model with a ring sliced from 5 in. diameter schedule 40 pipe at the center as shown in Figure 3-22 was used to evaluate the shrinkage stress. With a  $41^{\circ}$ F temperature drop applied at the surface of the concrete, the hoop tensile stress surrounding the conduit in the concrete is approximately 360 psi. The stress profile surrounding the conduit at the construction joint surface is shown in Figure 3-46. These stresses are based upon conservative shrinkage strains, but suggest sufficient magnitude to initiate cracking. Assuming a shrinkage strain of  $2.25 \times 10^{-5}$  in/in for the overall dome, the tensile stress surrounding the conduit is 36 psi.

3.4

#### CONCLUSIONS

It appears that a compression-tension interaction failure occurred. Effects which could have generated radial tension forces have been defined and discussed. Several of the effects such as radial tension due to prestressing, thermal effects, tendon alignment, stress concentrations and shrinkage in combination would have been sufficient when combined with biaxial compressive stresses and lower than normal direct tensile strength of the concrete to result in the delaminations. The complete fracture of the coarse aggregate on that surface and the variations in tensile strength values obtained from the direct tensile tests indicate that the fragility of the coarse aggregate permitted local cracking to propagate.

TABLE 3-1

INITIAL EXPLORATORY CORE HOLES

<u>Core No.</u>	<u>Diam. (in)</u>	<u>Location</u>		<u>Delamination</u>	
		<u>Az</u>	<u>Pour</u>	<u>Thickness (in)</u>	<u>Gap (in)</u>
1	1-3/4	90°	L	11-1/2	1-1/2
2	4	270°	L	13-3/8	1-5/8
3	4	90°	Q	15-1/4	1-3/4
4	4	270°	J	4-1/2	1/8
5	4	150°	L	14	2
6	4	30°	L	10-1/2	1-1/2
7	4	335°	L	13	1-3/4

TABLE 3-2

CORE STRENGTH TEST RESULTS

<u>Pour</u>	<u>Core</u>	<u>Compression</u>			<u>Split Tension</u>	<u>Remarks</u>
		<u>Compression Strength</u>	<u>Test Average</u>	<u>Moving Average of Three</u>		
G(W)	49	7000	-	-	-	
G(W)	50	6820	6910	-	-	
G(W)	51	-	-	-	-	
G(E)	55	5690	-	-	-	
G(E)	56	6330	6010	-	-	
G(E)	57	-	-	-	-	
G(N)	58	7080	-	-	-	
G(N)	59	6160	6620	6513	-	
G(N)	60	-	-	-	705	
G(S)	52	6680	-	-	-	
G(S)	53	5970	6320	6316	-	
G(S)	54	-	-	-	625	
H(SE)	45	6580	-	-	-	
H(SE)	13	5330	5950	6296	-	
H(SE)	46	-	-	-	710	
H(NW)	40	6860	-	-	-	
H(NW)	41	6180	6520	6263	-	
H(NW)	42	-	-	-	-	
H(SW)	43	6620	-	-	-	
H(SW)	12	6010	6310	6260	-	
H(SW)	44	-	-	-	730	

TABLE 3-2 (Cont'd)

Pour	Core	Compression			Split Tension	Remarks
		Compression Strength	Test Average	Moving Average of Three		
H(NE)	47	5440	-	-	-	
H(NE)	48	7090	6260	6363	-	
H(NE)	11	-	-	-	-	
J(5)	34	6990	-	-	-	
J(5)	35	6620	6800	6456	-	
J(5)	36	-	-	-	-	
J(6)	37	5220	-	-	-	
J(6)	38	6440	5830	6297	-	
J(6)	39	-	-	-	720	
K(7)	31	6920	-	-	-	
K(7)	32	6480	6700	6443	-	
K(7)	33	-	-	-	780	
K(7)	10	6510	-	-	-	Specimen test dry - not included.
K(8)	28	5940	-	-	-	
K(8)	29	6090	6010	6180	-	
K(8)	30	-	-	-	-	
L(9)	9	6250	-	-	-	Specimen tested dry - not included.
L(9)	25	4040	-	-	-	Flaw in specimen - not included.
L(9)	26	6560	-	-	-	
L(9)	61	5900	6230	6313	-	
L(9)	27	-	-	-	625	

TABLE 3-2 (Cont'd)

Pour	Core	Compression			Split Tension	Remarks
		Compression Strength	Test Average	Moving Average of Three		
M(10)	22	5890	-	-	-	
M(10)	23	6610	6250	6163	-	
M(10)	24	-	-	-	-	
N(11)	11	-	-	-	-	
N(11)	19	5370	-	-	-	
N(11)	20	6650	6010	6163	-	
N(11)	21	-	-	-	675	
P(12)	16	6360	-	-	-	
P(12)	17	6090	6220	6160	-	
P(12)	18	-	-	-	-	
Q(13)	8	6500	-	-	-	
Q(13)	14	5760	6130	6120	-	
Q(13)	15	-	-	-	800	

Notes

1. Number of compression test specimens = 34
2. Lowest average of three compression tests = 6130 psi
3. Lowest set of compression specimens + 500 psi = 5830 + 500 = 6330
4. Average compression stress = 6301 psi
5. Number of tension test specimens = 9
6. Average strength of tension test specimens = 708 psi

TABLE 3-3

CORE LOCATIONS AND MAIN DELAMINATION DETAILS

<u>Core #</u>	<u>Azimuth</u>	<u>Radius</u>	<u>Gap Dimension</u>	<u>Cap Thickness</u>	<u>Remarks</u>
1	92°16'30"	31'-10-1/4"	1-1/2"	11-1/2"	1-3/4" core
2	264°22'00"	32'-2-3/4"	1-5/8"	12-7/8"	
3	97°37'00"	3'-10-1/2"	1-3/4"	15'-4"	
4B	270°12'15"	50'-0"	1/8"	4-1/8"	
5	151°36'00"	30'-10"	2"	13-1/2"	
6	26°16'00"	32'-2"	1-1/2"	10-1/8"	
7	333°11'30"	31'-10-3/8"	1-3/4"	13"	
8A	6°06'00"	3'-9-3/4"	1-7/8"	14-7/8"	
8B	358°20'00"	3'-7-3/4"	2"	14-1/2"	
9	3°58'45"	31'-3"	1-5/8"	14-1/8"	
10	3°32'00"	36'-5-3/4"	1-1/2"	12-7/8"	
11	359°54'45"	50'-4-1/2"	1/8"	5-3/8"	
12B	119°38'30"	48'-11"	1/8"	4-5/8"	
13	238°26'15"	48'-6-1/4"	3/8"	4-1/8"	
14C	226°18'45"	3'-11-3/4"	1-5/8"	15"	
15	282°48'00"	8'-5-1/2"	2"	14-1/8"	
16B	42°56'15"	15'-2-1/2"	1-7/8"	13-1/4"	
17	186°08'00"	14'-3"	2-1/8"	13"	
18	323°26'45"	14'-4-3/4"	2"	14-3/4"	
19	355°51'00"	19'-3-1/2"	2"	13-5/8"	
20	115°57'30"	19'-4-7/8"	1-5/8"	13-3/4"	
21	246°22'45"	19'-3"	2"	12-1/8"	
22	42°54'00"	25'-5-1/2"	1-3/4"	13"	
23	180°42'00"	26'-10-1/2"	1-3/4"	14-1/8"	
24	326°56'15"	26'-0"	2-1/8"	12-3/4"	
25	116°21'45"	30'-9-3/8"	2-1/8"	9-1/8"	
26	230°15'45"	32'-1-1/2"	1-3/4"	11-3/8"	
27	329°21'00"	32'-9-1/2"	1-7/8"	13-3/8"	
28	349°02'45"	36'-6-3/8"	1-3/8"	13-3/4"	
29	37°58'15"	39'-4-3/4"	1-3/4"	10-3/8"	
30	102°29'00"	38'-7"	1-3/8"	8-3/4"	

TABLE 3-3 (Cont'd)

<u>Core #</u>	<u>Azimuth</u>	<u>Radius</u>	<u>Gap Dimension</u>	<u>Cap Thickness</u>	<u>Remarks</u>
31	157°20'00"	39'-6"	1"	13-5/8"	
32A	223°02'75"	38'-8-3/4"	1"	13-3/4"	
33	306°19'45"	36'-6-7/8"	1"	13-1/4"	
34D	34°52'30"	43'-10"	-	-	ND
35	131°04'45"	43'-4"	1"	10-7/8"	
36B	210°57'00"	45'-1-1/2"	1/4"	7-3/4"	
37	249°24'30"	44'-11-1/2"	1/2"	6-1/8"	
38	318°04'00"	43'-3-1/2"	5/8"	12-1/2"	
39	7°46'00"	43'-9-1/4"	3/8"	12-5/8"	
40B	7°18'45"	49'-7-1/4"	-	-	ND
41B	23°04'30"	49'-9-1/2"	-	-	ND
42	78°55'30"	49'-5"	1/2"	2-1/2"	
42A	76°04'45"	49'-5-1/4"	1/2"	4-1/8"	1-3/4" dia. core
42B	78°56'00"	46'-1-1/2"	1/8"	6-1/8"	1-3/4" dia. core
42C	79°00'00"	50'-3-1/2"	1/4"	2-1/8"	1-3/4" dia. core
42D	81°55'30"	49'-2-3/4"	1/2"	3-7/8"	1-3/4" dia. core
43	97°28'15"	49'-5"	1/8"	1-3/4"	
44	170°53'15"	48'-9-1/4"	1/8"	4-1/2"	
45	191°10'15"	49'-8-1/2"	-	-	ND
46	259°54'00"	47'-9-1/4"	-	-	ND
47B	280°24'30"	48'-7-1/2"	-	-	ND
48C	311°54'00"	51'-9-1/8"	-	-	ND
49	37°10'00"	55'-8-1/2"	-	-	ND
50	90°58'00"	55'-10"	-	-	ND
51	122°46'30"	53'-1-3/4"	-	-	ND
52A	146°10'00"	52'-11"	-	-	ND
53	183°15'00"	54'-11-1/2"	-	-	ND
54D	218°56'45"	55'-4-1/4"	-	-	ND
55	237°23'45"	52'-10-1/2"	-	-	ND
56	268°29'15"	55'-8-7/8"	-	-	ND
57	307°08'00"	55'-8"	-	-	ND
58	335°31'00"	56'-0-1/2"	-	-	ND
59D	351°06'45"	55'-1-1/2"	-	-	ND
60	24°51'45"	57'-1-1/4"	-	-	ND
61(VII)	83°49'00"	32'-0-1/8"	1-1/2"	10-7/8"	

TABLE 3-3 (Cont'd)

<u>Core #</u>	<u>Azimuth</u>	<u>Radius</u>	<u>Gap Dimension</u>	<u>Cap Thickness</u>	<u>Remarks</u>
I	73°49'45"	12'-3"	2"	13"	Construction joint examination
IIIA	226°06'45"	24'-0"	~1-1/2"	10-1/2"	Construction joint examination
IIIB	63°39'00"	23'-11-1/2"	1-1/2"	13"	Construction joint examination
IV	254°15'45"	30'-0"	2"	12-3/4"	Construction joint examination
VB	16°18'30"	35'-11-3/8"	1-1/4"	13-1/2"	Construction joint examination
VI	4°18'45"	41'-6-1/2"	1"	12-1/2"	Construction joint examination
VIII	156°25'45"	13'-0-5/8"	-	-	ND - Tensile test core
IX	336°46'30"	15'-0-5/8"	-	-	ND - Tensile test core
XII	63°38'00"	19'-1-5/8"	2"	13-5/8"	Tensile test core
XV	16°06'00"	32'-11-1/2"	1-5/8"	10-3/4"	Tensile test core
XVI	10°23'00"	20'-11-1/8"	2"	12-7/8"	Tensile test core
XVIII	113°21'15"	27'-8-3/4"	1-1/8"	13"	Tensile test core
-	0°00'00"	20'-0"	2-1/8"	11-1/2"	1-3/4" tendon survey core
-	90°00'00"	20'-0"	1-3/8"	13-5/8"	1-3/4" tendon survey core
-	180°00'00"	20'-0"	2-3/8"	11-3/4"	1-3/4" tendon survey core
-	270°00'00"	20'-0"	2"	11-1/8"	1-3/4" tendon survey core
-	0°00'00"	40'-0"	1"	10-1/4"	1-3/4" tendon survey core
-	90°00'00"	40'-0"	2"	8-3/8"	1-3/4" tendon survey core
-	180°00'00"	40'-0"	1-1/2"	11-1/4"	1-3/4" tendon survey core
-	270°00'00"	40'-0"	1-1/4"	10-1/8"	1-3/4" tendon survey core
-	90°00'00"	50'-0"	5/8"	2-7/8"	1-3/4" tendon survey core
-	180°00'00"	50'-0"	1/16"	4-7/8"	1-3/4" tendon survey core

Notes: a. Gap dimensions and cap thickness are radial measurements.

b. ND denotes no delamination.

TABLE 3-3A

## REACTOR BUILDING DOME

## SECONDARY CRACK LOCATIONS\*

D 1	33 3/4" deep, 19 1/2" x hairline, 13" x 1"
D 2	32 1/2" deep, 21 3/8" x hairline, 14 1/2" x 1 1/2"
D 3	32 1/4" deep, 26 3/8" x 1/16", 23" x hairline, 19 1/2" x 1/4" **, 12 3/4" x 2 1/8"
D 4	31" deep, 24 1/4" x hairline, 12 1/16" x hairline, 12" x hairline, 9 3/16" x 3/8", 6" x 11/16"
D 5	19 5/8" deep, hole not deep enough
D 6	32 1/8" deep, 25 3/4" x 1/32", 17 15/16" x 1/32", 17 13/16" x 1/32", 13 5/8" x 5/16", 10" x 1 1/8", 6 7/16" x 3/16"
D 7	32 1/2" deep, 19 1/2" hairline on North half, 13 5/8" x hairline, 12 1/4" x 5/8"
D 8	32 1/4" deep, 27 1/4" x 1/32", 15 13/16" x 5/16" **, 12 7/16" x 1 11/16", 10 3/4" x 1/8", 9 1/4" x 3/8" **, 8 1/2" x 1/2" **, 8 1/16" x 3/16" **
D 9	32 1/4" deep, 28 3/4" x 1/32", 19 1/2" x 1/8", 16 5/8" x 3/8", 13" x 2" with suspended slice of concrete, 9 5/8" x 3/16" **
D 10	33 3/8" deep, 25" x hairline, 22 1/2" x 1/32", 14 3/4" x 2 1/4"
D 11	31 1/2" deep, 25 1/2" hairline, 21 5/8" x 1/16", 12" x 2"
D 12	34 3/4" deep, 25 7/8" x hairline, 22 3/4" x 1/16", 13 5/8" x 2 1/8"
D 13	37 1/2" deep, 19" x 1/16", 17 1/2" x 1/16", 14" x 2"
D 14	34 1/2" deep, 23 5/16" x hairline, 13 7/16" x 1 7/8"
D 15	33" deep, 25" x 1/16", 20" x hairline, 17 1/16" x 7/16", 13 3/4" x 2
D 16	32 3/4" deep, 26 1/4" x hairline, 16" x ** in 1/8" crack, 9 11/16" x 13/16"
D 17	38 1/2" deep, 33 3/8" x hairline, 28 1/2" x hairline, 19 1/4" x 1/16" **, 19 3/8" x 1/16" **, 15" x 2"

\* For plan location see Figure 3-10D.

\*\*Multiple delamination indicated.

TABLE 3-3A (CONT'D)

D 18	34" deep, 27 3/8" x hairline, 18 1/4" x 1/8" **, 13 5/8" x 2"
D 19	34 1/4" deep, 29 1/8" x hairline, 16" x hairline, 13 1/4" x 2"
D 20	34 1/4" deep, 23 1/4" x 1/32", 17 5/8" x 1/16", 11 11/16" x 1 3/4"
D 21	34" deep, 26 7/16" x hairline, 23 3/8" x 1/32", 20 3/8" x 1/8", 14 1/8" x 2"
D 22	35 3/8" deep, 25 9/16" x hairline, 19 1/4" x hairline, 12 3/16" x 1 9/16"
D 23	32 1/4" deep, 16 11/16" x 3/32", 11 1/8" x 1", 10" x 3/8"
D 24	34 5/8" deep, 9 3/4" x 3/8", 9" x 1/32"

\*\*Multiple delamination indicated.

TABLE 3-3B

AVERAGE LIFT-OFF DATA

<u>Tendon No.</u>	<u>Date Tensioned</u>	<u>Ave. Liftoff</u>	<u>Remarks</u>	
D108	12/9/74	1525	↑ Tendon was not detensioned ↓	
D114	12/11/74	1450		
D120	12/5/74	1448		
D121	11/19/74	1342		
D122	12/2/74	1498		
D127	12/5/74	1465		
D128	11/5/74	1355		
D129	11/19/74	1465		
D134	12/3/74	1515		
D137	12/10/74	1418		
D201*	11/14/74 (12/9/74)	1535		
D208	12/4/74	1500		
D214	12/6/74	1435		
D221	12/12/74	1490		
D228	12/2/74	1368		
D234	12/5/74	1535		
D308	12/6/74	1475		
D314	11/27/74	1453		
D321	11/20/74	1545		
D328	12/5/74	1523		
D334	12/4/74	1333		
<hr/>				
D101	11/26/74	1553		↓ Tendon detensioned ↑
D109	11/21/74	1485		
D117	11/21/74	1510		
D125	11/19/74	1373		
D133	11/18/74	1553		
D141	11/15/74	1577		
D201	11/14/74 (12/9/74)	1485		
D209	12/5/74	1523		
D217	11/19/74	1520		
D225	11/20/74	1420		
D233	11/22/74	1618		
D241	11/25/74 (4/2/75)	1488		
D301	11/25/74	1583		
D309	11/22/74	1577		
D317	11/21/74	1546		
D325	11/19/74	1593		
D333	11/18/74	1600		
D341	11/15/74	1474		
Average		1491		

Predicted Design Value =  $141K/IN^2 \times 9.72 IN^2/TENDON = 1370K$

\*Denotes tendon subsequently detensioned.

Dates in parentheses are for final retensioning, see Table 3-7

TABLE 3-4

DOME EPOXY AND CONCRETE STRENGTH TESTS

<u>Pour</u>		<u>Epoxy</u>		<u>28 Day Concrete</u>			<u>90 Day Concrete</u>		
<u>Date</u>	<u>No.</u>	<u>PSI</u>	<u>Avg. to Date</u>	<u>PSI</u>	<u>Avg/ Set</u>	<u>Moving Average of Three</u>	<u>PSI</u>	<u>Avg/ Set</u>	<u>Moving Average of Three</u>
2/18/74	976-RB (G-1a)	6340	7831	6560 6190 6470 6030	6312		7060 6580 6830 5820	6622	
2/20/74	978-RB (G-1b)	5240	7776	6330 6690	6510		6370 7029	6695	
2/25/74	780-RB (G-2a)	6320	7746	4600 5910	5255	6026	7420 6930	7175	6830
2/25/74	981-RB (G-2b)	D.O.	D.O.	5560 6010	5785	5850	6720 4860	5790	6553
3/1/74	783-RB (H-3a)	8590	7763	5280 5680 4820 4630	5102	5381	5980 6380 5860 5380	5762	6242
3/4/74	985-RB (H-3b)	9190	7791	5540 5910	5725	5537	6770 5790	6780	6110
3/6/74	987-RB (H-4a)	8680	7809	6050 4850	5450	5426	6280 6160	6220	6254
3/7/74	988-RB (H-4b)	8425	7821	5800 5320	5560	5578	6070 6000	6035	6345
3/12/74	992-RB (J-5)	8000	7824	6540 5870 5430 6470	6078	5696	6380 6580 6790 6580	6580	6278

TABLE 3-4 (Cont'd)

Pour		Epoxy		28 Day Concrete			90 Day Concrete		
Date	No.	PSI	Avg. to Date	PSI	Avg/ Set	Moving Average of Three	PSI	Avg/ Set	Moving Average of Three
3/13/74	994-RB* (H-2a)	(10,175)	-	5310 4790 4880 4780	4940	5526	6000 5610 6190 6400	6050	6221
3/14/74	995-RB (J-6)	9840	7862	5570 5840 6470 5590	5868	5629	7590 6190 6490 7070	6835	6488
3/18/74	996-RB (R-2b)	(9170)	-	4980 5040 5180 4970	5028	5279	5960 6150 5360 6240	5928	6271
3/20/74	997-RB (K-7)	8530	7874	4420 5110 5360 4780	4918	5271	6420 6930 6240 6130	6430	6397
3/22/74	998-RB (R-1a)	(5220)	-	5090 4560 6360 4900	4978	4984	6700 6460 6240 5890	6322	6226
3/22/74	999-RB (R-1b)	D.O.	-	4950 4810 - -	4880	4925	5390 5870 - -	5630	6127

\* Pour location can not be identified.

3-20

TABLE 3-4 (Cont'd)

Pour		Epoxy		28 Day Concrete			90 Day Concrete		
Date	No.	PSI	Avg. to Date	PSI	Avg/ Set	Moving Average of Three	PSI	Avg/ Set	Moving Average of Three
3/26/74	1000-RB (K-8)	7370	7865	5410 4690 5620 5500	5305	5054	6440 6370 5840 6700	6338	6096
4/4/74	1004-RB (L-9)	5560	7825	4860 4920 4580 4560 4320 4240	4571	4919	4920 6620 5960 - 5780 -	5820	5929
7/8/74	1009-RB (M-10)	7200	7814	7040 6980 6400 6050 6600 6420	6583	5486	6720 7420 7360 7420 6920 7070	7185	6447
7/12/74	1010-RB (N-11)	5530	7775	6560 6760 6540 6610	6618	5924	7070 7410 7270 6950	7175	6726
7/17/74	1012-RB (P-12)	7170	7765	6560 6670 6230 5910	6342	6514	6930 7040 6690 6420	6770	7043
7/22/74	1014-RB (Q-13)	7475	7760	6560 6440 6790 6970	6670	6543			

TABLE 3-5

DOMES POUR LOG

<u>Pour No.</u>	<u>Date</u>	<u>Location</u>
G1	2-18-74	45° - 135°
G1	2-20-74	225° - 315°
G2	2-25-74	135° - 225°
G2	2-25-74	315° - 45°
H3	3-1-74	180° - 270°
H3	3-4-74	0° - 90°
H4	3-6-74	90° - 180°
H4	3-7-74	270° - 360°
J5	3-12-74	45° - 225°
J6	3-14-74	225° - 45°
K7	3-20-74	135° - 315°
K8	3-26-74	315° - 135°
L9	4-4-74	0° - 360°
M10	7-8-74	0° - 360°
N11	7-12-74	0° - 360°
P12	7-17-74	0° - 360°
Q13	7-22-74	0° - 360°

TABLE 3-6  
PRESTRESSING SEQUENCES

<u>Sequence No.</u>	<u>Tendons</u>			<u>Sequence No.</u>	<u>Tendons</u>		
1.	D131	D211	D331	22.	D102	D240	D302
2.	D127	D215	D327	23.	D106	D236	D306
3.	D123	D219	D323	24.	D110	D232	D310
4.	D119	D223	D319	25.	D114	D228	D314
5.	D115	D227	D315	26.	D118	D224	D318
6.	D111	D231	D311	27.	D122	D220	D322
7.	D107	D235	D307	28.	D126	D216	D326
8.	D103	D239	D303	29.	D130	D212	D330
9.	D135	D207	D335	30.	D134	D208	D334
10.	D139	D203	D339	31.	D138	D204	D338
11.	D141	D201	D341	32.	D140	D202	D340
12.	D137	D205	D337	33.	D136	D206	D336
13.	D133	D209	D333	34.	D132	D210	D332
14.	D129	D213	D329	35.	D128	D214	D328
15.	D125	D217	D325	36.	D124	D218	D324
16.	D121	D221	D321	37.	D120	D222	D320
17.	D117	D225	D317	38.	D116	D226	D316
18.	D113	D229	D313	39.	D112	D230	D312
19.	D109	D233	D309	40.	D108	D234	D308
20.	D105	D237	D305	41.	D104	D238	D304
21.	D101	D241	D301				

TABLE 3-6  
PRESTRESSING SEQUENCES

<u>Sequence No.</u>	<u>Tendons</u>			<u>Sequence No.</u>	<u>Tendons</u>		
1.	D131	D411	D331	22.	D102	D240	D302
2.	D127	D215	D327	23.	D106	D236	D306
3.	D123	D219	D323	24.	D110	D232	D310
4.	D119	D223	D319	25.	D114	D228	D314
5.	D115	D227	D315	26.	D118	D224	D318
6.	D111	D231	D311	27.	D122	D220	D322
7.	D107	D235	D307	28.	D126	D216	D326
8.	D103	D239	D303	29.	D130	D212	D330
9.	D135	D207	D335	30.	D134	D208	D334
10.	D139	D203	D339	31.	D138	D204	D338
11.	D141	D201	D341	32.	D140	D202	D340
12.	D137	D205	D337	33.	D136	D206	D336
13.	D133	D209	D333	34.	D132	D210	D332
14.	D129	D213	D329	35.	D128	D214	D328
15.	D125	D217	D325	36.	D124	D218	D324
16.	D121	D221	D321	37.	D120	D222	D320
17.	D117	D225	D317	38.	D116	D226	D316
18.	D113	D229	D313	39.	D112	D230	D312
19.	D109	D233	D309	40.	D108	D234	D308
20.	D105	D237	D305	41.	D104	D238	D304
21.	D101	D241	D301				

TABLE 3-7

ACTUAL TENDON STRESSING LOG

<u>Date</u>	<u>Tendons</u>
10-25-74	D331
10-30-74	D211
10-31-74	D130
11-4-74	D215
11-5-74	D128
11-7-74	D327, D219
11-8-74	D323, D123, D319
11-11-74	D223, D115, D227, D315, D111, D311, D119
11-12-74	D231, D107, D235, D307, D239*
11-13-74	D103*, D102*
11-14-74	D207, D303, D135, D201*, D335
11-15-74	D139, D339*, D341, D203, D141
11-18-74	D204, D338, D137*, D133, D210, D333, D213
11-19-74	D329, D129, D125, D325, D217, D121
11-20-74	D221*, D225, D321
11-21-74	D117, D317, D113, D313, D229, D109
11-22-74	D233, D309, D105
11-25-74	D238, D241*, D305, D301
11-26-74	D302, D104, D101, D240, D236, D232
11-27-74	D306, D310, D314, D106, D110, D114*
12-2-74	D118, D122, D318, D228, D322, D326
12-3-74	D224, D330, D216, D220, D132, D212, D126, D134
12-4-74	D138, D208, D334, D336, D337, D340, D140, D205, D222, D226
12-5-74	D230, D332, D234, D328, D237, D136, D131, D127, D209, D124, D120, D116
12-6-74	D206, D320, D324, D316, D312, D308, D304, D202, D214, D218
12-9-74	D112, D108, D201, D103
12-10-74	D137
12-11-74	D114, D102
12-12-74	D221
3-31-75	D339
4-2-75	D239, D241

\*Denotes tendons which were detensioned and retensioned at a later date to satisfy Nonconformance Reports.

TABLE 3-8

TENDON STRESSING/CUMULATIVE DAILY TOTALS

<u>Date</u>	<u>Layer 1</u>	<u>Layer 2</u>	<u>Layer 3</u>
10-28-74	0/1	0/0	1/1
10-30-74	0/0	1/1	0/1
10-31-74	1/1	0/1	0/1
11-1-74	1/2	0/1	0/1
11-4-74	0/2	1/2	0/1
11-7-74	0/2	1/3	1/2
11-8-74	2/4	0/3	2/4
11-11-74	2/6	2/5	2/6
11-12-74	1/7	3/8	1/7
11-13-74	2/9	0/8	0/7
11-14-74	1/10	2/10	2/9
11-15-74	2/12	1/11	2/11
11-18-74	2/14	3/14	2/13
11-19-74	3/17	1/15	2/15
11-20-74	0/17	2/17	1/16
11-21-74	3/20	1/18	2/18
11-22-74	1/21	1/19	1/19
11-25-74	0/21	2/21	2/21
11-26-74	2/23	3/24	1/22
11-27-74	3/26	0/24	3/25
12-2-74	2/28	1/25	3/28
12-3-74	3/31	4/29	1/29
12-4-74	2/33	4/33	4/33
12-5-74	6/39	4/37	2/35
12-6-74	0/39	4/41	6/41
12-9-74	2/41	0/41	0/41

## 4.0 DELAMINATED STRUCTURE

### 4.1 INTRODUCTION

The delaminated dome condition was evaluated for the various critical design bases assuming an effective 24" thickness except in the proximity of the ring girder where field investigations revealed an approximate thickness of 36". The resulting analytical model consisted of a shell of symmetric configuration, theoretical radii and the aforementioned effective concrete thicknesses (i.e. deep cracks were not represented). The dome model's geometry considered in the analyses is shown in Figure 4-1.

### 4.2 APPLICABLE CODES AND STANDARDS

For the evaluation of the delaminated dome the following documents were considered:

1. Crystal River Unit 3 FSAR Docket No. 50-302.
2. ASME Boiler and Pressure Vessel Code, Section III, Division 2, 1975. (liner strains only)

### 4.3 CRITERIA

The applicable criteria are given in Table 2-2.

### 4.4 EVALUATION

The objective of the analyses of the delaminated structure was twofold:

1. to confirm hand calculations related to the safety of the structure,
2. to investigate the serviceability of the structure without major modification.

The load combinations investigated with the exception of the small break accident are given in Table 2-3. The evaluation which follows was based on an in-place strength of concrete of 6000 psi (refer to Section 3.3.1).

The results are presented for the delaminated structure using FSAR and ASME Code Section III Division 2 (liner only) acceptance criteria. These criteria as they apply to extreme fiber compression stresses, membrane stresses and liner strains are given for each load combination. The acceptability of the dome for shear was evaluated by the following procedures:

The minimum capacity of the concrete,  $\phi V_c$ , was compared with the ultimate shear,  $V_u$ , that exists on the section. If a case results where this minimum concrete capacity was less than the ultimate shear, then the actual section capacity was computed using the FSAR criteria.

The shear capacities described above represent ultimate capacities. For assessing the section adequacy in shear, the ultimate shear  $V_u$ , was calculated by applying a load factor of 1.5 to the net shears resulting from load combination a, b, and c in Table 2-3. A load factor of 1.0 was applied to the net shears for load combination d.

The shear provisions of section 2.3.2 were applied in the delaminated dome shear investigations.

The location of the stations in degrees noted on the shear figures is shown in Figure 4-1.

The consideration of radial tension in combination with radial shear is discussed in Appendix I.

The structural analysis of the containment was performed using KALNIN'S Static Computer Program described in Appendix D. The individual loads which comprise the load combinations were input separately, and their results were combined internally in the program where possible. This was not possible for the Structural Integrity Test and Accident Condition load combinations due to the different Young's Modulus ( $E$ ) values for the concrete under the sustained loads ( $D$ ,  $F$ , and  $T_0$ ) and the rapidly applied loads ( $P_a$  and  $T_a$ ). In these cases, stresses for each of the two types of loads were combined externally to the computer. The effects of shrinkage and creep were considered as discussed below.

a. Shrinkage

The effect of concrete shrinkage on the overall structural response (stress resultants) was insignificant due to the large volume to surface ratios of the cylindrical wall, ring girder, and dome.

In the prestress loss calculations a conservative value for long term shrinkage strain of 100 micro in/in was used to be consistent with the original design. This is the value recommended in Reference (12) for calculating prestress losses in  $f'_c = 5000$  psi concrete. Actually, use of the shrinkage equation appearing in this reference for time = 40 yr. and volume to surface ratio = 24" results in a shrinkage strain of 10 micro in/in at end of plant life.

b. Creep

The effect of concrete creep under the prestress loads was included in the prestress loss calculations and in the structural analysis. The creep curves appearing in Reference (12) allow specific creep strains to be determined considering both concrete age at loading and duration of load. Actual creep strains were calculated from these specific creep strains for use in determining prestress losses. Also, the reduction in concrete stresses, which results in an increase in liner stresses, caused by concrete creep under

sustained loads was taken into account in the structural analysis by using an effective Young's Modulus,  $E'_c$ . This modulus is expressed in terms of specific creep as

$$E'_c = \frac{E_c}{1 + sc E_c}$$

where:

$E_c$  = instantaneous concrete Young's Modulus =  $4 \times 10^6$  psi,

sc = specific creep (micro in/in/psi)

Analysis of the containment for load combinations a, b, and c (Table 2-2) was based on calculated prestress losses and a sustained load (D, F,  $T_a$ )  $E'_c = 2.7 \times 10^6$  psi corresponding to the present time. In load combination c (SIT), the results for  $1.15P_a$  were based on  $E_c = 4.0 \times 10^6$  psi.

For investigation of the containment under load combination d (LOCA), 40 year calculated values of prestress losses and  $E'_c = 1.8 \times 10^6$  psi were used. The  $1.5P_a$  and  $T_a$  parts were based on  $E_c = 4 \times 10^6$  psi.

c. Prestress Losses

The calculated prestress losses (ksi) and effective prestress (ksi) are given below:

	<u>Elastic Shortening</u>	<u>Creep</u>	<u>Steel Relaxation</u>	<u>Shrinkage</u>	<u>Total Losses</u>	<u>Effective Prestress</u>
<u>Present</u>						
Vertical	3.6	3.9	2.2	2.9	12.6	155.4
Hoop	6.4	7.0	2.2	2.9	18.5	146.2
Dome	10.4	11.3	2.2	2.9	26.8	141.2
<u>40 yr.</u>						
Vertical	3.6	9.1	3.4	2.9	19.0	149.0
Hoop	6.4	16.2	3.3	2.9	28.8	136.0
Dome	10.4	26.2	3.4	2.9	42.9	125.1

The membrane and extreme fiber stress results presented in this section were those obtained directly from the KALNIN'S Static Computer Program analyses (i.e. linear, elastic, uncracked). At locations in the dome where tensile stresses exceeded the allowable values given in Table 2-2, the concrete was assumed to be cracked. Cracked section investigations were performed to calculate concrete compressive and rebar tensile stresses. In the cracking investigation, the axial force (P) and moment (M) stress resultants applied on the section were computed from the uncracked stresses (plotted). The only exception to this was for the Normal Winter Operating Condition load combination. In this case, the cracked section reduced the effect of the through thickness gradient ( $\Delta T$ ) part of the  $T_0$  term in the load combination. Therefore, the uncracked stresses due to  $\Delta T$  were subtracted from the plotted stresses prior to computing P and M. Then, the effect of  $\Delta T$  applied to the section with P and M was considered in a manner similar to that described in ACI 505-54. Cracked section stresses, calculated as described above, are shown at selected locations in some of the figures for this section.

#### 4.4.1

##### Structure Prior to Operation

For this load combination, the allowable extreme fiber stress according to the FSAR is  $0.6 f'_c$  compression and zero tension. This results in an allowable stress of 3600 psi compression for 6000 psi concrete. For an uncracked section, the results in Figure 4-2 indicate that the stresses near the ring girder are tensile. Thus, a cracked section investigation was required. This resulted in a peak compressive stress of 3326 psi. Figure 4-3 shows a peak compressive hoop stress of 2413 psi. No hoop tensile stresses exist.

The allowable membrane compression stress using the FSAR is  $0.45 f'_c$ . This results in an allowable compressive stress of 2700 psi for 6000 psi concrete. Results shown in Figure 4-4 indicate a maximum membrane compression stress of 2470 psi. No membrane tension exists.

The ASME Code limits for liner strain for this load combination are a compression strain of 0.002 and tension strain of 0.001. Figure 4-5 shows a maximum compression strain of 0.0011 in the meridional direction and a maximum tensile strain of 0.000002 in the hoop direction.

The shear stress limits noted in the FSAR were used in this evaluation. Figure 4-6 shows that the available shear capacity is in excess of the required shear capacity. Thus the delaminated structure was considered serviceable for this load combination.

Figure 4-12 shows that the available shear capacity is in excess of the actual shears using the FSAR criteria.

#### 4.4.3 Structural Integrity Test

The allowable extreme fiber stresses according to the FSAR are  $0.6 f'_c$  compression and zero in tension. This results in an allowable stress of 3600 psi compression for 6000 psi concrete. The uncracked results shown in Figures 4-14 and 4-15 show a peak compressive stress of 1655 psi and a peak tensile stress of 186 psi. Based on a cracked section investigation, a concrete compressive stress of 1682 psi and compressive stress in the rebar exists at this location since the cracking does not extend far enough into the section to reach the inside face rebar.

For the condition of membrane stress the FSAR limit is  $0.45 f'_c$  compression and zero tension. This results in an allowable compressive stress of 2700 psi for 6000 psi concrete. Figure 4-16 shows the peak membrane compressive stress to be 902 psi, which is below allowable values. No membrane tension exists.

Liner strain limits given in the ASME Code are a compressive strain of 0.002 and a tensile strain of 0.001. Figure 4-17 shows a peak liner compressive strain of 0.00057. For this condition the analysis indicates no liner tensile strain.

Using FSAR criteria, Figure 4-18 shows the available shear capacity exceeds the required capacity.

#### 4.4.4 Accident Condition

The delaminated structure was investigated for a late plant life (40 years) loss of coolant accident condition. The 40 year prestress losses, accompanied by a sustained load reduced concrete modulus,  $E_c$ , were considered. The accident temperature effect on the liner up to 36 ksi yield produces a tensile force in the concrete and was included. The results for an uncracked analysis are shown in Figures 4-20 and 4-21.

The membrane stresses illustrated in Figure 4-20 are tensile over most of the dome. In accordance with the Design Criteria, Table 2-2, the concrete is assumed to have zero tensile capacity. Since the delaminated dome does not have sufficient reinforcement to resist these membrane tension forces, a cracked analysis of the dome was performed relying on the resistance of the unbonded tendon system.

For the accident condition, the tendon stress is limited by the ASME Code to  $0.9 f_{py}$ , which is equivalent to  $0.72 f_{pu}$ . The allowable liner strains from the ASME Code are 0.005 in compression and 0.003 in tension. This analysis did not consider the 5 inch schedule 40 pipe as reinforcement.

$1.15P_a$ , membrane tension occurs (25 psi) in the hoop direction, approximately half way up the dome as shown in Figure 4-22. For purposes of calculating conservative values of tendon stress and tensile liner strains, the balance of the accident pressure, i.e.,  $1.5P_a - 1.15P_a$ , was assumed to be resisted solely by the tendon network.

At  $1.15P_a$ , total tendon stresses (resulting from prestress increase added to effective prestress) and liner compressive strains up to liner yield were calculated. The liner strains at assumed cracking are shown in Figures 4-23 and 4-24 as solid lines. The maximum tendon stress at  $1.15P_a$  was calculated to be 137 ksi.

The tendon stresses and liner tensile strains were calculated for  $1.5P_a - 1.15P_a$ . The effect of accident temperature on the liner is to produce compressive strains, whose magnitude depends on the degree of restraint provided by the concrete. For purposes of calculating maximum tensile liner strains, the restraint of the cracked concrete was assumed to be zero and, hence, no compressive liner strains occur beyond the  $1.15P_a$  pressure stage. The liner strains beyond  $1.15P_a$  were, therefore, tensile and their values are shown in Figures 4-23 and 4-24 as solid-dot lines. The total liner strain results are shown in Figures 4-23 and 4-24 as dashed lines and the maximum tensile value is 0.000178.

The maximum tendon stress increase beyond  $1.15P_a$  was calculated as 27 ksi. When this was added to the stresses up to  $1.15P_a$ , a total tendon stress of 164 ksi resulted, which is less than  $0.72 \times 240 = 173$  ksi.

b. Maximum Predicted Compressive Liner Strains

The maximum compressive liner strain occurs when the pressure is at its minimum; therefore, the load condition corresponding to  $D + F + P_a + T_a$  was investigated. For this condition the concrete did not undergo any through thickness cracking as shown in Figure 4-25. Liner compressive strains up to  $275^{\circ}\text{F}$  (max  $T_a$ ) were calculated and added to those due  $D + F + P_a$ . The results are presented in Figure 4-26 with a maximum compressive strain of 0.002267, which is less than the 0.005 allowable per the ASME Code.

Using FSAR shear criteria, Figure 4-27 shows that the available shear capacity exceeds the required capacity.

#### 4.5 SUMMARY AND CONCLUSION

The results of this section indicate that the structural response of the delaminated structure to critical load combinations would, in general, be satisfactory. This is due, in part, to considering the actual in place concrete and steel strengths. The in place concrete strength as justified by test cylinder results is  $f'_c = 6000$  psi (see Section 3.3.1). The minimum yield strength of meridional and hoop reinforcement based on mill test results is  $f_y = 45,000$  psi.

However, two aspects of the analyses deserve further comment:

1. the evaluation of the compressive stresses on the inside face of the dome near the ring girder for the normal winter operation load combination (see Section 4.4.2).

and

2. the evaluation of dome strength during the LOCA load combination (see Section 4.4.4).

Considering item 1 above, the compression stress due to the normal winter operating condition has been presented in Figure 4.8 with a maximum stress of 3613 psi. The calculated value is acceptable within engineering accuracy when compared to a working stress allowable of 3600 psi. When the compression steel on the inside face of the dome near the ring girder is considered and the liner is neglected, the peak concrete compression stress is reduced to 3488 psi and the calculated compression steel stress is 25,733 psi (see Figure 4-8). The ASME Code allowable for compression steel for the normal winter operation load combination is  $0.67f_y$  or 30,000 psi.

Referring to the second item above concerning dome strength during the LOCA load combination, the analyses presented in Section 4.4.4 indicate the delaminated structure is theoretically acceptable if evaluated according to the current criteria of the ASME Code. However, reinforcing steel was included in the repaired dome to control and distribute cracking. This reinforcement enhances the strength of the repaired structure and is discussed in Section 5.0.

The analyses presented in this section support the conclusion that the delaminated structure would be serviceable subsequent to the repair activities described in Section 5.0.

This conclusion was further supported by the results of the investigation of the dome and included:

1. The measured response of the structure to a 14.6% detensioning was acceptable when compared with predicted response.
2. A series of cores drilled into the structure indicated the absence of crushed concrete. There was lower level cracking, but the concrete is sound parallel to the plane of the dome.
3. The dome prestress as measured by lift-off tests was greater than predicted, indicating that the delaminated structure was stiffer than assumed and the prestressing forces were not reduced by the delaminations.

## 5.0 CORRECTIVE ACTION

### 5.1 INTRODUCTION

Based on the analyses and investigations presented in the previous sections, it was concluded that the CR3 dome would be satisfactorily repaired subsequent to the actions described in this section.

The delaminated cap was safely removed; meridional, hoop, and radial reinforcement provided and a new cap placed. The integration of the new reinforcement with the lower prestressed structure was accomplished to control and distribute cracking associated with the LOCA load combination.

### 5.2 REPAIR METHOD

The repair sequence was as illustrated in Figure 5-25 as described by the following:

1. Instrumentation installed and monitored
2. 18 tendons detensioned
3. Holes drilled (Figures 5-1 and 5-2) into the lower concrete
4. Delaminated cap removed
5. Inspection of 24" structure
6. Lower level cracks grouted with epoxy
7. New reinforcement placed
8. New cap poured and cured
9. 18 tendons partially re-tensioned
10. Structural Integrity Test conducted
11. Dome surfacing

#### 5.2.1 Instrumentation

##### a. Instrumentation for Detensioning and Drilling Grout Holes

Instrument stations were established in the dome on two (2) orthogonal axes at distances of 15, 30 and 45 feet from the apex (See Figures 5-3 thru 5-10). The data recovered at these stations consisted of the following:

1. The hoop and meridional concrete strain changes near the upper and lower surfaces of the delaminated top portion of the dome using Ailtech Concrete Embedment Gages with a 4" gage length.

2. The hoop and meridional concrete strain changes near the upper surface of the lower portion of the dome using Ailtech Concrete Embedment Gages with a 4" gage length.
3. The hoop and meridional steel strain changes on the liner using SR4 three element electrical resistance strain gages attached to the inside surface of liner.
4. The change in width of gap between the top and lower levels of the dome using linear potentiometers (infinite resolution type).
5. The change in elevation of the top surface measured by survey techniques with  $\pm 0.012$  inches accuracy.
6. The vertical displacement of the liner, inside surface, measured at three (3) azimuths and at radial distances of 0, 29, 49 and 56 feet from the apex using extensometers.
7. The radial displacement of the liner measured at the 49 and 56 foot radii with the extensometers.
8. The movement of the top of the liner at the apex monitored by survey techniques using a stainless steel pin attached to the liner. This measurement was used to correlate the inside and outside vertical movements.
9. The air temperature at three (3) locations; outside the dome, in the gap and inside the dome.

In addition to these instruments which were added for the repair program, instrumentation previously installed for the SIT test was also monitored. The data recovered consisted of:

The reinforcing bar strain changes on the outside face of the dome at three (3) azimuths at approximately 50 feet from the apex. The gages are SR4 linear strain gages.

The reinforcing bar strain changes on the outside face of the containment cylinder wall at three (3) azimuths and at seven (7) elevations were also monitored with SR4 gages.

Instrumentation readings except for those recovered by survey techniques were recorded using a Vidar Model Autodata 8 data acquisition system. The data was printed out at least once every hour. The survey readings mentioned previously were taken at least twice a day.

b. Instrumentation for Other Operations and Repairs

During operations prior to SIT, the apex displacement was measured as well as the concrete and steel strains using existing gages.

c. Instrumentation for SIT

The Reactor Building's structural response to the SIT was monitored by utilizing the existing instrumentation described in the FSAR and supplementary instrumentation installed within the repaired dome (see Appendix J for communications with the NRC).

Instrumentation within the repaired dome consisted of stations established in the dome on two (2) orthogonal axes at distances of approximately 15, 30 and 45 feet from the apex (see Figures 5-3 and 5-11). The data recovered at these stations consisted of the following:

1. The hoop and meridional steel strain changes on the liner using SR4 three-element electrical resistance strain gages attached to the inside surface of the liner.
2. The hoop and meridional concrete strain changes near the upper surface of the lower portion of the dome using Ailtech Concrete Embedment Gages with a 4-inch gage length.
3. The hoop and meridional reinforcing bar strain changes of both layers of steel within the new concrete cap. These measurements were obtained from SR4 linear strain gages attached to #4, Grade 60 sister bars.
4. The reinforcing bar strain changes of the #6, Grade 60 radial reinforcement. The gages are SR4 linear strain gages.

Gross structural deformations were measured by extensometers attached to the steel liner plate at the locations identified on Figure 5-9. This instrumentation provided the following data:

The vertical displacement of the liner, inside surface, measured at three (3) azimuths and at radial distances of approximately 0, 29, 49 and 56 feet from the apex.

The radial displacement of the liner measured at approximately the 49 and 56 foot radii.

5.2.2

Dome Detensioning

A symmetrical group of 18 tendons (see Table 5-1) was detensioned and the effects on the structure were studied. The results of this load reduction is reported in Section 3.

### 5.2.3 Drilling Radial Holes

The presence of lower level cracks was established by initial drilling (see Section 3.1). While the delaminated cap was still in place and provided a smooth, regular work surface, approximately 1850 radial holes one (1) inch in diameter were drilled into the dome. These holes were located as shown in Figures 5-1 and 5-2. Figures 5-12 and 5-13 illustrate the location of the holes relative to the tendons. These holes served three purposes. They provided:

1. a means for inspecting for lower level cracking.
2. grouting and venting holes (see Section 5.2.6).
3. holes for placing radial reinforcement (see Section 5.2.7).

### 5.2.4 Delaminated Cap Removal

After the holes were drilled, the delaminated cap was removed to the extent defined in Figure 5-14. Removal work began at the apex in the following sequence, pours Q, P, N, M, L, K, and J, and continued toward the ring girder until concrete above the main delamination was removed and lower concrete exposed.

Reinforcing steel at the lower edge of the dome (Pours J and H) was cut at the location of the construction joint between pours J and K. After the loose concrete from pour J had been removed to sound concrete, the final surface concrete was terraced in steps as shown on Figure 5-15.

### 5.2.5 Inspection of the 24" Structure

In addition to the investigations described in Section 3.1.3, the upper surface of the 24" structure was visually inspected and boroscope inspection logs were made for the radial holes. The findings of the inspection were:

1. There was no evidence of crushed concrete or radial cracks.
2. The surface of the 24" structure between adjacent conduits runs generally from near the top of the conduit at lower elevation to near the mid-plane of the conduit at higher elevation. There were a number of localized delaminations forming small lenses (layers) of concrete usually adjacent to the high side of the conduits. Loose lenses of concrete were carefully removed.
3. Exposed straps attached to the conduits appeared to be in good condition. There was no evidence of any movement of the conduit relative to the surrounding concrete, including those conduits containing detensioned tendons, or of cracks, crushing, or high stresses at the tendon concrete interface.

The conclusion from these observations was that the 24" structure was in good condition and capable of performing in accordance with the design requirements. Appendix E contains photographs illustrating the condition of the structure during delaminated cap removal.

#### 5.2.6 Lower Level Crack Grouting

The presence of lower level cracks was established by core drilling (see Sections 3.1 and 5.2.3). The cracks were grouted with epoxy through the holes described in Section 5.2.3. Figure 5-16 illustrates the device (packer) used during grouting to isolate one level of cracks from other levels in a given hole. A packer was placed in each hole and epoxy grout applied under pressure until grout appeared in adjacent holes or when flow of grout ceased. See Supplement 2, Attachment 2 for additional information.

#### 5.2.7 New Reinforcement

To enhance the tensile capacity of the structure to resist the LOCA load combination and control cracking of the concrete in tension, non-prestressed meridional and hoop reinforcement was provided. This reinforcement is sufficient to resist, at  $0.9f_y$ , the membrane tensile forces shown in Figure 4-20. This reinforcement is as shown in Figures 5-17 through 5-19 and consists of deformed bars conforming to ASTM 615-68 Grade 60. Figures 5-20 and 5-21 compare the area of reinforcement provided versus that required. See Appendix H for cadweld requirements.

The principal radial reinforcement for the repaired structure is a #6 deformed bar and is illustrated in Figure 5-19. This reinforcement was installed in each radial hole with Masterflow 814 cement grout. Approximately 1850 #6 bars were provided.

The test program outlined in Supplement 1, pages S-11, S-12, S-13, was expanded to include testing of eleven (11) #6 radial reinforcement test specimens. Test specimens consisted of #6 Grade 60 deformed bar installed in 1"  $\phi$  hole, 15 inches deep, and grouted with Masterflow 814 cement grout. Specimens were tested in concrete blocks with an in-place compressive strength of 2400 to 5000 psi. Grout cubes tested at 4,265 to 7,215 psi compressive strength.

The first observed distress in the test specimens was the development of a shallow secondary failure cone of concrete as illustrated in Figure 5-26. This "secondary failure cone" condition occurred at an average load of 31.5 kips (3.3 kips above the guaranteed minimum yield strength of #6, Grade 60 bar). Failure occurred at an average load of 40.1 kips due to rupture of the #6 bar at welds for testing apparatus attachments.

The radial tension force for which the #6 bar was designed is a function of the level of membrane stress in the new concrete. Figure 5-22 indicates the level of radial stresses in the 24" structure, which are all compressive. Future tensile stresses are a function of the transfer of stresses between the new and old concretes due to creep and retensioning. Figure 5-23 indicates the final predicted distribution of radial stresses at the end of plant life. The #6 radial bar was designed to resist, at  $0.5f_y$ , the tensile force corresponding to the radial stress of 21.4 psi. The consideration of radial tension in combination with radial shear is discussed in Appendix I.

#### 5.2.8

##### New Cap

The concrete materials for the new cap satisfied the requirements of FSAR Section 5.2.2.1. Figure 5-24 indicates the pour sequence used and Figures 5-14 and 5-15 illustrate a typical section. The new material was "wet" cured for fourteen (14) days to minimize creep and shrinkage.

#### 5.2.9 Dome Retensioning

The 18 tendons which were detensioned (see Section 3.1.3) constituted 14.6 percent of the tendons in the dome. The average prestress force per tendon computed on the basis of the lift-off data of Table 3-3B was 1491 kips. The design value used in the calculations was 1370 kips. Therefore, the actual prestress forces in the delaminated structure were 9% higher than those used in the design. The force per tendon in the 18 tendons required to return the structure to the design condition was 646 kips per tendon.

The 18 tendons were retensioned to that load using the reverse of the detensioning sequence given in Table 5-1 after the new concrete had been "wet" cured for seven (7) days and had achieved a minimum compressive strength of 4000 psi.

#### 5.2.10 Structural Integrity Test (SIT)

The SIT provided evidence of the adequacy of the repaired structure. The forces on the structure during the SIT consisted of dead load, prestressing and 1.15 times design pressure ( $P_a$ ) along with changes in environmental conditions which occurred during testing. Measurements and observations recorded during the test were evaluated and compared with predictions of the expected structural behavior (see Supplement 2, Attachment 1). The repaired dome was well behaved and the SIT provides quantitative justification of the repair approach utilized.

#### 5.2.11 Dome Surfacing

A silicone urethane waterproofing membrane will be applied to the dome surface.

TABLE 5-1

DOME DETENSIONING SEQUENCE

<u>Sequence</u>	<u>Top</u>	<u>Middle</u>	<u>Bottom</u>
1.	D101	D241	D301
2.	D141	D201	D341
3.	D117	D225	D317
4.	D125	D217	D325
5.	D109	D233	D309
6.	D133	D209	D333

6.0

QUALITY ASSURANCE

The Quality Assurance Program as described in FSAR Section 1.7 was implemented during all activities for accomplishing the dome repair.

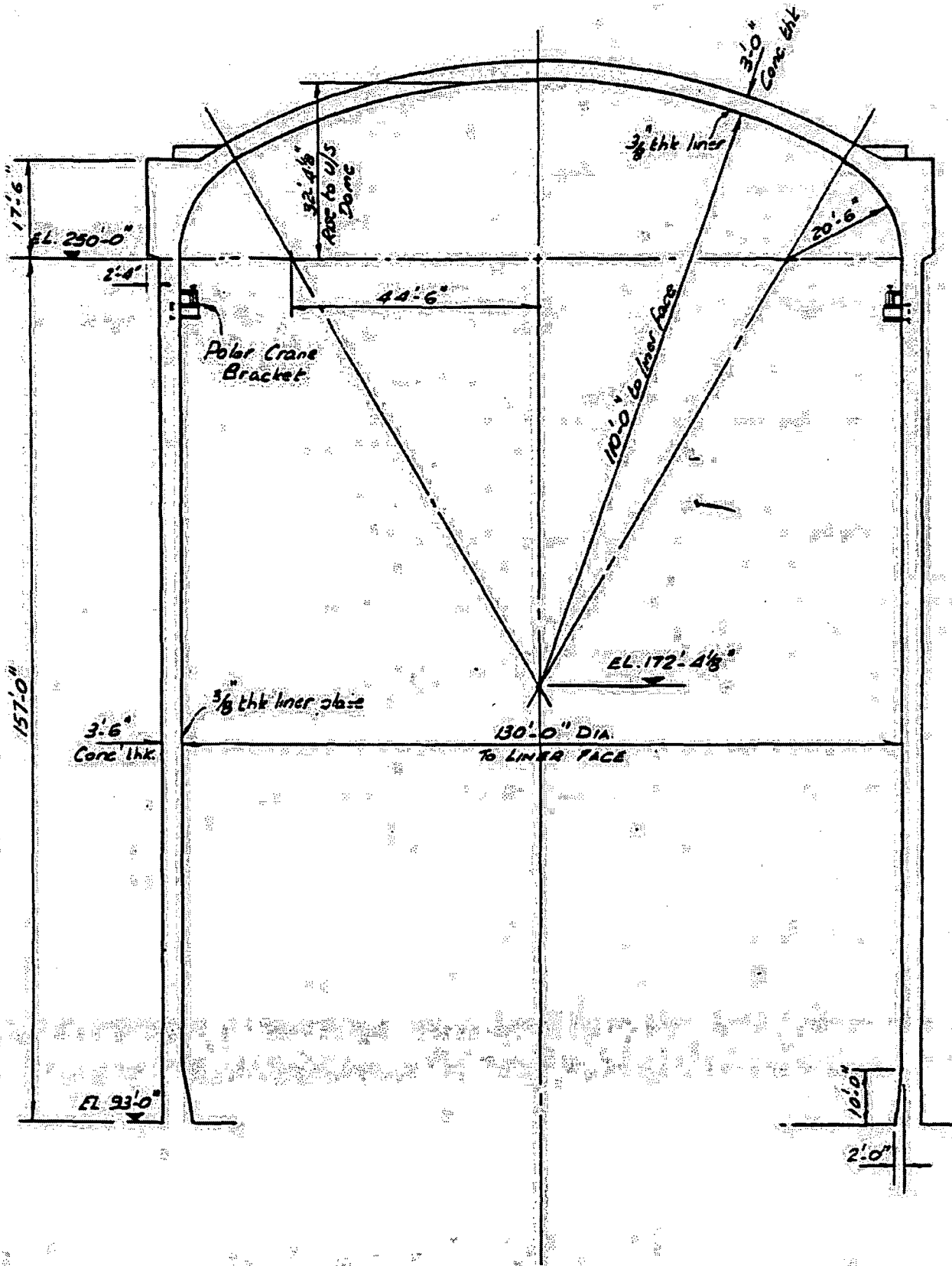
This Quality Program was in effect during the entire Crystal River #3 construction phase.

In accordance with that program, approved written procedures were in effect, and were enforced by appropriate quality control methods. Records of activities and audit of those activities will be maintained.

The Program was supplemented by additional technically qualified Engineering and Quality Program personnel, with stop-work authority, who were in attendance during all work on the dome.

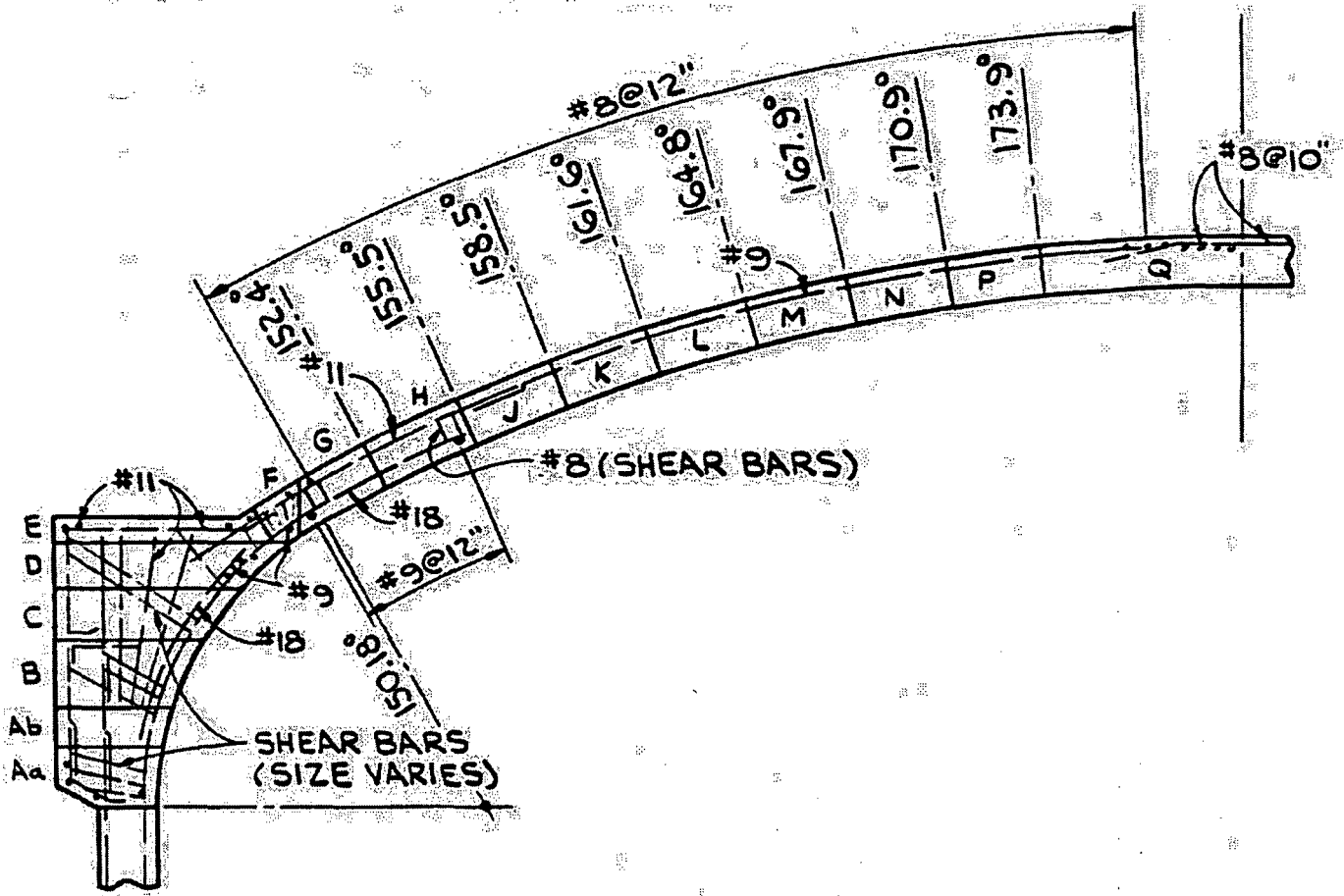
REFERENCES

1. Thomas T.C. Hsu, "Mathematical Analysis of Shrinkage Stresses in a Model of Hardened Concrete", ACI Journal March 1963, p. 371-390.
2. Hubert Woods, "Durability of Concrete Construction", American Concrete Institute Monograph No. 4, 1968.
3. American Society for Testing and Material, "Significance of Tests and Properties of Concrete and Concrete Making Materials," ASTM Special Technical Publication No. 169-A, 1966.
4. Israel Rosenthal and Joseph Glucklich, "Strength of Plain Concrete Under Biaxial Stress," ACI Journal, November 1970, p. 903-914.
5. G. N. Savin, "Stress Concentration Around Holes," Pergamon Press, New York, 1961.
6. R. E. Peterson, "Stress Concentration Factors," John Wiley & Sons, New York, 1974.
7. William Griffel, "Handbook of Formulas for Stress and Strain," Frederick Ungar Publishing Company, New York, 1966.
8. Helmut Kupfer, Hubert K. Hilsdorf and Hubert Rusch, "Behavior of Concrete Under Biaxial Stresses," ACI Journal, August 1969, p. 656-666.
9. Oral Buyukozturk, Arthur H. Nilson, and Floyd O. Slate, "Stress-Strain Response and Fracture of a Concrete Model in Biaxial Loading," ACI Journal, August 1971, p. 590-599.
10. Tony C. Y. Liu, Arthur H. Nilson, and Floyd O. Slate, "Stress-Strain Response and Fracture of Concrete in Uniaxial and Biaxial Compression," ACI Journal, May 1972, p. 291-295.
11. S. Timoshenko and J. N. Goodier, "Theory of Elasticity," Second Edition, McGraw Hill Book Company, New York, 1951, p. 58-66.
12. Three Mile Island Nuclear Station Unit 2, PSAR, Docket No. 50-320, Appendix 5J.
13. Adam M. Neville, "Hardened Concrete-Physical and Mechanical Aspects," (2. Nature of Strength of Concrete), ACI & University of Iowa, ACI Monograph #6, 1971.
14. Stress Concentration in Prestressed Concrete, Group H, Paper 47, From: Proceedings, Conference on Prestressed Concrete Pressure Vessels, Church House, Westminster, S.W.1. 13-17, March 1967, The Institution of Civil Engineers, London 1968.
15. Turkey Point Unit 3 Containment Dome, Delamination of the Dome Concrete During Post-Tensioning, Docket 50-250.



REACTOR BUILDING DIMENSIONS

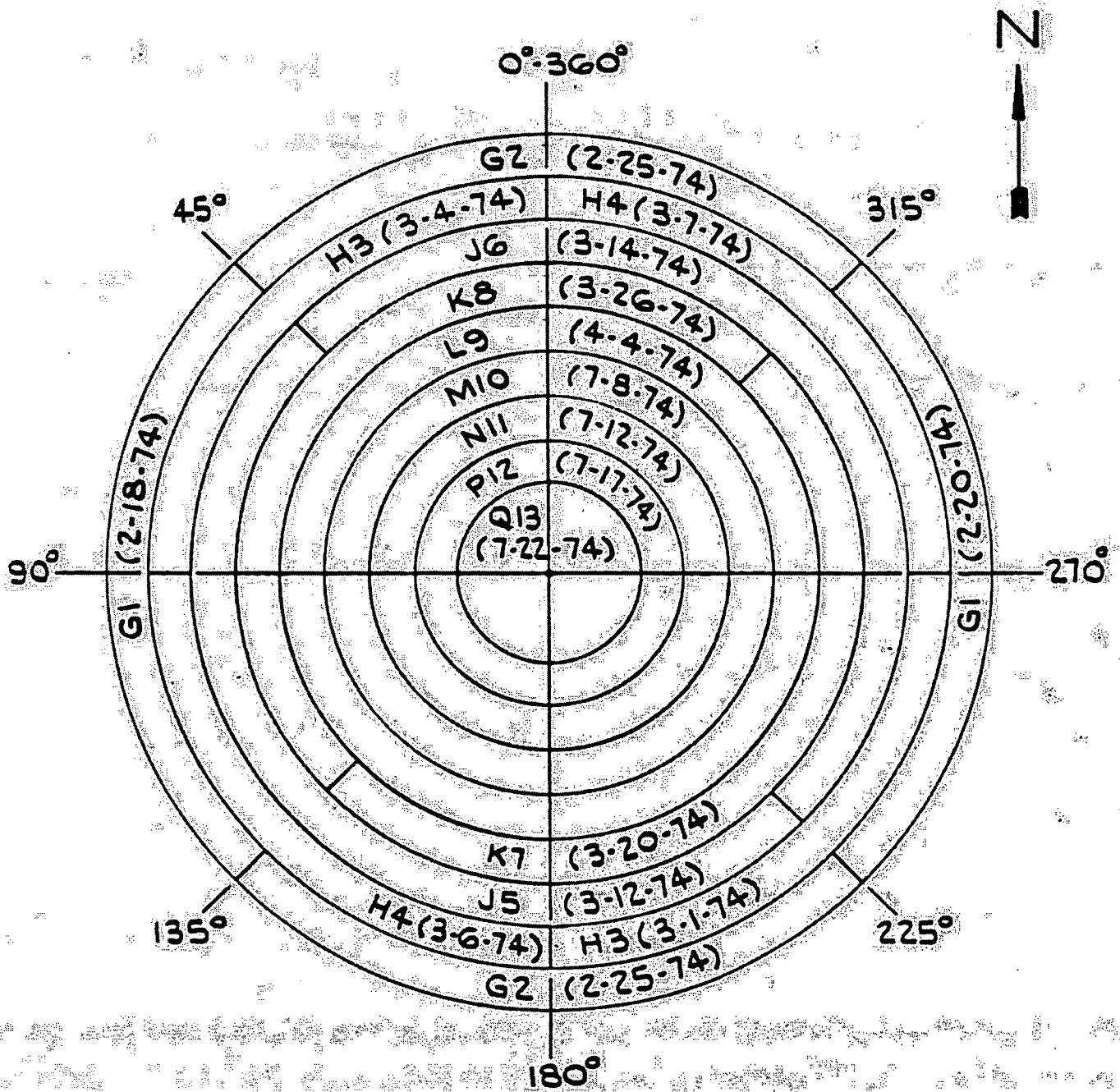
FIGURE 2-1



NON-PRESTRESSED REINFORCEMENT

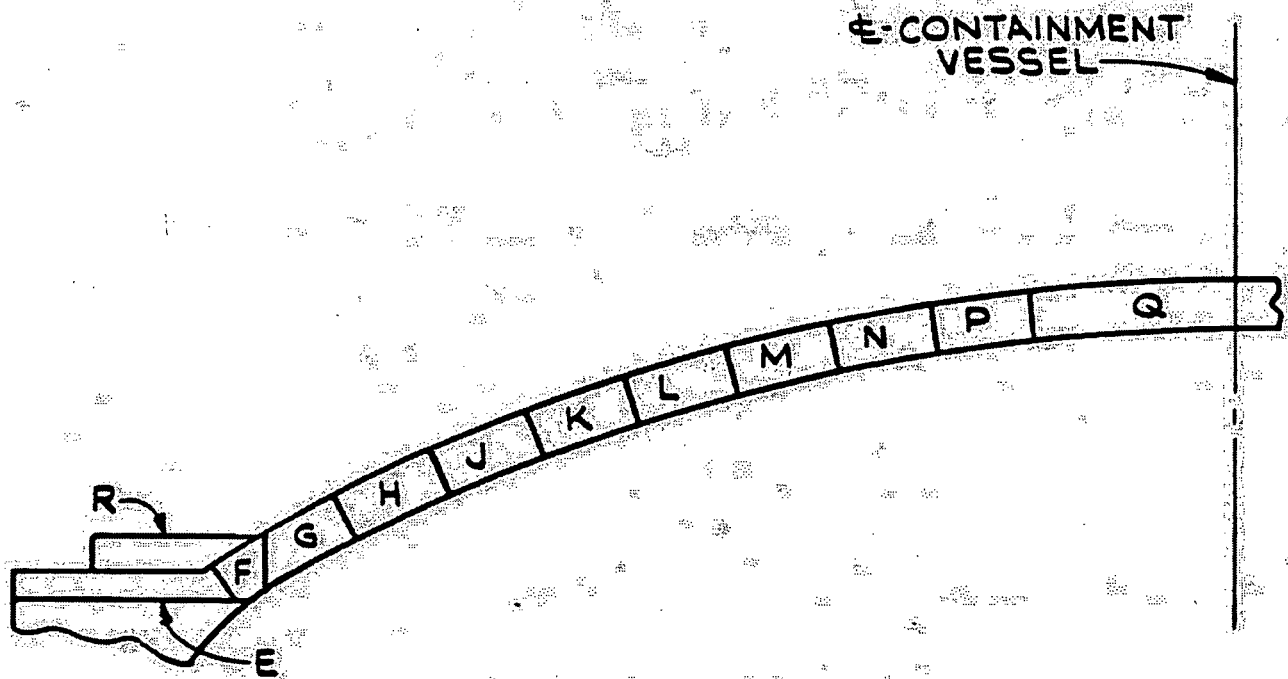
FIGURE 2-2

Revised: 8-10-76



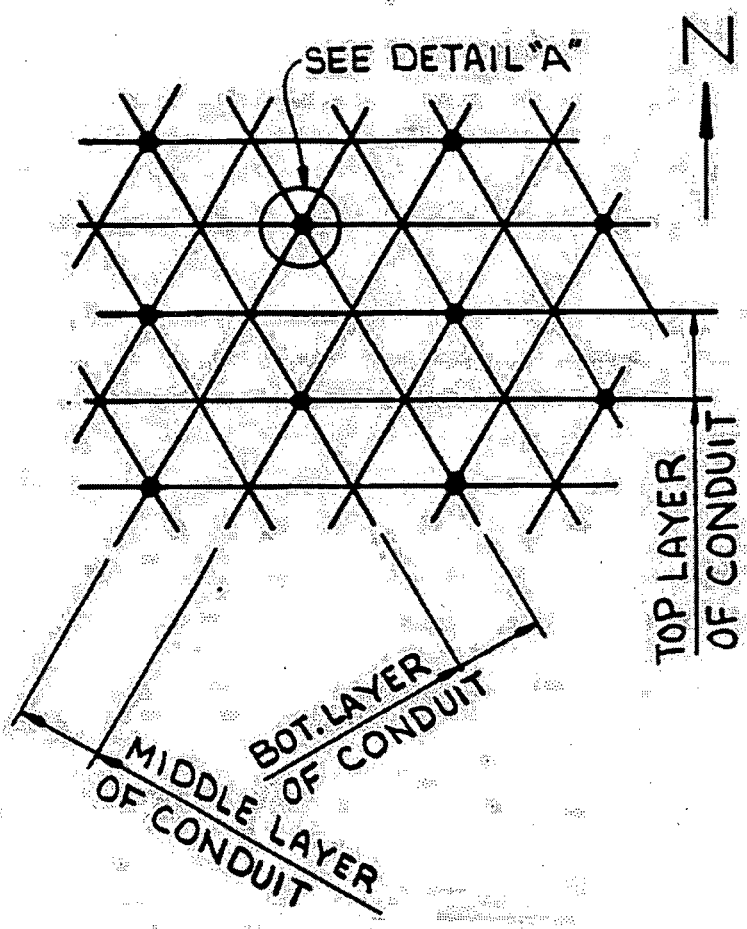
DOME CONCRETE PLACEMENT - PLAN

FIGURE 2-3



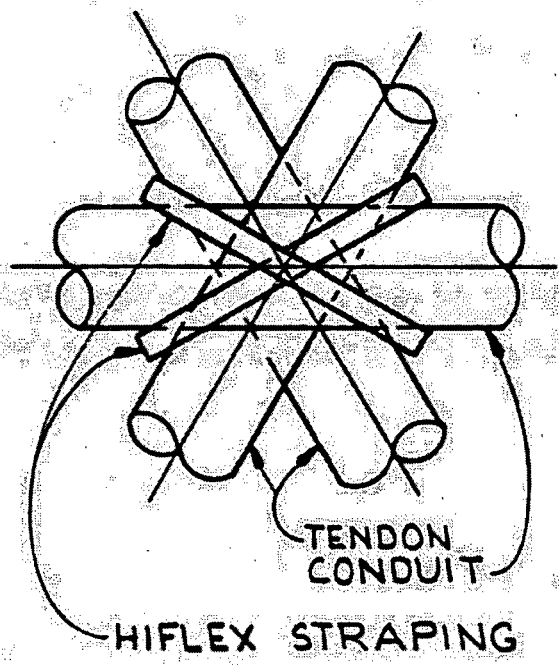
*DOME CONCRETE PLACEMENT - SECTION*

*FIGURE 2-4*



PLAN

CONDUIT STRAPPING  
DETAIL

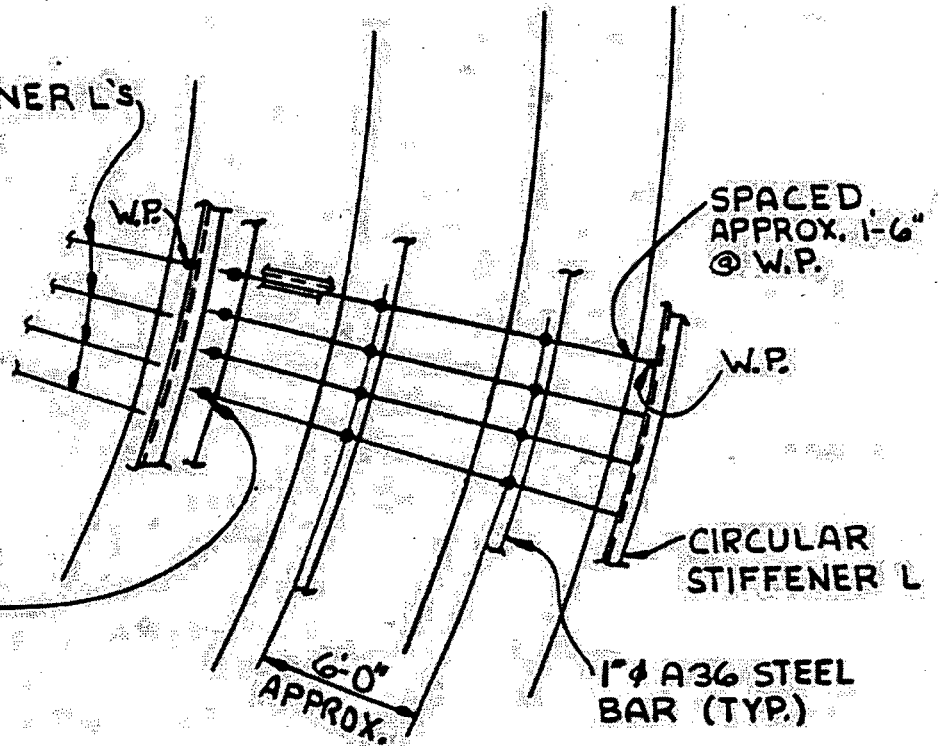


DETAIL "A"

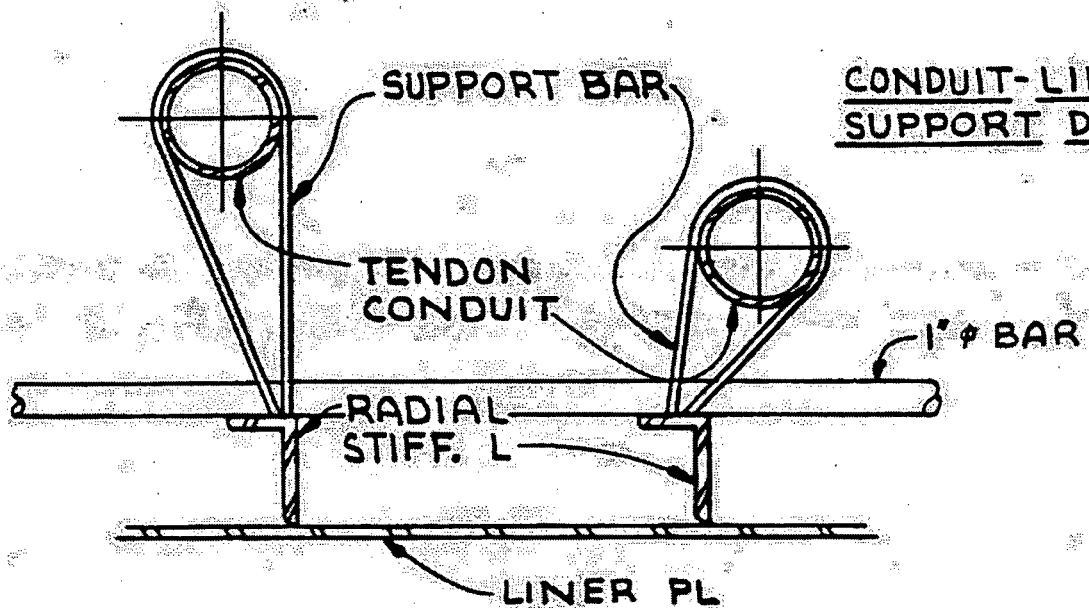
FIGURE 2-5

RADIAL STIFFENER L'S  
SPACED APPROX.  
1'-6" @ W.P.

SUPPORT (TYP.)  
SEE DETAIL

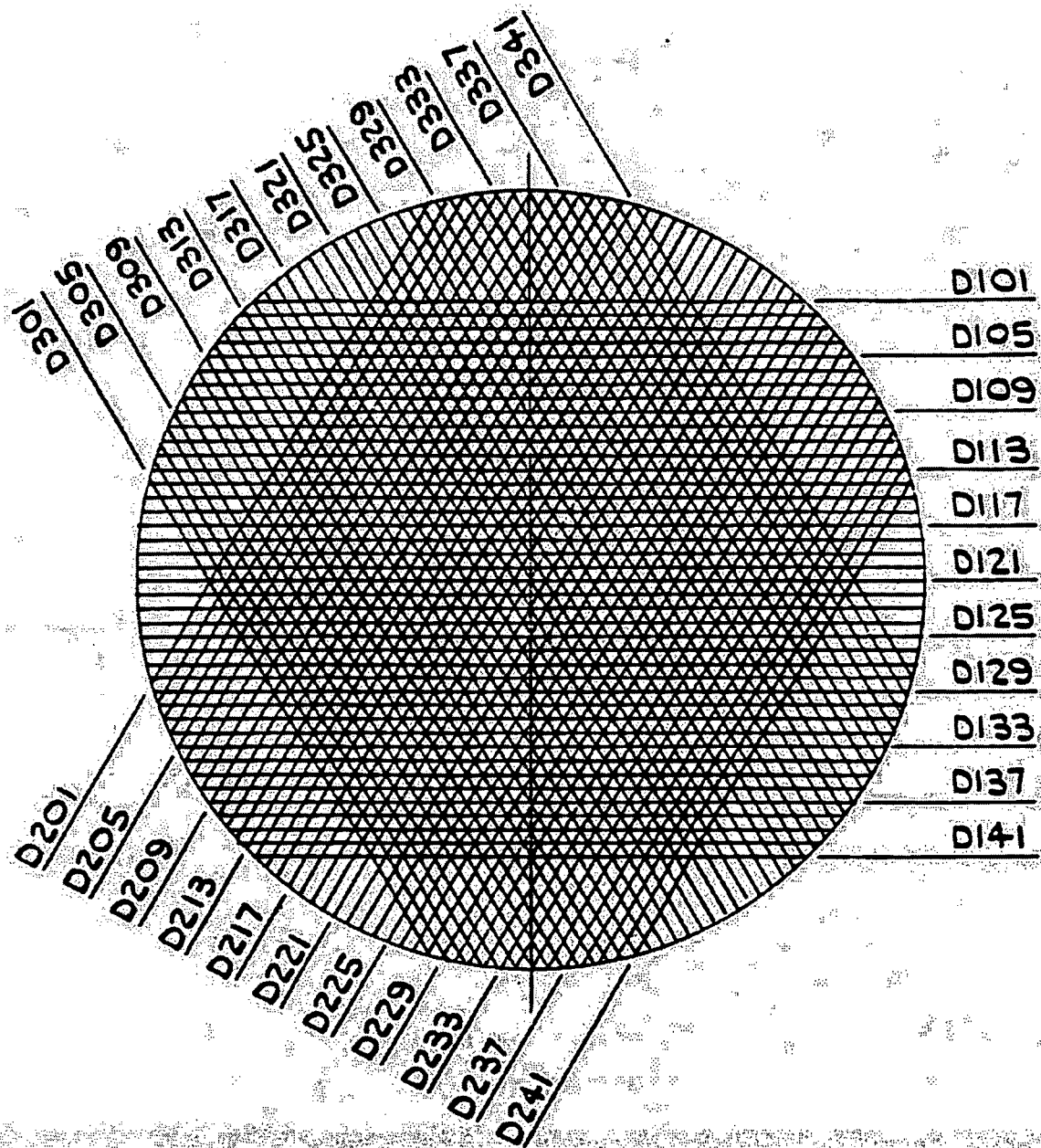


PLAN



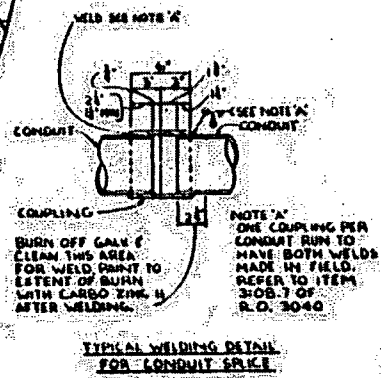
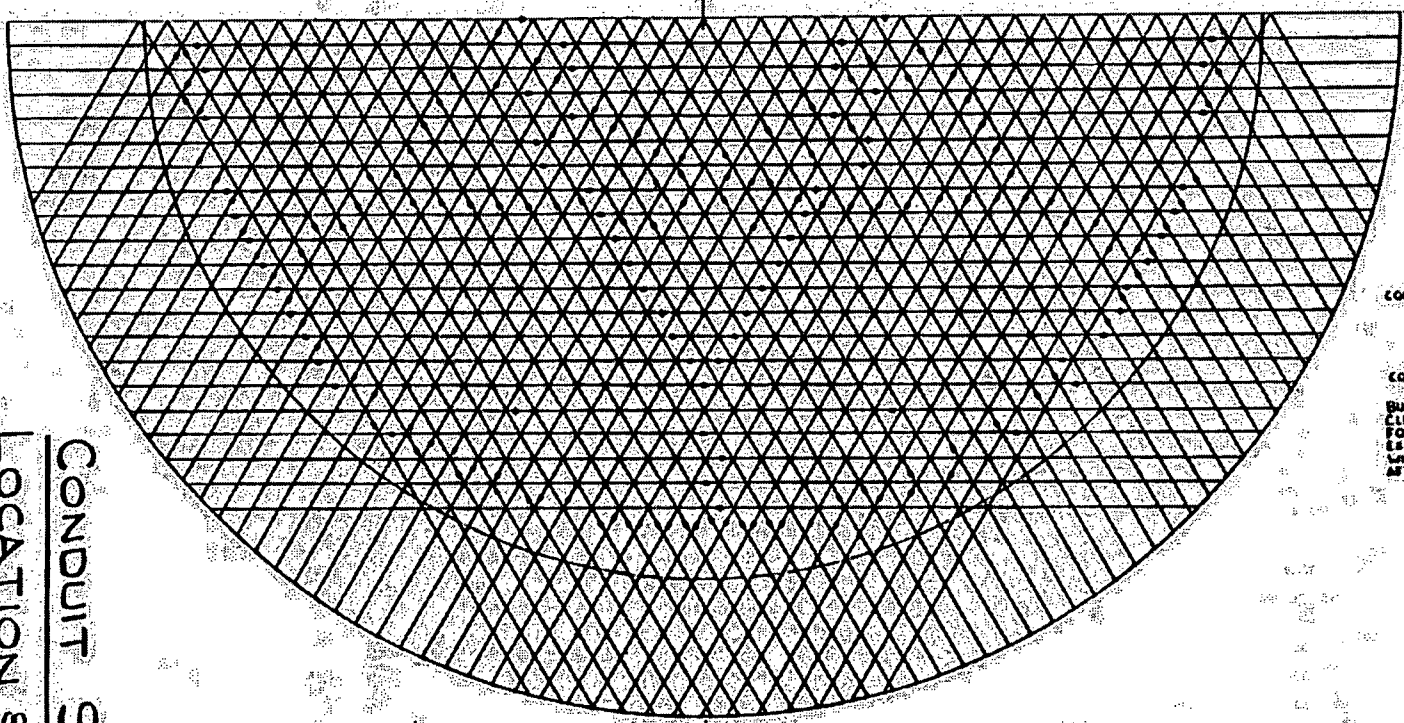
SUPPORT DETAIL

FIGURE 2-6



DOME TENDON LOCATION PLAN

FIGURE 2-7



COUPLING

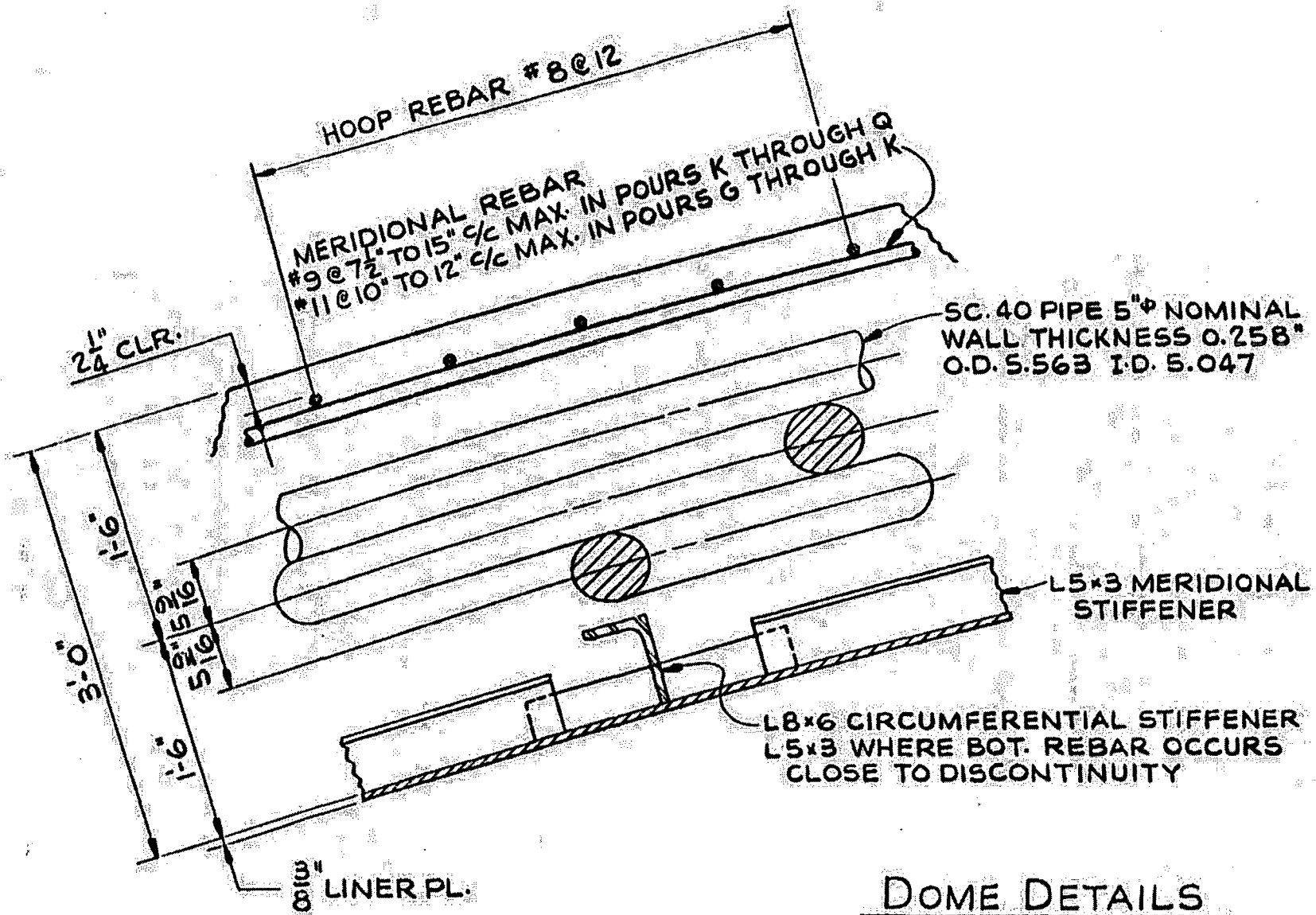
BURN OFF GALV. & CLEAN THIS AREA FOR WELD JOINT TO EXTENT OF GUN WITH CARBO KING 11 AFTER WELDING.

180°

TOP PLAN OF PIPE

CONDUIT SPLICES  
LOCATION & DETAIL

Figure 2-8



DOME DETAILS

FIGURE 2-9

Revised: 9-22-76

**APPENDIX D**

**COMPUTER PROGRAM  
VERIFICATION AND DESCRIPTION**

## KALNINS-STATIC

KALNINS-STATIC uses a multisegment method of direct numerical integration of boundary value problems and was developed by Arturs Kalnins and published in the Journal of Applied Mechanics, Vol. 31, September 1964, pp. 467-476, and in the Journal of the Acoustical Society of America, Vol. 36, July 1964, pp. 1355-1365. The program calculates elastic deflections and stresses in a thin-walled, axisymmetric shell when subjected to any arbitrary surface, edge and/or ring loads. The solution is based on the linear theory of elasticity and takes into consideration bending as well as membrane action of the shell in response to applied load. Results are in terms of resultant forces and couples with stresses calculated by assuming a linear distribution through the thickness.

This program has been widely used for thin shell analysis since its release to the public domain in 1968. The program is being executed on Gilbert Associates, Inc., Reading, Pa., IBM 370/155 computer under IBM operating system O/S 21.8 MVT with HASP 3.2.

#### SAP IV

SAP IV is a large scale linear, three-dimensional general purpose structural analysis program having static and dynamic capabilities. SAP IV has an extensive finite element library. Nodal points can have six degrees of freedom. No restriction is made on the number of nodal points or finite elements used. Temperature, hydrostatic, inertia and surface loadings may be used. General orthotropic material properties can be modeled.

SAP IV was developed by the University of California at Berkeley. The program has been widely used for structural analysis since its release to the public domain in 1973. The program has been verified by comparison to published results. It is being executed at United Computing Systems, Inc., Kansas City, Missouri on multiple CDC Main Frames (i.e., 6600, CYBER 7418, CYBER 175) under APEX Release SL7.

**ARTURS KALNINS**  
*Consulting Engineer*  
R.D. 5 - BINGEN ROAD  
BETHLEHEM, PENNSYLVANIA 18015 U.S.A.  
TELEPHONE (215) 868-3148

May 11, 1976

Dr. F. L. Moreadith  
Gilbert Associates, Inc.  
P. O. Box 1498  
Reading, Pennsylvania 19603

Dear Dr. Moreadith:

Upon your request, I have completed the running of 18 test cases with the KALNINS Static Computer Program for the analysis of axisymmetric shells. The test cases were designed to test the following features of the program:

1. Geometry of a shell (standard surfaces)
2. Elastic foundation
3. Orthotropy of material
4. Variable surface loads
5. Variable thickness
6. Edge loads
7. Springs
8. Branches and box branches
9. Ring loads
10. Layers with different material
11. Dead weight loads
12. Torsion
13. Subcase addition

In all cases, the results given by the program agreed with independently calculated values which were obtained either from published results or from a global equilibrium requirement. All cases were run first on Lehigh University's CDC 6400 computer and then rerun on Gilbert Associates IBM 370/155 computer. In all cases, there was agreement between the two (2) outputs.

I believe that these test cases provide a satisfactory verification of the validity of the KSHELL computer program.

Sincerely yours,

*Arturs Kalnins*  
Arturs Kalnins

GFD:AK:flg

**APPENDIX E**

**PHOTOGRAPHS OF EXISTING STRUCTURE**

Revised: 9-22-76

APPENDIX E

PHOTOGRAPHS OF EXISTING STRUCTURE

PHOTO NO. 1 - Surface of Concrete Illustrating the Relative Position of Failure Plane and Conduit

PHOTO NO. 2 - Surface of Concrete Illustrating the Position of Failure Plane and Lens on Surface

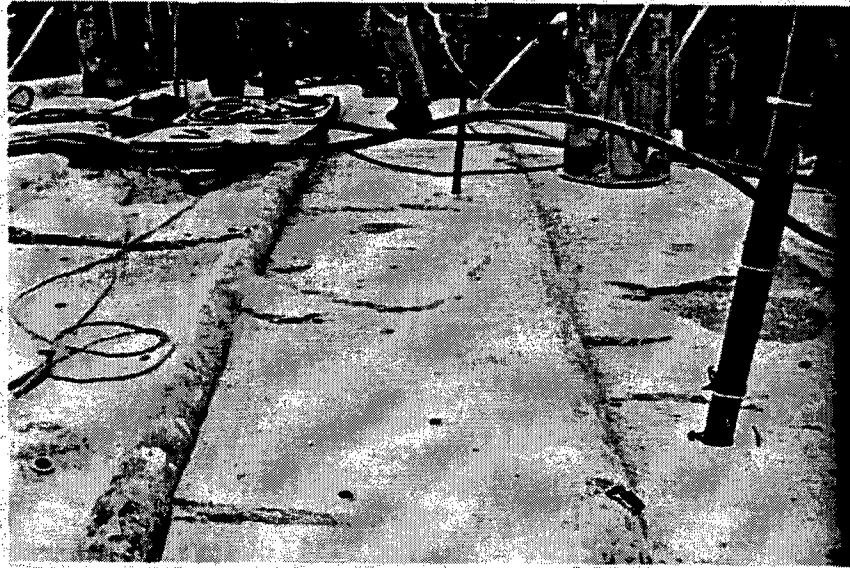


PHOTO NO. 1

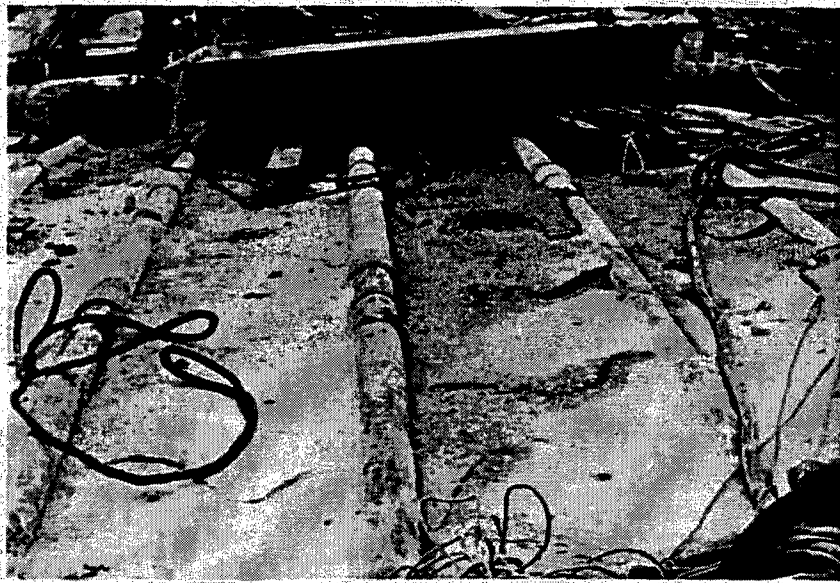


PHOTO NO. 2

APPENDIX E (Cont'd.)

PHOTO NO. 3 - Loose Concrete Lens Extending to the Top of the Tendon Duct

PHOTO NO. 4 - Tight Concrete at the Top of a Tendon Duct (at Different Location than Photo No. 3)



PHOTO NO. 3

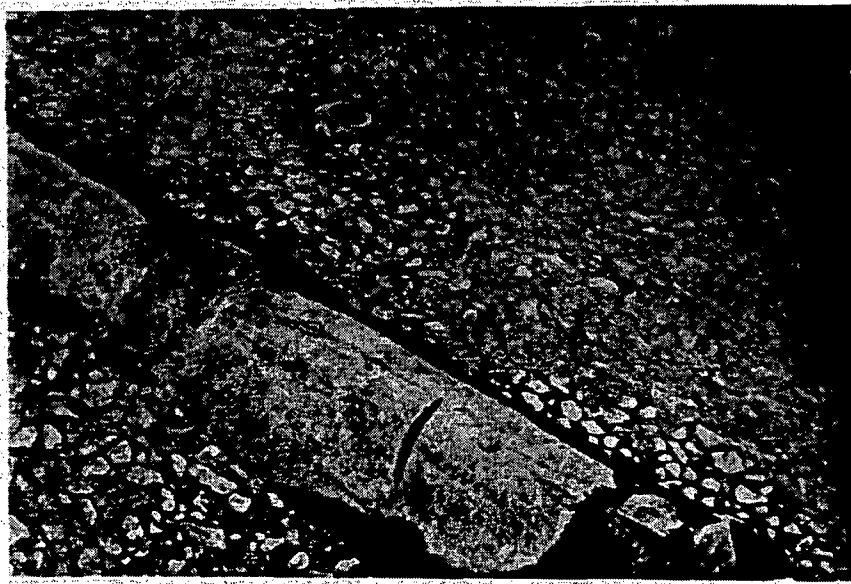


PHOTO NO. 4

**APPENDIX E (Cont'd.)**

**PHOTO NO. 5 - Close up of Delamination as it goes across a Tendon Conduit**

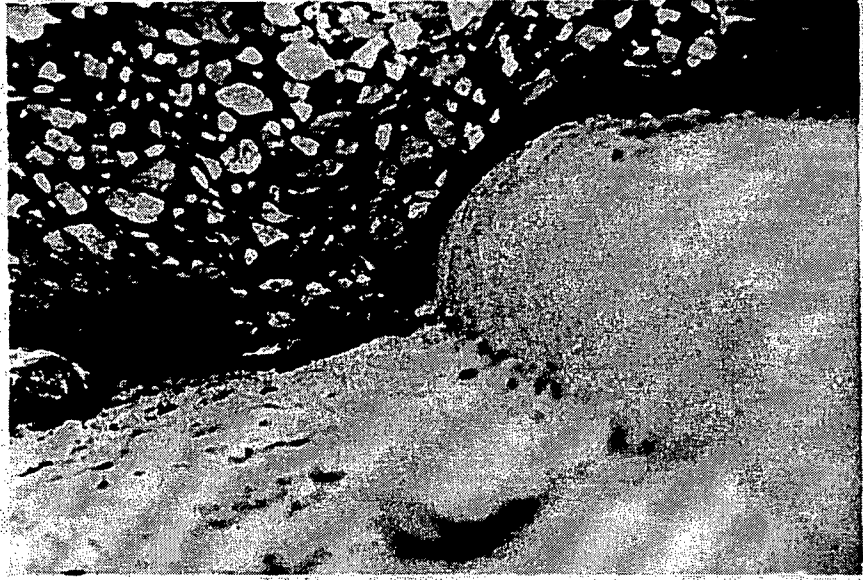


PHOTO NO. 5

APPENDIX E (Cont'd.)

PHOTO NO. 6 - Bottom Surface of Delaminated Cap

PHOTO NO. 7 - Bottom Surface of Delaminated Cap



PHOTO NO. 6



PHOTO NO. 7

**APPENDIX F**

**DISCUSSION OF REPAIR METHOD**

Revised: 9-22-74

APPENDIX F

DISCUSSION OF REPAIR METHOD

*Hansen, Holley and Biggs Inc.* CONSULTING ENGINEERS

ROBERT J. HANSEN • MYLE J. HOLLEY, JR. • JOHN M. BIGGS Box 88, MIT Branch PO, Cambridge, Massachusetts 02139

August 6, 1976

Dr. Fred L. Moreadith  
Gilbert Associates, Inc.  
P.O. Box 1498  
Reading, PA 19603

Re: Crystal River #3  
Dome Delamination

Dear Dr. Moreadith:

This is written to summarize my present judgments relative to the subject structural problem and proposed corrective measures.

CAUSES OF DELIMINATION

The delamination represents a concrete tensile failure in a tri-axial stress field comprised of two substantial compression stress components and a small tensile stress component. The average tensile stress across the failure surface was modest ( $\approx 40$  psi), but it reflected an "active" radial force; i.e., a force unrelieved by local cracking.

There were many sources of local stress concentration which, in some combination, could produce local stress states exceeding the concrete strength.

It appears that the concrete used in this structure fractured through the aggregate when loaded in tension. This suggests the possibility that the concrete is unusually "notch sensitive," that is, subject to tensile fracture in regions of high stress concentration. In the presence of the active radial force, such local fractures would trigger propagating cracks. The head of such a crack is itself a region of severe stress concentration, in a field of average tensile stress which increases as the crack spreads.

In summary,

- a) Geometric discontinuities and reductions in effective section, occasioned by the conduit grid, easily could produce locally concentrated stress states in excess of the strength of this concrete.
- b) The concrete was unusually notch sensitive; that is, likely to fail in a brittle manner at points of local stress concentration.
- c) The radial tension force was essentially unrelieved by the cracking, until the cracked area and crack thickness were large. Indeed as the cracks spread, thereby reducing the area resisting the radial force, the magnitude of the average radial stress was increased.

## Appendix F Cont'd.

- d) Under the impetus of the unrelieved radial tension force, a crack initiated at a point of stress concentration (and subsequently generating its own point of stress concentration) would spread very rapidly.

### CONDITION OF REDUCED DOME

Thus far exploration of the concrete in the reduced dome has been by a substantial number of core holes driven through the cap into the reduced dome below. Secondary laminar cracks have been found, particularly in regions away from the boundary. Apart from these cracks, the exploratory coring has not disclosed any signs of distress; e.g., crushing or spalling of the concrete. Indeed the fact that the core drilling has not, itself, caused any evidence of spalling may be an indication that it has not penetrated any zones of unexpectedly high compression stresses. I do not know of any studies of damage due to core drilling into stressed concrete, as a function of stress level. Nevertheless, I would expect such damage to occur as the stress level approaches the cylinder strength of the concrete. The absence of any damage associated with the core drilling, to date, is at least encouraging. It may or may not verify that stresses do not exceed the calculated values, which are well below the cylinder strength.

It is my impression that the lift-off forces (in the 18 tendons checked) imply, on the average, smaller prestress losses than would be predicted by the creep relationship used to predict 40-year effective prestress values. This is further, indirect, evidence that the concrete in the reduced dome is in generally sound condition.

Additional verification of the sound condition of the reduced dome must await removal of the old cap. This will permit the first, direct, visual inspection. If the results of that inspection are favorable, repair measures which utilize the existing dome will be justified.

If visual inspection of the dome does not disclose any severe, unexpected, damage, there would appear to be no necessity to de-tension the tendons. Indeed, the present stress and strain condition of the structure must reflect a history of inelastic, as well as elastic, strains; and the response to de-tensioning (essentially elastic) cannot be expected to return the dome to a zero condition of stress and strain. Thus de-tensioning might cause further cracking, might open cracks which now are small, and might cause separation of conduits from the concrete. These are undesirable effects which should be avoided if possible. Unless stress analyses indicate that the tendons must be detensioned (and re-tensioned after a new cap has been joined to the dome), or unless visual inspection reveals unexpectedly severe damage, de-tensioning is not recommended.

### REQUIRED DOME BEHAVIOR

It is obvious that delamination caused the prestress forces (only slightly reduced) to be resisted by a dome of lesser thickness. That is,

Appendix F Cont'd.

it caused a significant increase in meridional and hoop membrane stresses. Since the conduit zone is a larger portion of the thickness of the reduced zone than of the original dome, the distribution of membrane stresses through the thickness also could have been altered. For example, stresses in the zone between conduits and liner might have been increased by this latter effect as well as by the reduction in dome thickness, per se. To whatever extent such changes in the distribution and intensities of membrane stresses may have occurred, the accompanying membrane strains could lead to altered shear and bending moment distributions in the discontinuity zone at, and near, the perimeter.

As already noted, there is no evidence, in the form of crushing or spalling, to indicate that the stress changes in the reduced dome have included the development of regions of very high compressive stress. Moreover, the relatively small tendon stress losses during the 19 months since delamination suggest that abnormally high concrete stresses have not developed. This seems to indicate that the conduit zone is sufficiently stiff to accept a substantial portion of the membrane forces.

Under accident conditions, it is clear that the inward radial pressure which can be developed by the tendon grid is substantially in excess of the active outward pressure ( $1.5 \times 55 = 82.5$  psi). Preferably the inward and outward pressures will be in balance at a membrane strain which does not imply the possibility of large cracks in the concrete. In verifying that this desired condition will obtain, it appears prudent to assume that the concrete has zero tensile strength.

To achieve the above-described desired behavior under accident load conditions, it is essential that the tendons not experience any unexpected, large, loss of tension. This, in turn, implies that the dome must not undergo any unexpected, large, compression strain. Lift-off measurements have shown prestress losses, to date, to be modest. This, in turn, demonstrates that no unusually large concrete compressive strains (elastic, and/or inelastic) have developed thus far. For this reason one may have confidence in analytical predictions of the prestress losses which may occur over the next 40 years. Such analyses indicate that the residual tendon forces will be sufficient to cause inward and outward pressures to balance either at a small net concrete compressive stress, or at a net concrete tensile stress within the capacity of bonded rebar which will be placed in the new cap. Accordingly it appears that uncontrolled concrete cracking will not occur under the accident condition.

In addition to avoidance of uncontrolled membrane cracking, it is essential that the dome possess adequate resistance to the radial shears and bending moments which may develop, in the transition zone, during the accident load condition. Fortunately it appears that this zone suffered very little damage (e.g., secondary cracks) as a result of the delamination. Your analyses appear to indicate that the shear and bending effects are less severe in the accident condition than in the normal winter operating condition. If the transition zone does not experience any "failure" during normal operation, it should be well able to resist the shears and bending moments associated with the accident condition.

#### Appendix F Cont'd.

Let us next consider the behavior of the dome during normal operating conditions. In regions well away from the boundary the new cap will slowly assume some small portion of the compressive membrane forces currently being resisted entirely by the reduced dome. Thus the stress state in the reduced dome in these regions of essentially membrane behavior can only improve with time. Because of the absence of substantial shear force in these regions, the secondary (laminar) cracks are not a threat to the membrane compressive strength of the repaired dome. Even without the addition of radial anchor bars the region should not experience any distress. However, the contemplated radial bars are required to mobilize the membrane compression capacity of the new cap, and they will improve the membrane compressive strength of the concrete in the reduced dome.

In the boundary zone your analyses indicate high meridional compressive stress due to the combined effects of membrane force and bending moment. This stress, which is the subject of continuing analyses, may be slightly in excess of the  $0.6f_c$  FSAR limit. If so, this does not necessarily indicate that the dome can not safely withstand normal operating load conditions. First, it should be noted that the meridian compression stress in question is only 20 percent smaller for the D.L. + prestress condition than for the normal winter operating condition; the D.L. + prestress condition has existed for 19 months, and has not caused any evidence of distress. Second, the computed high compression stress results from linear analysis. Analyses which account for increased elastic and creep strains with increased stress should indicate some reduction in the section bending moment, more favorable distribution of the compression stresses on the section, and greater participation of the meridional compression rebars. All of these effects should lead to a lower value of computed stress. Third, it should be noted that the load (mainly D.L. + prestress) is very reliably known for the operating conditions. Under these known loads the section bending moment is well below the ultimate section capacity. Finally, it should be remembered that the high compression stress vanishes under the accident condition.

Based on the immediately preceding discussion,

- a) The actual maximum meridional compression stress in the boundary zone probably is less than the computed value, and may be below the FSAR limit of  $0.6 f_c$ .
- b) The high computed compression stress does not signify any threat of catastrophic failure (e.g., collapse) under normal operating conditions.

#### PROPOSED NEW CAP

I am in complete agreement with the decision to remove, and replace, the old cap. Not only will this permit better inspection of the reduced dome, but it will permit the installation of an improved grid of bonded rebars in the cap zone. The quantity of meridional rebar which can be

## Appendix F Cont'd.

developed is limited by the existing quantity of these bars outside the cap boundary. However, the quantity of hoop rebars can be increased. For the accident loading there is a region over which hoop membrane force exceeds the concrete pre-compression. That is, computed net concrete stress is tensile. The increased hoop rebar quantity will be sufficient to resist these net tensile forces, thus precluding unconstrained growth in crack widths. Finally, Cadweld splices, rather than lap splices, will be used for rebars in the new cap.

It is my understanding that the new cap will be of essentially the same thickness as the old cap. Because the new cap concrete will be placed on the prestressed reduced dome (i.e., with only 15% of the dome tendons de-tensioned), the membrane compression stress in the new cap will be substantially less than in the old cap (prior to delamination). Re-tensioning of the 15% of tendons that have been de-tensioned will produce only small membrane compression stress in the new cap, and this will be reduced by shrinkage strain. It must be expected that the structural integrity test loading will produce net tensile stress in the new cap in excess of its tensile strength; thus cracking will occur. Upon removal of the test loading the membrane stress probably will again be compression, but small. Creep strain, over many years, may be expected to cause a modest increase in the cap compression stresses and a corresponding, but smaller, decrease in membrane compression stress in the reduced dome.

I have reviewed C. Chen's analysis of the maximum (i.e., long-term) membrane compression stress that may develop in the new cap. I agree with his conclusion that the cap compression stress will not exceed 1200 psi; it may be substantially less. This implies that the average tension stress across the cap-to-dome interface will not exceed 21.4 psi, in regions where the cap is 12" thick. In regions of lesser cap thickness the radial stress will be proportionately smaller. It is my understanding that the radial anchor bars securing the new cap to the reduced dome will be proportioned for the above dome radial tension stress, at a bar tension of  $0.5 f_y$ . This is reasonable and conservative.

### CORE DRILLING, GROUTING, AND RE-DRILLING

Most of the secondary cracks are in regions away from the boundary, that is, they are in regions of essentially membrane behavior. For this reason they may be of little or no significance to the dome strength. Nevertheless, I believe the decision to (epoxy) grout all of the secondary cracks is prudent. Unfortunately this operation together with the radial anchor installation will require repeated core drilling. The crack grouting operation will fill the radial holes drilled for that purpose with grout. A second set of holes, essentially co-axial with the grout holes, but of larger diameter, must be drilled to accommodate the anchor bars. I am not familiar with any research on the effects, if any, of drilling small diameter holes into biaxially compressed concrete. However, there has been no evidence of any damage associated with the substantial number of exploratory holes drilled into the dome thus far. Despite the fact that the new cap will develop smaller interface radial tension stresses than were associated with the old cap, the fact of the earlier delamination

Appendix F Cont'd.

dictates some positive radial connection of the new cap to the reduced dome. Paul Mast's suggestion, that the new cap be tied to the outer conduits, is interesting, but it is not clear that there is a reliable practical means to accomplish this. Therefore radial ties appear to be necessary, and it is advantageous to extend them deep enough to cross the secondary cracks in the reduced dome. Accordingly the risk that the drilling may cause some damage to the stressed concrete appears to be both small and justified.

SUMMARY

- 1) The decision to utilize the reduced dome, unless visual inspection reveals unexpectedly severe damage, is sound.
- 2) The decision not to de-tension the tendons, beyond the present 15% de-tensioning, is sound.
- 3) The decision to cast a new cap of essentially the same thickness as the original cap, and to place adequate, Cadweld-spliced, bonded rebars in the new cap should assure satisfactory behavior of the dome.
- 4) The radial tension stress across the cap-to-dome interface has been conservatively computed.
- 5) The decision to grout the secondary cracks is prudent.
- 6) The use of deep radial anchor bars, tying cap to dome and bridging the secondary cracks is sound. There is no basis for certainty that the necessary core drilling will cause no damage to the compressed concrete. However, the risk of such damage seems small, and is justified in view of the advantages gained by the use of such bars.
- 7) It is believed that continuing analyses may show that the high concrete meridional compressive stress near the boundary is not excessive. However, regardless of the results of these analyses, it does not appear that a modest overstress in this zone has any adverse implications for the performance of the containment structure.

I look forward to the opportunity to discuss all the above with you and your colleagues at our next meeting, on August 9, 1976.

Sincerely,



Myle J. Holley, Jr.

MJH/jm

**APPENDIX G**

**COMPARISON OF DESIGNS**

COMPARISON OF DESIGNS

SUMMARY OF RESULTS

STRUCTURE: 36-Inch Dome (FSAR - 5000 psi Concrete)

Item No.	Description	Dead Load + Prestress @ Early Plant Life	Norm. Winter Operating Condition @ Early Plant Life	Structural Integrity Test	LOCA @ 40 Years		
I	Design compressive strength of concrete (psi)	5000	5000	5000	5000		
	Design dome tendon prestress (ksi)	148	148	148	137		
	Deflection of dome apex (in)	-1.56 <sup>2</sup>	-1.52 <sup>2</sup>	+0.75 <sup>3</sup>	+1.02 <sup>4</sup>		
II	Maximum tensile liner strain (micro in/in)	None	None	None	None		
	Allowable tensile liner strain (micro in/in)	1000	1000	1000	1000		
III	Maximum compressive liner strain (micro in/in)	948	1240	510	2057		
	Allowable compressive liner strain (micro in/in)	5000	5000	5000	5000		
IV	Pressure at which first concrete cracking occurs through section thickness (psi)	No Thru Cracking	No Thru Cracking	No Thru Cracking	No Thru Cracking		
	Maximum pressure for transient (psi)	0	0	63	83		

<sup>1</sup>Maximum calculated tensile stress (148 psi) is less than allowable value (+212 psi).

<sup>2</sup>Referenced to unstressed condition.

<sup>3</sup>Due to 1.15 P<sub>a</sub>

<sup>4</sup>Due to 1.5 P<sub>a</sub> + T<sub>a</sub>

G-1

Revised: 9-22-76

SUMMARY OF RESULTS

STRUCTURE: 36-Inch Dome (FSAR - 5000 psi Concrete)

Item No.	Description	Dead Load + Prestress @ Early Plant Life	Norm. Winter Operating Condition @ Early Plant Life	Structural Integrity Test	LOCA @ 40 Years		
V	Maximum concrete <u>membrane compressive stress</u> (psi)	1836	1759				
	Maximum concrete <u>membrane tensile stress</u> (psi)			-469 <sup>1</sup>	148		
	Allowable <u>membrane stress</u> (psi) (compression -/tensile +)	-2250/0	-2250/0	-2250/0	-2250/+212		
VI	Maximum <u>compressive concrete extreme fiber stress</u> (psi) - Uncracked analysis value	2666	3538				
	Cracked section investigation value - Calculate when actual uncracked is greater than allowable	Not Req'd	3038				
	Allowable <u>compressive extreme fiber stress</u> (psi)	3000	3000	3000	3000		
VII	Maximum concrete <u>tensile extreme fiber stress</u> in areas without reinforcement (psi)	None	None	None	None		
	Allowable concrete <u>tensile extreme fiber stress</u> in areas without reinforcement (psi)	0	0	0	424		

<sup>1</sup>No tension occurs; minimum compression indicated.

G-2

Revised: 9-22-76

SUMMARY OF RESULTS

STRUCTURE: 36-Inch Dome (FSAR - 5000 psi Concrete)

Item No.	Description	Dead Load + Prestress @ Early Plant Life	Norm. Winter Operating Condition @ Early Plant Life	Structural Integrity Test	LOCA @ 40 Years		
VIII	Calculated shear at point of minimum margin (kips/ft)	53	17	15	10		
	Allowable shear at point of minimum margin (kips/ft)	55	25	23	23		
	Location of minimum shear reinforcement margin	153.8°	158.4°	155.6°	156.6°		
IX	Maximum tensile stress in reinforcing bar (psi)	Section Not Cracked	2192	=0	25125		
	Allowable stress in reinforcing bar (psi)	20000	20000	20000	36000		

G-3

Revised: 9-22-76

## Appendix G Cont'd.

## SUMMARY OF RESULTS

STRUCTURE: 24-Inch Dome ("In-Place" Concrete Strength - 6000 psi)  
 (See Table 2-2 for allowable criteria)

Item No.	Description	Dead Load + Prestress @ Early Plant Life	Norm. Winter Operating Condition @ Early Plant Life	Structural Integrity Test	LOCA @ 40 Years		
I	Design compressive strength of concrete (psi)	6000	6000	6000	6000		
	Design dome tendon prestress (ksi)	141	141	141	125		
	Deflection of dome apex (in)	-1.83 <sup>1</sup>	-1.79 <sup>1</sup>	+0.90 <sup>2</sup>	+2.07 <sup>3</sup>		
II	Maximum tensile liner strain (micro in/in)	2	None	None	178		
	Allowable tensile liner strain (micro in/in)	1000	1000	1000	3000		
III	Maximum compressive liner strain (micro in/in)	1100	1560	570	2267		
	Allowable compressive liner strain (micro in/in)	2000	2000	2000	5000		
IV	Pressure at which first concrete cracking occurs through section thickness (psi)	No Thru Cracking	No Thru Cracking	No Thru Cracking	63		
	Maximum pressure for transient (psi)	0	0	63	83		

<sup>1</sup>Referenced to unstressed condition.

<sup>2</sup>Due to 1.15 P<sub>a</sub>

<sup>3</sup>Due to 1.5 P<sub>a</sub> + T<sub>a</sub>

SUMMARY OF RESULTS

STRUCTURE: 24-Inch Dome ("In-Place" Concrete Strength - 6000 psi)  
 (See Table 2-2 for allowable criteria)

Item No.	Description	Dead Load + Prestress @ Early Plant Life	Norm. Winter Operating Condition @ Early Plant Life	Structural Integrity Test	LOCA @ 40 Years		
V	Maximum concrete <u>membrane compressive stress</u> (psi)	2470	2380				
	Maximum concrete <u>membrane tensile stress</u> (psi)			-585 <sup>1</sup>	445 <sup>2</sup>		
	Allowable <u>membrane stress</u> (psi) (compression -/tensile +)	-2700/0	-2700/0	-2700/0	-2700/0		
VI	Maximum <u>compressive concrete extreme fiber stress</u> (psi) - Uncracked analysis value	3266	4082				
	Cracked section investigation value - Calculate when actual uncracked is greater than allowable	Not Req'd	3613				
	Allowable <u>compressive extreme fiber stress</u> (psi)	3600	3600	3600	3600		
VII	Maximum concrete <u>tensile extreme fiber stress</u> in areas without reinforcement (psi)	None	None	None	980 <sup>2</sup> (Uncracked)		
	Allowable concrete <u>tensile extreme fiber stress</u> in areas without reinforcement (psi)	0	0	0	0		

<sup>1</sup>No tension occurs; minimum compression indicated.

<sup>2</sup>Since calculated values exceed allowables and no reinforcement exists, LOCA resisted as described in report Section 4.4.4.

Appendix G Cont'd.SUMMARY OF RESULTS

STRUCTURE: 24-Inch Dome ("In-Place" Concrete Strength - 6000 psi)

Item No.	Description	Dead Load + Prestress @ Early Plant Life	Norm. Winter Operating Condition @ Early Plant Life	Structural Integrity Test	LOCA @ 40 Years		
VIII	Calculated shear at point of minimum margin (kips/ft)	45	55	6	10		
	Allowable shear at point of minimum margin (kips/ft)	55	55	7	23		
	Location of minimum shear reinforcement margin	151.5°	152.0°	161.0°	160.0°		
IX	Maximum tensile stress in reinforcing bar (psi)	748	7081	=0	Rebar not available over most of dome		
	Allowable stress in reinforcing bar (psi)	20000	20000	20000	36000		

(See Table 2-2 for allowable criteria)

G-6

Revised: 9-22-76

Appendix G Cont'd.

SUMMARY OF RESULTS

STRUCTURE: 36-Inch Dome, Including New Reinforced Cap

Item No.	Description	Dead Load + Prestress @ Early Plant Life	Norm. Winter Operating Condition @ Early Plant Life	Structural Integrity Test	LOCA @ 40 Years		
I	Design compressive strength of concrete (psi)	6000	6000	6000	6000		
	Design dome tendon prestress (ksi)	141	141	141	125		
	Deflection of dome apex (in)	-1.87 <sup>3</sup>	-1.83 <sup>3</sup>	+0.90 <sup>1,4</sup>	+2.07 <sup>1,5</sup>		
II	Maximum tensile liner strain (micro in/in)	=0	0	0	178 <sup>1</sup>		
	Allowable tensile liner strain (micro in/in)	1000	1000	1000	3000		
III	Maximum compressive liner strain (micro in/in)	1100 <sup>1</sup>	1560 <sup>1</sup>	570 <sup>1</sup>	2267 <sup>1</sup>		
	Allowable compressive liner strain (micro in/in)	2000	2000	2000	5000		
IV	Pressure at which first concrete cracking occurs through section thickness (psi)	No Thru Cracking	No Thru Cracking <sup>2</sup>	No Thru Cracking <sup>2</sup>	63 <sup>1</sup>		
	Maximum pressure for transient (psi)	0	0	63	83		

<sup>1</sup>Tensile strength of concrete in cap taken as zero. Cap reinforcement has practically no effect on dome stiffness. Therefore, values are practically same as for 24" dome.

<sup>2</sup>Due to assumed zero concrete tensile strength, cap cracks at 0+ psi pressure. Remaining 24" dome thickness is sufficiently prestressed to preclude cracking.

<sup>3</sup>Referenced to unstressed condition.

<sup>5</sup>Due to 1.5 P<sub>a</sub> + T<sub>a</sub>

<sup>4</sup>Due to 1.15 P<sub>a</sub>

G-7

Revised: 9-22-76

SUMMARY OF RESULTSSTRUCTURE: 36-Inch Dome, Including New Reinforced Cap

Item No.	Description	Dead Load + Prestress @ Early Plant Life	Norm. Winter Operating Condition @ Early Plant Life	Structural Integrity Test	LOCA @ 40 Years		
V	Maximum concrete <u>membrane compressive stress (psi)</u>	2498	2712 <sup>1</sup>				
	Maximum concrete <u>membrane tensile stress (psi)</u>			-552 <sup>2</sup>	445 <sup>3</sup>		
	Allowable <u>membrane stress (psi)</u> (compression -/tensile +)	-2700/0	-2700/0	-2700/0	-2700/0		
VI	Maximum <u>compressive concrete extreme fiber stress (psi) - Uncracked analysis value</u>	3219	3999				
	Cracked section investigation value - Calculate when actual uncracked is greater than allowable	Not Req'd	3540 <sup>4</sup>				
	Allowable <u>compressive extreme fiber stress (psi)</u>	3600	3600	3600	3600		
VII	Maximum concrete <u>tensile extreme fiber stress in areas without reinforcement (psi)</u>	None	None	None	None		
	Allowable concrete <u>tensile extreme fiber stress in areas without reinforcement (psi)</u>	0	0	0	0		

<sup>1</sup>2712 occurs in bottom 24"; corresponding cap stress is 365 psi tensile. (Sta 161.1<sup>0</sup>).

<sup>3</sup>Cap reinforcement added to resist all net membrane tension. See Figures 5-20 and 5-21.

<sup>2</sup>No tension exists in bottom 24" section of dome; minimum

<sup>4</sup>Occurs at Sta 150.2<sup>0</sup>.

G-8

Revised: 9-22-76

SUMMARY OF RESULTSSTRUCTURE: 36-Inch Dome, Including New Reinforced Cap

Item No.	Description	Dead Load + Prestress @ Early Plant Life	Norm. Winter Operating Condition @ Early Plant Life	Structural Integrity Test	LOCA @ 40 Years		
VIII <sup>1</sup>	Calculated shear at point of minimum margin (kips/ft)	45	55	6	10		
	Allowable shear at point of minimum margin (kips/ft)	55	55	7	23		
	Location of minimum shear reinforcement margin	151.5°	152.0°	161.0°	160.0°		
IX	Maximum tensile stress in reinforcing bar (psi)	7482 <sup>2,3</sup>	7081 <sup>2,3</sup>	11000 <sup>4</sup>	54000 <sup>4</sup> @ Sta 161.1° (Fig. 2)		
	Allowable stress in reinforcing bar (psi)	20000 <sup>3</sup>	20000 <sup>3</sup>	30000 <sup>4</sup>	54000 <sup>4</sup>		

<sup>1</sup>Since cap is cracked after SIT, shear results are same as those for 24-Inch Dome.

<sup>2</sup>Practically the same as for 24-Inch Dome.

<sup>3</sup>In location where Grade 40 reinforcement exists.

<sup>4</sup>In location where Grade 60 reinforcement exists, 0.5f<sub>y</sub> for SIT and 0.9f<sub>y</sub> for LOCA.

G-9

Revised: 9-22-76

**APPENDIX H**

**CADWELDING REQUIREMENTS**

Revised: 9-22-76

## APPENDIX H

### CADWELDING REQUIREMENTS

#### 1.0 Applicable Codes, Standards, and Reference Documents

The WORK shall be in accordance with applicable portions of the following codes, standards, and reference documents:

1. American National Standards Institute (ANSI) N45.2.2-1972, "Packaging, Shipping, Receiving, Storage, and Handling of Items for Nuclear Power Plants."
2. American Society for Testing and Materials (ASTM):
  - a. A 370-75, "Standard Methods and Definitions for Mechanical Testing of Steel Products."
  - b. A 513-73, "Electric-Resistance-Welded Carbon and Alloy Steel Mechanical Tubing."
  - c. A 519-73, "Seamless Carbon and Alloy Steel Mechanical Tubing."
  - d. A 615-68, "Standard Specification for Deformed and Plain Billet-Steel Bars for Concrete Reinforcement."

#### 2.0 Cadweld Splices

##### 2.1 General:

Splice samples shall be sister splices (removable splices made in place next to production splices and under the same conditions).

##### 2.2 Cadweld Operator or Crew Qualification:

1. Prior to performing the actual splices of reinforcing bars each member of the splicing crew (or each crew, if the members work as a unit) shall prepare two qualification splices for each of the bar sizes (identical to those to be used in the structure) to be used in the production work. The completed qualification splices will be visually inspected and tested for tensile strength.
2. Each member of the splicing crew (or each crew, if the members work as a unit) is subject to requalification if a) splicing has not been done for 3 months or more or b) completed splices fail to pass the visual inspection test or fail to pass the tensile test requirements or c) there is any reason to question their ability. The requalification procedure shall be identical to the original qualification procedure.

## APPENDIX H (Cont'd)

### 2.3 Acceptance Criteria for Cadweld Splices:

1. Sound, nonporous filler material shall be visible at both ends of the splice sleeve and at the top hole in the center of the sleeve. Filler material is usually recessed 1/4 inch from the end of the sleeve due to the packing material and is not considered a poor fill.
2. Splices which contain slag or porous metal in the riser, tap hole, or at the ends of the sleeve shall be rejected. A single shrinkage bubble present below the riser is not detrimental and should be distinguished from general porosity as described above.
3. There shall be evidence of filler material between the sleeve and the reinforcing bar for the full 360 degrees; however, the splice sleeves need not be exactly concentric or axially aligned with the reinforcing bars.
4. In order to qualify, the completed splices shall also meet the acceptance requirements of Erico Products "Inspection of the Cadweld Rebar Splice," Standard RB5M-274.
5. Splice samples shall be subjected to tensile tests by using loading rates set forth in ASTM A 370 to determine conformance with the following acceptance criteria:

a. Individual splice strength criteria:

The tensile strength of each sample tested shall be equal to or exceed 125% of the minimum yield strength specified in ASTM A 615 for the grade of reinforcing bar being used.

b. Group splice strength criteria:

The average tensile strength of each group of 15 consecutive samples shall equal or exceed the guaranteed ultimate strength for that grade of reinforcing bar as specified in ASTM A 615.

### 2.4 Positioning of Reinforcing Bars for Sister Splices:

Sufficient extra lengths of reinforcing bars shall be positioned in those areas of reinforcement where splices will be required prior to any splicing taking place in that concrete pour. The reinforcing bar shall be secured in position so that it cannot be displaced during splicing. The positioning of the reinforcing bar shall be such that the location and orientation of the sister splice are similar to the splices it will represent.

APPENDIX H (Cont'd)

2.5 Availability of Sample Test Results:

Test results for the samples shall be available and be certified as being in conformance with the requirements before concrete is placed.

3.0 Frequency of Testing

3.1 Separate test cycles will be established for splices for each bar size and for each splicing crew in accordance with the following frequency:

1. One sister splice of the first ten production splices.
2. Four sister splices for the next 90 production splices.
3. Three sister splices for the next and subsequent units of 100 splices.

**APPENDIX I**  
**RADIAL TENSION AND SHEAR**

## APPENDIX I

### RADIAL TENSION AND SHEAR

#### GENERAL

Fundamentally, radial tension is directly related to compression stresses in the plane of the dome. The importance of considering these stresses in conjunction with radial shear stresses is dependent on the load condition being considered; i.e., service or abnormal.

For abnormal load combinations, where in-plane tension exists at the top surface, radial tension stresses become compressive. Therefore, radial shear stresses are considered separately.

For service load combinations where cracking does not occur, radial tension and shear stresses should be combined. Mohr's Circle graphical method is an appropriate technique for accomplishing the combination.

The critical location in the existing structure for radial tension and shear in combination is in the pours outside the main delamination; e.g., pours G and H. Those pours are reinforced (original design) through the thickness of the dome with #8 (J) reinforcement (see Figure 2-2). The minimum area of steel provided perpendicular to the plane of the membrane is approximately 0.79 in.<sup>2</sup> of steel per 432 in.<sup>2</sup> of concrete.

#### SERVICE LOAD

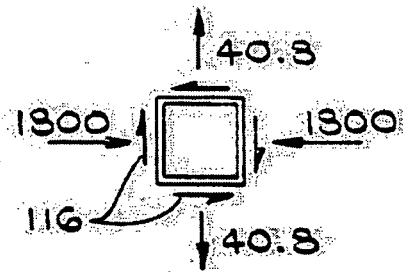
To illustrate the combination of radial tension and shear for service loads, an example state of stress for the original structure will be evaluated. Considering the middle of the outer tendon conduit as the critical section for radial stress, an average value of 40.8 psi of radial tension stress is defined in Figure 3-15. The state of membrane compression stress compatible with that value is approximately 1800 psi (original design, see Figure 2-12). To define a complete state of stress, a radial shear of 50 kips/ft (from Figure 2-14 at analytical station 154°) or 116 psi nominal shear stress for 36" thickness is used for example purposes. This shear is larger than the shear that occurs at the same location in the structure as the radial tension and compression stresses. Figure I-1 indicates the principle tension stress is 48.1 psi and that plane on which it occurs is approximately the plane of the membrane. Therefore, the steel stress (for each #8 bar) is,

$$f_s = \frac{48.1 \text{ psi} \times 432 \text{ in.}^2}{0.79 \text{ in.}^2} = 26,300 \text{ psi}$$

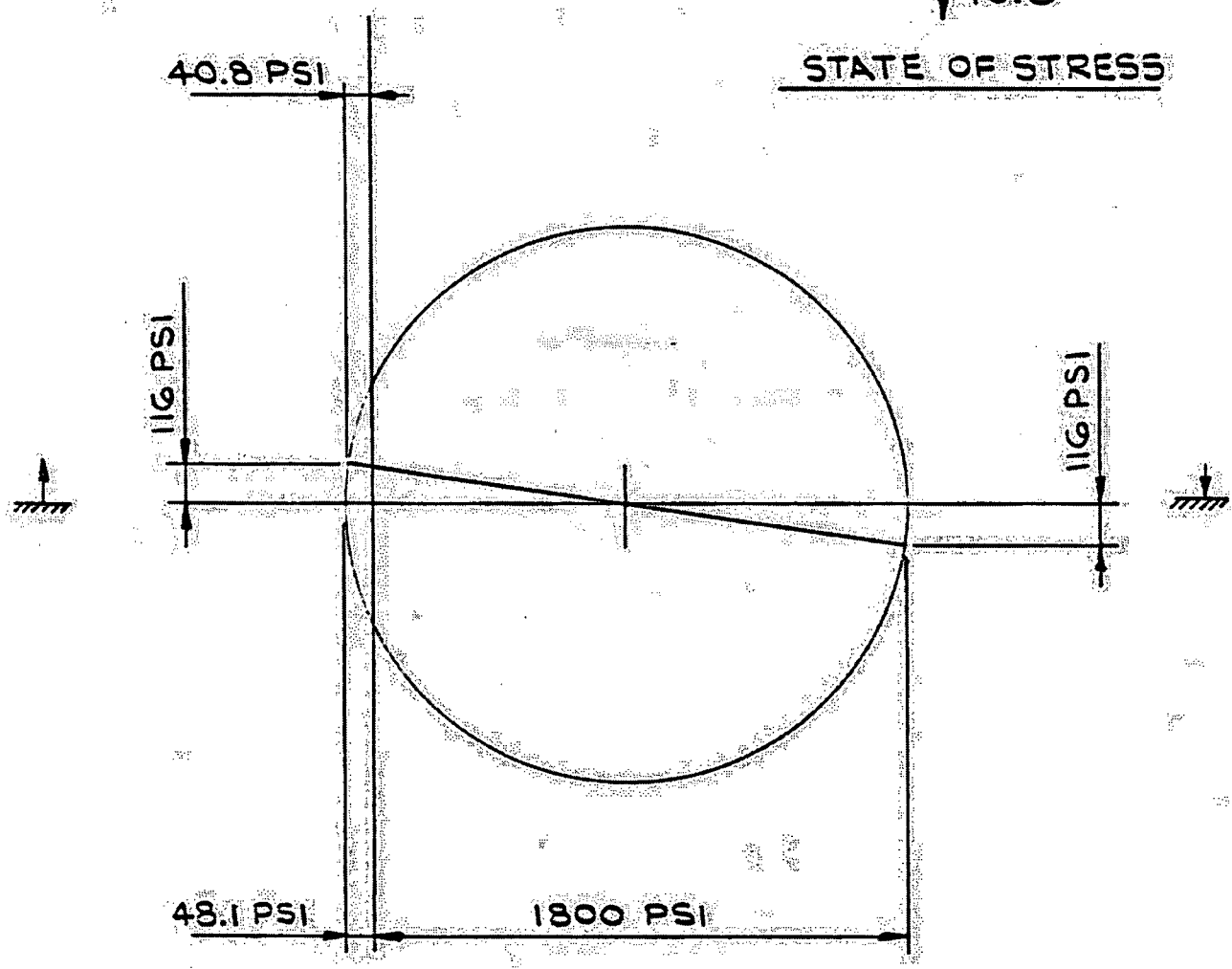
which is 0.48f<sub>y</sub> for f<sub>y</sub> = 55,000 psi (minimum mill test result) and is acceptable. This steel stress is an upper bound solution for pours G and H (original, delaminated and repaired structures) since the combined membrane compression, radial tension and radial shear state of stress anywhere in those pours is less critical than the example case.

### FACTORED LOADS

Radial shear capacity (as a measure of diagonal tension) is of importance in factored load considerations to preclude premature failure. Each of the governing load combinations has been investigated for the existing structure with regard to shear capacity required for factored loads (see Figures 4-6, 4-12, 4-18 and 4-27).



STATE OF STRESS



MOHR'S CIRCLE

COMBINED STRESSES

FIGURE I-1  
Revised: 9-22-76

**APPENDIX J**  
**NRC CORRESPONDENCE**  
**SIT INSTRUMENTATION**

Revised: 9-22-76

APPENDIX J

NRC CORRESPONDENCE

SIT INSTRUMENTATION

September 1, 1976

TO: MR. LEON ENGLE

FROM: F. L. MOREADITH

THE ATTACHED LETTER IS SENT TO YOU PER INSTRUCTIONS BY  
MR. B. L. GRIFFIN AND MR. J. T. RODGERS AND DESCRIBES THE  
EXTENT TO WHICH INSTRUMENTATION DESCRIBED IN THE FSAR WILL  
BE SUPPLEMENTED AS A RESULT OF THE CRYSTAL RIVER #3 DOME REPAIR.

SHOULD YOU HAVE ANY QUESTIONS CONCERNING THE DESCRIPTION,  
PLEASE FEEL FREE TO CONTACT ME.

FLM:cd

APPENDIX J (Cont'd)

August 31, 1976

FPC/DR-52

Mr. B. L. Griffin  
Vice President and Manager of  
Crystal River Unit #3 Dome Repair  
Florida Power Corporation  
P. O. Drawer 1057  
Crystal River, Florida 32629

Re: Crystal River Unit #3 Dome Repair  
Instrumentation

Dear Mr. Griffin:

The Containment Building's structural response to the SIT will be monitored by utilizing the existing instrumentation described in the FSAR and supplementary instrumentation installed within the repaired dome.

Instrumentation within the repaired dome will consist of a series of instrumentation stations established in the dome on two (2) orthogonal axes at distances of 15, 30 and 45 feet from the apex (see Figures 1 and 2). The data recovered at these stations consist of the following:

1. The hoop and meridional steel strain changes on the liner using SR4 three-element electrical resistance strain gages attached to the inside surface of the liner.
2. The hoop and meridional concrete strain changes near the upper surface of the lower portion of the dome using Ailtech Concrete Embedment Gages with a 4-inch gage length.
3. The hoop and meridional reinforcing bar strain changes of both layers of steel within the new concrete cap. These measurements are obtained from SR4 linear strain gages attached to #4, Grade 60 sister bars.

APPENDIX J (Cont'd)

Mr. B. L. Griffin  
FPC/DR-52  
August 31, 1976  
Page Two

4. The reinforcing bar strain changes of the #6, Grade 60 radial anchors. The gages are SR4 linear strain gages.

Gross structural deformations will be measured by extensometers attached to the steel liner plate at the locations identified on Figure 3. This instrumentation provides the following data:

1. The vertical displacement of the liner, inside surface, measured at three (3) azimuths and at radial distances of 0, 29, 49 and 56 feet from the apex.
2. The radial displacement of the liner measured at the 49 and 56 foot radii.

All instrumentation readings are processed and recorded using a Vidar Model Autodata 8 data acquisition system. The data sampling rate will be sufficient to adequately evaluate the structural response of the structure.

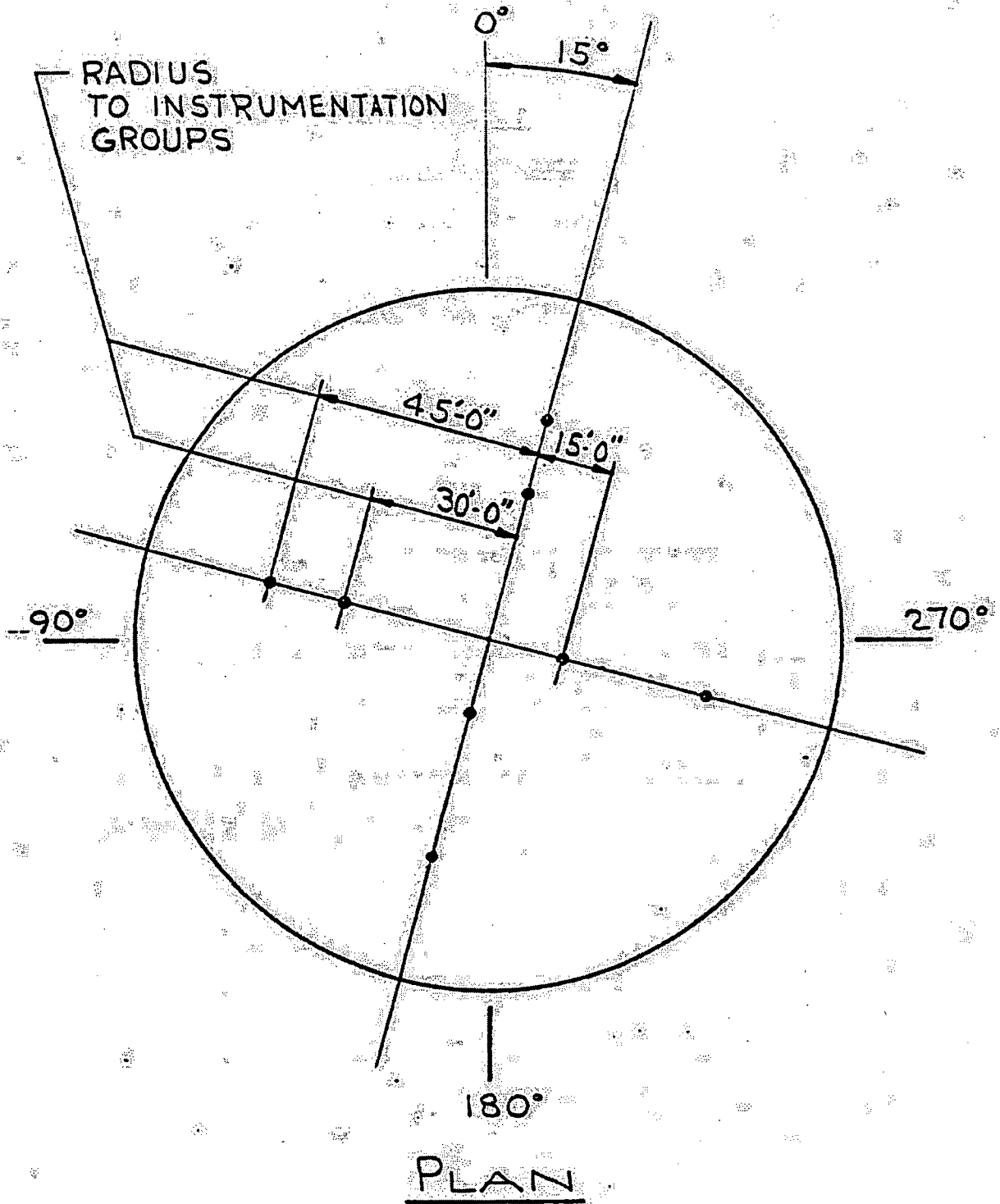
Sincerely yours,



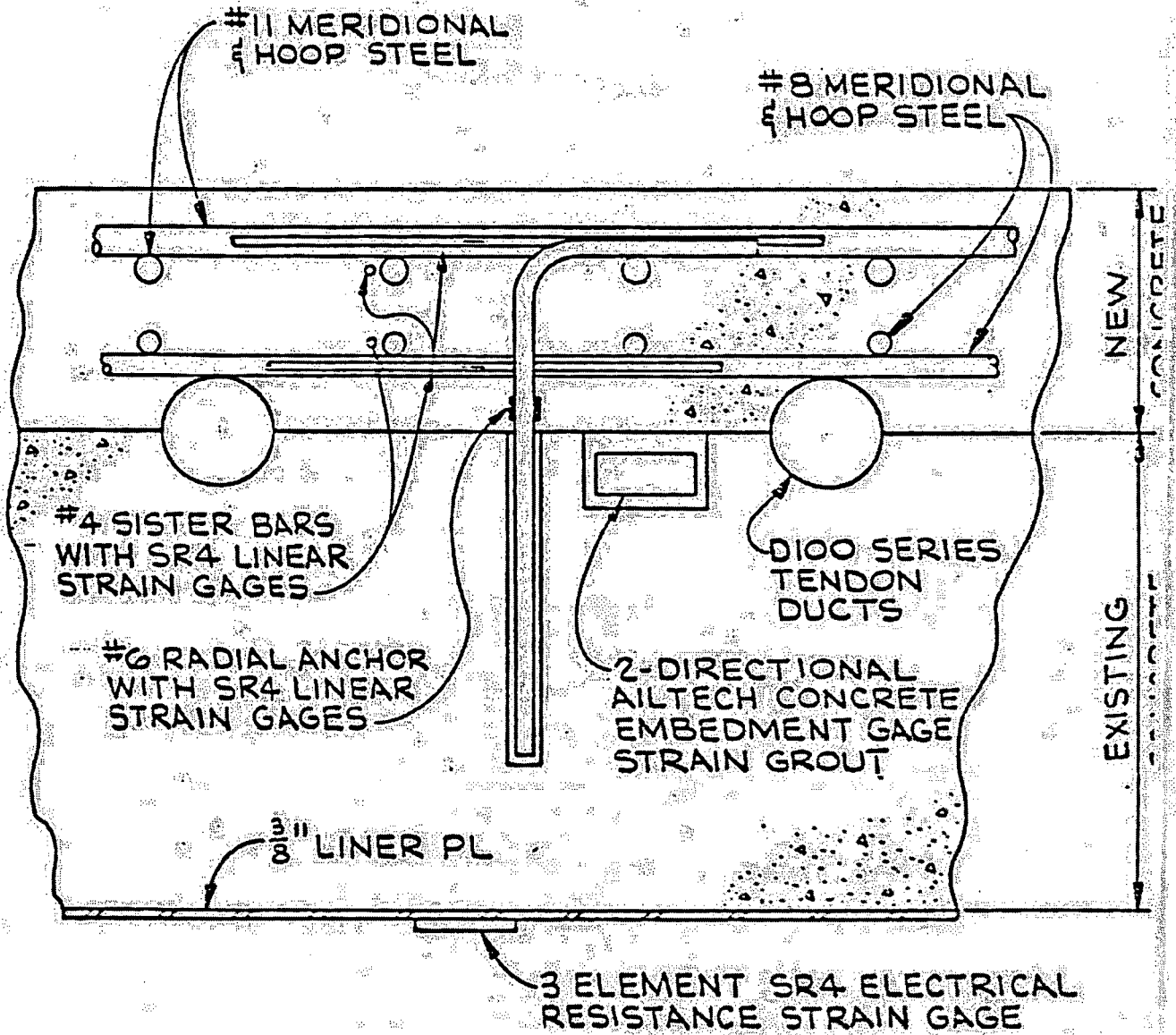
F. L. Moreadith  
Project Manager  
Crystal River Unit #3 Dome Repair

TDB:cd

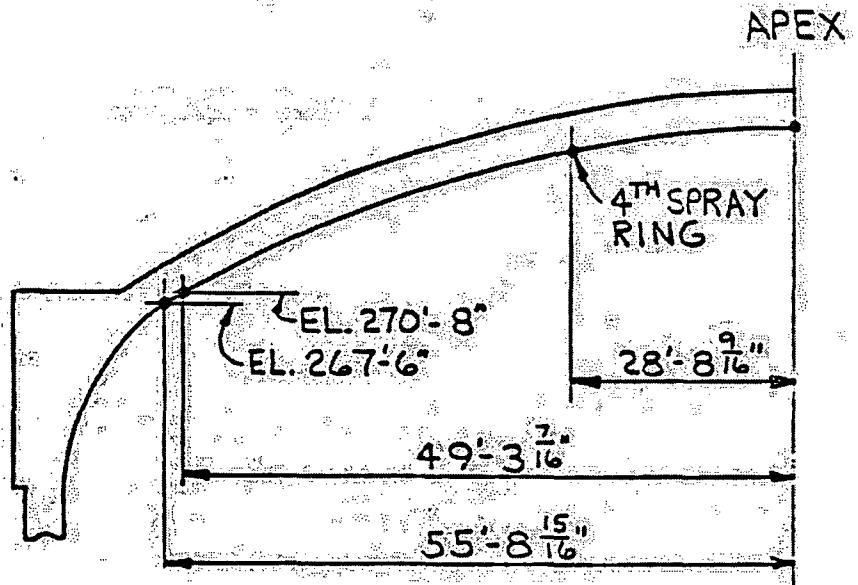
cc: B. L. Griffin  
J. Alberdi  
R. S. Burns  
C. E. Jackson  
J. E. Colby  
A. L. Gomez



STRAIN INSTRUMENTATION FOR MONITORING STRUCTURAL RESPONSE DURING SIT



TYPICAL SECTION AT INSTRUMENTATION LOCATION



LOCATION		DIR. OF MEASMT.
AZ 90°	EL. 270'-8"	RADIAL
AZ 200°	↓	
AZ 333°55'	↓	
AZ 90°	EL. 267'-6"	
AZ 200°	↓	
AZ 333°55'	↓	
AZ 90°	4 <sup>TH</sup> SPRAY RING	VERTICAL
	EL. 270'-8"	
	EL. 267'-6"	
AZ 200°	4 <sup>TH</sup> SPRAY RING	
	EL. 270'-8"	
	EL. 267'-6"	
AZ 333°55'	4 <sup>TH</sup> SPRAY RING	
	EL. 270'-8"	
	EL. 267'-6"	
	DOME APEX	↓

EXTENSOMETERS ON LINER  
FOR DISPLACEMENT MEASUREMENT

FIGURE 3  
Revised: 9-22-76

APPENDIX J (Cont'd)

SEPTEMBER 14, 1976

FPC/DR-75

MR. LEON ENGLE  
DIVISION OF PROJECT MANAGEMENT  
NUCLEAR REGULATORY COMMISSION  
WASHINGTON, D.C. 20555

RE: CRYSTAL RIVER UNIT #3 DOME REPAIR  
INSTRUMENTATION  
RESPONSE TO C. P. TAN'S TELEPHONE  
CALL OF SEPTEMBER 13, 1976

DEAR MR. ENGLE:

IN RESPONSE TO DR. TAN'S TELEPHONE CALL, THE FOLLOWING ADDITIONAL INFORMATION IS PROVIDED WITH REGARD TO INSTRUMENTATION DESCRIPTION.

THE EXTENSOMETERS BEING USED AS PART OF THE INSTRUMENTATION FOR THE CRYSTAL RIVER UNIT #3 DOME REPAIR AND SIT CONSIST OF A TRANSDUCER ELEMENT WHICH IS AN INFINITE RESOLUTION LINEAR POTENTIOMETER. OUTPUT OF THE POTENTIOMETER IS A VOLTAGE THAT IS PROPORTIONAL TO THE DISPLACEMENT OF THE MOVABLE CONTACT (SEE ATTACHED FIGURE) WITH RESPECT TO THE POTENTIOMETER. MOVEMENT OF THE LINEAR POTENTIOMETER IS ACTIVATED BY INVAR WIRES ATTACHED TO THE LINER PLATE AND THE MOVABLE CONTACT. THE INVAR WIRES ARE KEPT UNDER CONSTANT TENSION BY CONSTANT LOAD LINEAR SPRINGS.

SPECIFIC CHARACTERISTICS OF THE EXTENSOMETERS BEING EMPLOYED ARE:

MOVEMENT RANGE	1.75 INCH
RESOLUTION	0.001 INCH
ACCURACY	0.005 INCH
LINEAR SPRING FORCE	20 POUNDS

TO ASSURE THAT THE MEASURED DEFLECTIONS ARE DUE TO MOVEMENT OF THE CONTAINMENT STRUCTURE AND NOT THE SUPPORTING STRUCTURE THE FRAME OF THE TRANSDUCER UNIT IS ATTACHED TO A "FIXED" REFERENCE STRUCTURE. ATTACHMENT STRUCTURES FOR THE TRANSDUCER UNITS WITHIN THE CONTAINMENT BUILDING ARE THE TOP OF THE SECONDARY SHIELD WALL AT ELEVATION 180'-6" AND THE OPERATING FLOOR AT ELEVATION 160'-0". THE EXTENSOMETER TRANSDUCER FRAMES HAVE BEEN DIRECTLY ATTACHED TO THESE REFERENCE STRUCTURES OR TO SPECIALLY PROVIDED STRUCTURAL FRAMES ATTACHED TO THE REFERENCE STRUCTURE.

APPENDIX J (Cont'd)

MR. LEON ENGLE  
NUCLEAR REGULATORY COMMISSION  
SEPTEMBER 14, 1976  
PAGE TWO

IF THE ABOVE INFORMATION IS NOT FULLY RESPONSIVE TO DR. TAN'S REQUEST, PLEASE CONTACT US FOR FURTHER INFORMATION.

SINCERELY,

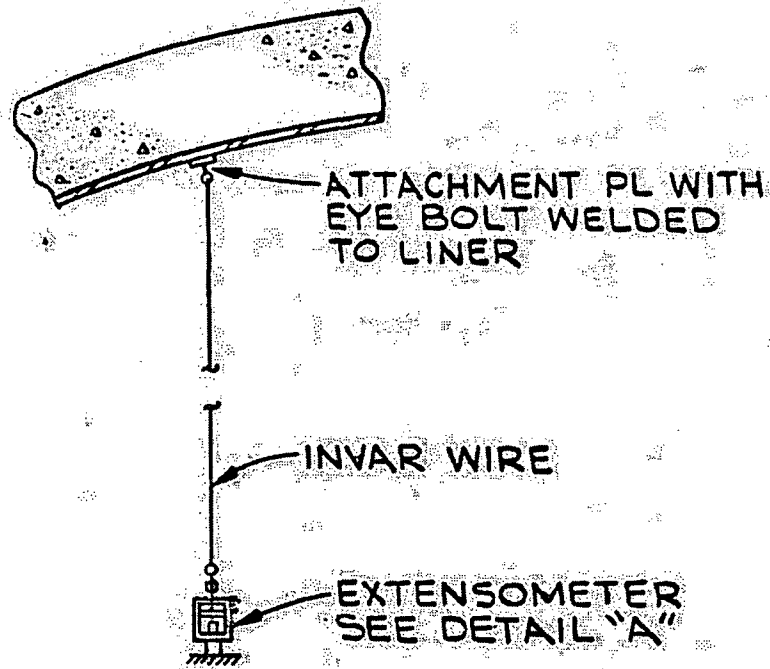


F. L. MOREADITH  
PROJECT MANAGER  
CRYSTAL RIVER UNIT #3 DOME REPAIR

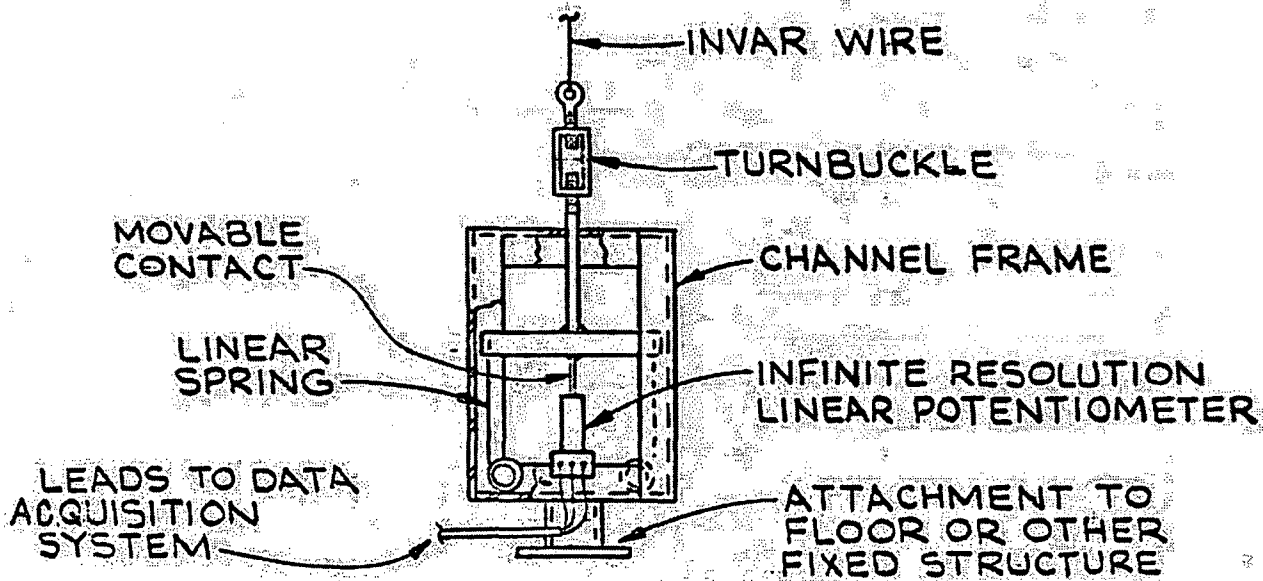
FLM:cd

ATTACHMENT

cc: B. L. Griffin  
J. T. Rodgers  
W. R. Zimmerman



TYPICAL DETAIL OF  
EXTENSOMETER INSTALLATION



DETAIL "A"

FIGURE I

9/15/76 3:40 pm

APPENDIX J (Cont'd)

Mr. Engle called with the following:

Mr. J. T. Rodgers:

Re: SIT Instrumentation  
Crystal River #3 Dome.

We have reviewed the information on SIT instrumentation for the dome as contained in the September 1, 1976 telecon from F. L. Moreadith to Leon Engle.

It is our understanding the extensionometers // which are for measuring the deflections at pertinent locations of the dome will be used in combination with strain gauges on concrete, reinforcing bars and steel liners.

We concur that the proposed instrumentation if properly installed should provide information required for adequate assessment of this structural integrity of the repaired dome.

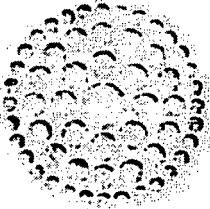
Unless you have some questions pertaining to the telecon, you should consider "go ahead" on SIT instrumentation for CR#3.

Leon Engle

B.1/4-

Fred should include the above Sept 1 & Sept 14 telecon information into the "Interim Report" revision being submitted on Sept 22 to NRC

Thanks



**Florida  
Power**  
CORPORATION

August 10, 1976

United States Nuclear Regulatory Commission  
Washington, D.C. 20555

Attention: Mr. John F. Stolz, Chief  
Light Water Reactor Branch No. 1  
Division of Project Management

Re: Florida Power Corporation  
Crystal River Unit #3  
Docket No. 50-302

Gentlemen:

In accordance with your letter of July 30, 1976 relative to the request for information concerning our interim report, "Reactor Building Dome Delamination," June 11, 1976, we submit the attached response as supplement number 1. Forty (40) copies are included.

We have prepared this response for submittal at this time per your request as a supplement to the interim report and in the next two weeks we will forward the agreed upon correction/addition pages to amend the report to reflect the repair procedures being followed subsequent to July 27, 1976.

It is anticipated that the format being followed will allow a single report to suffice in furnishing the necessary information for you and your staff. Additional supplemental pages will be submitted as required by your review.

We will discuss this matter with Mr. Engle today after our presentation on the repair status.

Very truly yours,

J. V. Rodgers  
Assistant Vice President

JTR:cd

cc: Mr. Norman Moseley  
Atlanta, Georgia  
Region II Inspection & Enforcement

**APPENDIX K**

**DISCUSSION OF CONCRETE AND AGGREGATE PROPERTIES**

Revised: 12-10-76

APPENDIX K

DISCUSSION OF CONCRETE AND AGGREGATE PROPERTIES

217 356-4598

R.F.D. 3, Champaign, Illinois 61820

November 24, 1976

Dr. Frederick L. Moreadith  
Project Manager, Crystal River  
Unit 3 Dome Repair  
Gilbert Associates, Inc.  
P. O. Box 1498  
Reading, PA. 19603

Dear Dr. Moreadith:

RE: Crystal River Unit 3 Dome Delamination

The cause of the delamination that occurred in the dome of Crystal River Unit 3, presumably during prestressing, is not clear but is most likely related in a major sense to the quality of the aggregate.

The coarse aggregate was obviously weak although it met what were considered, by the owner, to be the pertinent ASTM C33 requirements. The low strength of the coarse aggregate is indicated by:

1. a loss of 41.4 percent in the Los Angeles abrasion test, even though this was within specification limits,
2. the nature of the particles, many of which were fossiliferous with high porosity and permeability, and
3. the fracture of all of the coarse aggregate particles at the delaminated surfaces

Normally, concrete is a more ductile material than cement paste because the aggregate particles act as crack arresters and more energy is required to propagate a crack in concrete. For the concrete in question, the fracture resistance of the aggregate was probably less than that of the cement paste; certainly it was no greater. Concrete of this type would be expected to exhibit, comparatively, a more brittle and sudden failure than concretes made with good quality aggregates. Also, the tensile strength would be expected to be low and was measured in tests at from 230 to 505 psi.

The average tensile stress in the dome concrete as determined by Gilbert Associates is 41 psi, or perhaps twice this amount if allowance is made for the area occupied by the tendons. However, a finite analysis indicated high local tensile stresses in the concrete at the interface between the concrete and the tendon ducts by, I believe, assuming the concrete to be a linear elastic material. Had the dome been made with concrete containing good quality aggregates it would not be a linear elastic material and the maximum tensile stresses would be considerably less than those computed.

APPENDIX K (Cont'd)

Dr. Frederick L. Moreadith  
November 24, 1976  
Page 2

The maximum stress would also be influenced by shrinkage, creep and microcracking. Furthermore, concretes by their very nature are abundant in flaws, cracks and irregularities which are all stress raisers. Therefore, the effect of the conduit in a dome made of concrete with good quality aggregates may be nil, certainly, it would not be the effective stress raiser that the elastic analysis approach would indicate.

However, the concrete in the dome of Crystal River Unit 3 was made with a weak coarse aggregate. These aggregate particles apparently did not act as crack arresters in the concrete and thus the concrete was probably as brittle, or nearly so, as cement paste. For this reason the elastic analysis approach suggests a source of high stress which could initiate cracks. This is not to say that the stresses are as high as computed but a fraction of their computed value is sufficient to cause failure in this particular concrete.

If there is merit to this approach and the dome concrete is as brittle as speculation indicates, little energy would be adsorbed by the dome concrete ahead of a crack and a crack could propagate with relative ease.

The weak coarse aggregate particles appear to have had a compound effect: (1) they increased the brittleness of the concrete which in turn resulted in an increased maximum tensile stress, (2) they resulted in a concrete with low tensile strength and (3) they permitted cracks to propagate with low energy input.

While more data is needed, it seems that although delamination of the dome occurred when this particular aggregate was used in the concrete it would not have occurred had good quality aggregate been used.

Sincerely yours,

Clyde E. Kesler

CEK:cds

SUPPLEMENT 1  
RESPONSES TO  
NRC COMMENTS TO THE CRYSTAL RIVER #3  
REACTOR BUILDING DOME DELAMINATION REPORT  
DATED JUNE 11, 1976  
DOCKET NO. 50-302

GENERAL

1. For easy reference, provide a list of tables and figures in the Table of Contents.

Answer: The material suggested has been incorporated into the Table of Contents.

## SECTION 1.2

1. The staff considers the establishment of the causes of the dome delamination to be important in assessing the adequacy of the repair program and in providing assurance that another crack will not occur again during the life of the structure. The potential contributing factors should, therefore, be identified indicating the magnitude of radial tensile stresses created in the concrete.

**Answer:** The material has been incorporated into the report in Section 1.2.

2. The use of radial anchors will enhance the capability of the dome to resist radial tension. However, they will not eliminate tension in concrete, and therefore small cracks may still exist. Provide an analysis to indicate that such cracks will not jeopardize the required structural integrity of the dome to resist all combinations of loadings for which it is designed.

**Answer:** These cracks exist primarily in regions where membrane behavior dominates, i.e., negligible shear stress across the cracks.

Despite the presence of the cracks, the membrane compression capacity of the concrete is adequate. Under LOCA or SIT, there is radial compression across the cracks.

It is of interest to note that under 15% detensioning (admittedly a nominal stress change) deflections were less than predicted. If the cracks were contributing any significant effect to the response, larger rather than smaller deflections would be expected.

In addition to the above considerations, secondary cracks will be epoxy grouted and the radial reinforcing will cross virtually all these cracks.

SECTION 2.3 AND TABLE 2-2

1. Clarify the definition of tensile capacity of concrete. Explain how principal tension is related to shear and diagonal tension as indicated in Section 2.3.1, and what is the difference between the shear discussed in this section and that in the next section (2.3.2).

Answer: The material in sections 2.3.1 and 2.3.2 have been rearranged in the report, section 2.3.1 title is "Flexural and Membrane Tensile Stresses" and section 2.3.2 is entitled "Shear".

2. Provide and describe with examples of actual design, the conditions under which each of the criteria (a) and (b) in Section 2.3.1 is applied.

Answer: The material requested now appears in section 2.3.2. Attachment #1 is a design example.

3. Since the stress/strain distribution is tri-axial, the limits of  $3\sqrt{f'_c}$  and  $6\sqrt{f'_c}$  may not be directly applicable to this problem and their use should be justified.

Answer: The state of stress in the dome may be regarded as being biaxial since the stress in the radial direction is very small in comparison with the membrane stresses. The interactions for tension-tension and tension-compression are not significant at least until the compression exceeds about 60% of the compressive strength of the concrete (Kupfer, Hilsdorf and Rusch, ACI Journal Aug. 1969) (Ref. 8 of the Report). Thus the limits of  $3\sqrt{f'_c}$  and  $6\sqrt{f'_c}$  are justified.

4. If  $0.85f'_c$  as extreme compression in ultimate strength design is used, it may not be directly applicable for the same reason as in the above comment and should be justified.

Answer: Although criteria indicate that under factored load concrete stresses would be allowed to reach  $0.85f'_c$  they do not. The actual stresses are much lower and do not appear critical since the dominant stress is bi-axial compression the strength should be higher.

5. The shear strength of concrete is influenced by stresses orthogonal to the axis of the element; therefore, this effect should be considered.

Answer: Hoop tension stresses should have little or no effect on radial shear strength, since sufficient bonded hoop rebar has been provided to preclude hoop tensile "Failure".

NRC Question 2.3.2 - Shear Design ExamplesCase a. Membrane tension or membrane comp. < 100 psi

Example | LOCA 36" Dome (Fig 2-30 & 2-32)  
Sta. 157.5°

From shell analysis

$$V = 9.4 \text{ k/l}, \quad M_{\phi} = 172 \frac{\text{k}}{\text{l}} \text{ (Ten of)} \quad \bar{T}_{\phi} = 98 \text{ psi (comp) membrane}$$

Since  $\bar{T}_{\phi} = 98 \text{ psi (comp)} < 100 \text{ psi (comp)}$ , use 318-63, Ch 17.

Calculate conc. capacity using (17-2) with (17-3).

$$\frac{\phi A_s d f_y}{S} = 0 \text{ since no shear rein. avail. at } 157.5^\circ.$$

From (17-3),

$$M' = M - N \left( \frac{4t-d}{8} \right) = 172 - 42.3 \left( \frac{4 \times 36 - 31.8}{8 \times 12} \right) = 122.5 \frac{\text{k}}{\text{l}}$$

$$N = 98 \text{ psi} \times 12" \times 36" = 42.3 \text{ k/l}$$

$$t = 36" \quad d = 31.8" \text{ (dist. from IF to OF rebar)}$$

From (17-2),

$$V_c = \phi \left( 1.9 \sqrt{F_c'} + 2500 \rho_w \frac{V_d}{M'} \right) \quad \left( \rho_w = \frac{A_s}{bd} = \frac{1.20}{12 \times 31.8} = 0.003 \right)$$

$$V_c = 0.85 \left[ 1.9 \sqrt{5000} + 2500 (0.003) (9.4) (31.8) / 122.5 \right]$$

$$V_c = 129.8 \text{ psi} < 3.5 \phi \sqrt{F_c'} @ 210 \text{ psi}$$

$$V_c = bd V_c = \frac{(12)(31.8)(129.8)}{1000} = \boxed{49.5 \text{ k/l}} \quad \text{Fig 2-32}$$

$$\text{Ultimate applied shear, } V_u = V = 9.4 \text{ k/l}$$

$$\boxed{49.5 \text{ k/l capacity} > 9.4 \text{ k/l} \therefore \text{section OK}} \quad \text{Fig 2-32}$$

NRC Question 2.3-2 — Shear Design ExamplesCase b. Membrane Compression  $> 100$  psi

Example	Norm. winter Oper. Cond.	36" Dome (Figs 2-18 & 2-20)
	Sta. 138.3°	

From shell analysis

$$V = 119.3 \text{ k/ft} \quad M_{\phi} = 277 \frac{\text{k}}{\text{ft}} \text{ (Ten OF)} \quad \bar{\sigma}_{\phi} = 1384 \text{ psi (comp)}$$

Membrane stress = 1384 psi comp  $> 100$  psi comp $\therefore$  use 318-63-Ch 26 (Pls Conc)Try to show OK using minimum concrete capacity  $> \phi V_c$ , plus shear rein.,  $\frac{\phi A_v d f_y}{s}$ .

If

$$\phi V_{cmin} + \frac{\phi A_v d f_y}{s} \geq V_u \quad \text{OK};$$

if not, calc  $V_c$  from (26-12) with FSAR exceptions.

$$\phi V_{cmin} = \phi (1.7 b' d) \sqrt{f_c'} \quad , \quad d = 18.4" \text{ (dist from extreme comp. fiber to cg tendons)}$$

$$= (0.85)(1.7)(12)(18.4) \sqrt{5000}$$

$$\phi V_{cmin} = 22,560 \text{ #/ft} = \boxed{22.6 \text{ k/ft}} \text{ concrete}$$

$$\frac{\phi A_v d f_y}{s} = \frac{(0.85)(0.79)(31.8)(40 \text{ ksi})}{4.5} = \boxed{189.8 \text{ k/ft}} \text{ shear rein.}$$

$d$  = dist. from extreme comp fiber to tension rein.  
 $s$  = 4'2" meridional spacing of #8 shear bars  
 (12" hoop spa)

$$\therefore \text{Conc + Rein} : \boxed{212.4 \text{ k/ft Capacity}}$$

$$\text{Applied (factored)} : V_u = 1.5V = 1.5(119.3 \text{ k/ft}) = \boxed{179.0 \text{ k/ft}}$$

$212.4 \text{ k/ft capacity} > 179.0 \text{ k/ft applied (factored)}, \therefore$   
 section is OK based on minimum conc shear capacity

NO. Question 2.3-2 — Shear Design ExamplesCase 6-1 Membrane Compression  $> 100$  psi

Example | Norm. Winter Oper. Cond. 36" Dome (Fig. 2-13(2-20))  
Sta 152.0°

From shell analysis

$$V = 45.5 \text{ k/l}, \quad M_{\phi} = 307 \frac{\text{k}}{\text{ft}} \text{ (Ten OF)}, \quad \bar{P}_{\phi} = 1488 \text{ psi (comp)}$$

$$V_u = 1.5V = 1.5(45.5) = 68.3 \text{ k/l}$$

Membrane stress = 1488 psi comp  $> 100$  psi comp

$\therefore$  use 313-63, Ch 26 (Pls Corc)

Try min  $V_c$  + shear rein (#8 @ 18" v sH)

$$\phi V_{c \text{ min}} = 22.6 \text{ k/l (obtained previously)}$$

$$\frac{\phi A_v d f_y}{s} = \frac{(0.85)(.79/1.5)(31.8)(40)}{18"} = \boxed{31.8 \text{ k/l}}$$

$$\text{total cap.} = 22.6 + 31.8 = 54.4 \text{ k/l} < 68.3 \text{ k/l}$$

$\therefore$  calc actual  $V_c$  from (26-12) w/FSAR exceptions

$$V_{ci} = K_{\Delta V} b' d \sqrt{f'_c} + \frac{M_{cr}}{\frac{M}{V} - \frac{d}{2}} + V_d$$

$$K_{\Delta V} = 1.75 - \frac{0.036}{np} + 4np$$

$$M_{cr} = \frac{I}{y} (6\sqrt{f'_c} + f_{pe} - f_d)$$

$f_{pe} - f_d$  = compressive stress in concrete due to prestress and dead load after all losses, at the extreme fiber of the section at which tension stresses are caused by applied loads

$M$  and  $V$  are due to all loads

$d = 18.4$ " (dist. from extreme comp. fiber to cg tendons)

Case b.-1 (cont)

Since Max. cur. is tension on OF,  $\rho = \rho_{OF}$ .

$$\rho = \rho_{OF} = A_s / bd = 1.60 / (12)(31.3) = 0.0042$$

$$n = 29/4 = 7.25$$

$$K_{AV} = 1.75 - \frac{0.036}{(7.25)(0.0042)} + 4(7.25)(0.0042) = 0.692 > 0.60$$

Use 0.60

$$I = \frac{1}{12} (12)(36)^3 = 46656 \text{ in}^4 \quad \rightarrow y = 36/2 = 18"$$

$$6\sqrt{f'_c} = 6\sqrt{5000} = 424 \text{ psi}$$

$$f_{pc} - f_d = -910 \text{ psi comp (D+F: -910 OF, -2300 IF)}$$

$$M_{CR} = \frac{46656 (6\sqrt{5000} + 910)}{18} \times \frac{1}{12000} = 288 \frac{\text{L-K}}{\text{I}}$$

$$V_{ci} = \frac{.6 (12)(18.4)(70.7)}{1000} + \frac{288}{\frac{307}{45.5} - \frac{18.4}{2 \times 12}} =$$

$$V_{ci} = 9.4 + 48.2 = 57.6 \text{ K/I}$$

From (26-13), diag. cr. shear ( $V_{cw}$ ).

$$V_{cw} = b'd (3.5\sqrt{f'_c} + 0.3 f_{pc})$$

$$f_{pc} = \bar{\sigma}_p = 1488 \text{ psi (comp)} \quad \rightarrow d = 0.80 \times 36" = 28.8"$$

(> 18.4")

$$V_{cw} = 12(28.8)(3.5\sqrt{5000} + 0.3 \times 1488)$$

$$V_{cw} = 240 \text{ K/I} > V_{ci}$$

$$\therefore \boxed{V_c = V_{ci} = 57.6 \text{ K/I}}$$

$$\text{Total Capacity of Conc + Rein} = 57.6 + 31.8 = 89.4 \text{ K/I}$$

$$\boxed{\text{Capacity @ } 89.4 \text{ K/I} > V_u @ 68.3 \text{ K/I} \therefore \text{section OK}}$$

Fig 2-20

SECTION 2.4:

1. In the paragraph in the middle of Page 2-4, you indicated that for structural integrity test and accident condition load combinations, stresses for sustained loads cannot be combined with those due to rapidly applied loads internally in the program and are combined externally. Provide an example of actual design to show how the stresses are combined externally and illustrate the combination on a stress-strain diagram.

Answer: See Attachment 2.

2. On Page 2-5 under Item b Creep, it is indicated that as a result of concrete creep there is a reduction in concrete stress and an increase in liner stress. Since the liner is relatively thin and may buckle under prestress, the liner should not be considered to contribute any strength to the containment vessel. However, in the design of the steel liner, strain due to creep of concrete should be considered to check its leaktightness integrity. Revise the concrete stresses in the report if they have been reduced.

Answer: A reduced modulus of elasticity of concrete has been used in the analysis and thus the effect of creep on concrete and liner stresses has been accounted for. Our analysis indicates that for the load combinations D+F and D+F + T<sub>0</sub>, the concrete stress is increased if the liner is removed in the analytical model. From the standpoint of concrete stress behavior for the SIT and LOCA load combinations, to remove the liner from the analytical model is not conservative.

The figures in the report have been modified to provide a comparison of both results at selected points.

3. Provide the procedure which you used in the design of the steel liner. In Table 2-2, you stated that no criteria on liner strains were used in the original design. Indicate the criteria you used for the steel liner design.

Answer: Table 2.2 has been modified to reflect liner design criteria.

4. Discuss in detail the effects of creep, including the following consideration:

Because of the different level of prestress in the wall in the vertical direction, the wall in the hoop direction, in the ring girder and in the dome the  $E_c'$  is different in all these directions and this effect should be considered in the analysis. The wall acts as an orthotropic element. The different parts of the structure have simultaneously different  $E_c'$  due to different specific creep.

Answer: The effect of creep has been accounted for by the use of reduced modulus. Although the different parts of the structure have different prestress, the specific creep (creep due to unit psi) should be the same for the same material. Thus the reduced modulus should be about the same for the various parts of the structure. A calculation is attached to demonstrate this (See Attachment 3).

5. In Table 2-3 add load combination equation for repairs. This equation should include the seismic load term.

Answer: The FSAR and the current ASME Code load combinations do not include earthquake effects in combination with construction loads.

## ATTACHMENT 2 FOR ANSWER TO QUESTION 2.4(1)

EXAMPLE OF SIT CALCULATION

24" CONCRETE SIT

Ref: Figs 4-4 thru 4-7

$$E_c = 3.1 \times 10^6 \quad \nu_c = 0.20$$

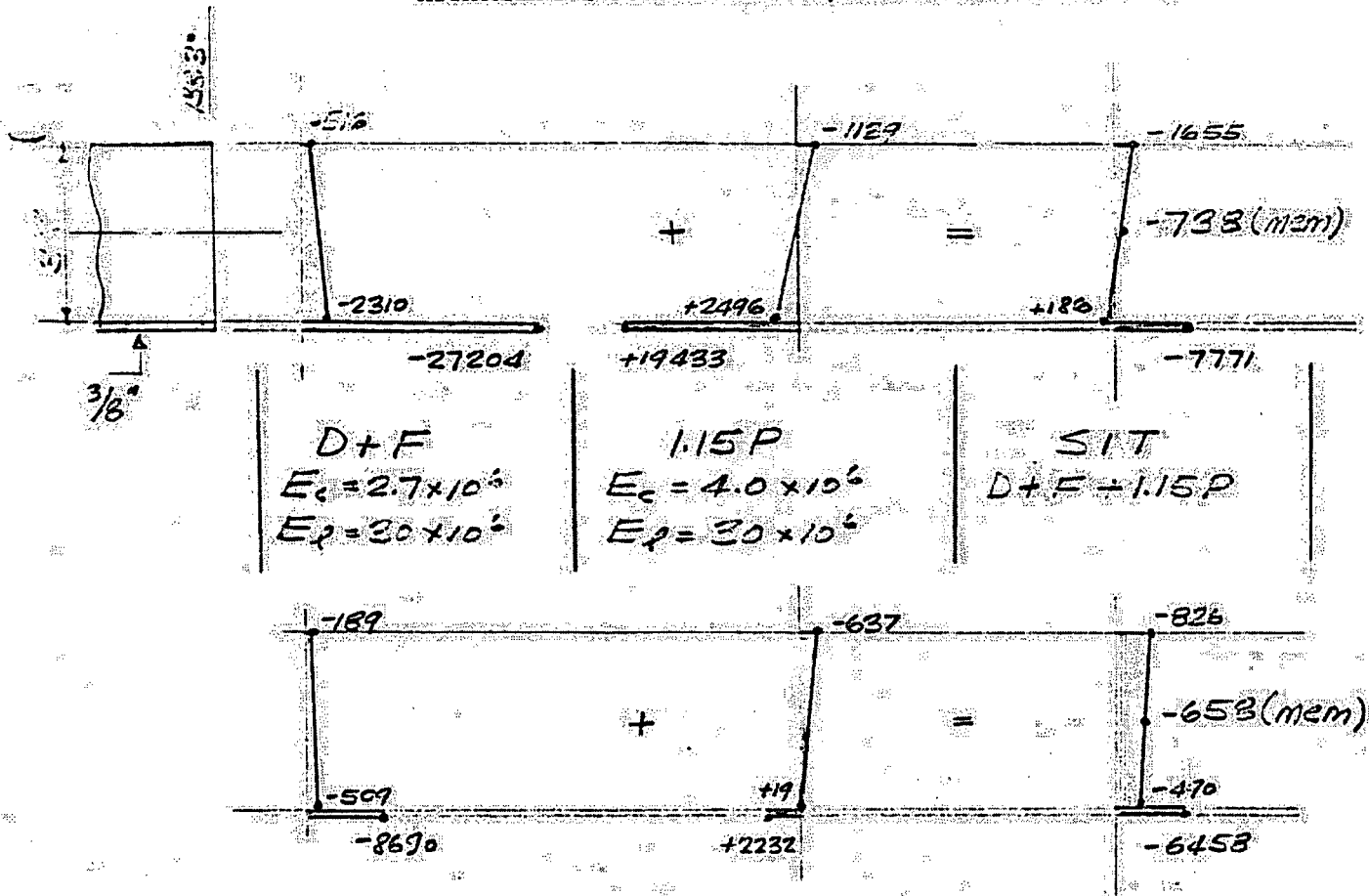
D+F

$$E_c = 4.0 \times 10^6 \quad \nu_c = 0.20$$

1.15P

$$E_c = 3.0 \times 10^6 \quad \nu_c = 0.30$$

ATTACHMENT 2 FOR ANSWER TO QUESTION 2.4(1) (Cont'd)



MECHANICAL (psi)  
From shell analysis

Fiber (psi)  
From shell analysis

Liner Strains

$$\epsilon_p = \frac{-7771 - 0.3(-6458)}{30 \times 10^6} = -0.000194 \frac{1}{11}$$

$$\epsilon_c = \frac{-6458 - 0.3(-7771)}{30 \times 10^6} = -0.000138 \frac{1}{11}$$

IF Conc. Strains

$$\epsilon_p = \frac{-2310 - 0.2(-509)}{2.7 \times 10^6} + \frac{+2496 - 0.2(19)}{4 \times 10^6} = -0.000195 \frac{1}{11}$$

$$\epsilon_c = \frac{-509 - 0.2(2310)}{2.7 \times 10^6} + \frac{19 - 0.2(2496)}{4 \times 10^6} = -0.000137 \frac{1}{11}$$

- (Total SIT Conc. Strains cannot be calc. from total conc stresses)

## ATTACHMENT 3 FOR ANSWER TO QUESTION 2.4(4) - CREEP

Creep of the concrete under sustained loads  $D$ ,  $F_v$ ,  $F_H$ , and  $F_D$  has several effects on tendon forces and containment stresses. The most obvious is to decrease the tendon forces with time. This effect is taken into account in the prestress loss calculations.

Another effect is to decrease concrete stresses and to increase liner stresses and strains, which are compressive over most of the containment structure. The decrease in concrete stress is due to the additive effects of the decrease in tendon force plus the creep straining of the concrete acting with a non-creeping liner, which tends to shed compressive stresses from the concrete to the liner. This latter effect is taken into account in the analysis through the use of the effective Young's Modulus,  $E'_c$ , appearing on page 4-3 of the report.

Using this approach, less concrete compression is calculated to be available to resist SII or LOCA conditions than would be calculated by considering the reduced tendon force alone.

With respect to liner stresses and strains, the structural analyses show that the  $E'_c$  effect ( $E'_c = 2.7 \times 10^6$  @ present and  $E'_c = 1.8 \times 10^6$  @ 40 yr versus  $E_c = 4 \times 10^6$  - "instantaneous") is much greater than that of the reduced tendon force. The net result is liner stresses and strains which have compressive values much greater than those which occur at initial prestress. The liner strains in the report include this.

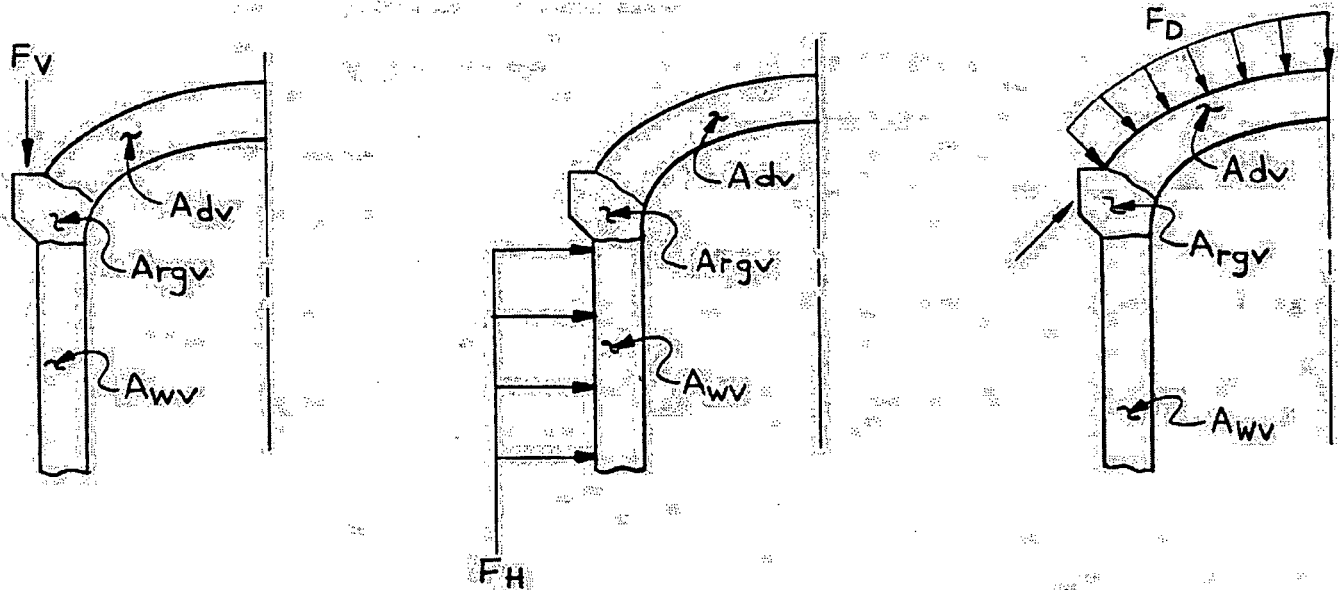
A third effect of concrete creep is to produce creep induced stresses which result only when the  $E'_c$  is not uniform over the containment structure. If  $E'_c$  is uniform, the stresses at any time are equal to those at initial prestress less tendon losses, in the case where the liner is not part of the model.

The  $E'_c$  values used in the structural analyses correspond to specific creep values,  $sc$ , which were calculated based on the 1) average age of the dome concrete at application of the dome prestress (average) and 2) the duration of this prestress to "present" and to "40 yrs". The resulting  $E'_c$  values were applied to the entire structure in the analyses for  $D + F$ . It was recognized that a different  $E'_c$  is associated with vertical ( $F_v$ ), hoop ( $F_H$ ), and dome ( $F_D$ ) prestress loading conditions. This is so only because the concrete age at application of each prestress load is different and the duration of each type is different. However,  $E'_c$  values were based on the dome concrete age and dome prestress since it is that part of the containment structure which is most effected by the delamination. Also, it was felt that these  $E'_c$  values would be an average for the wall since, chronologically,  $F_D$  was applied between  $F_v$  and  $F_H$ . Nevertheless, a more accurate determination of the creep effects due to the separate application and duration of the prestress is discussed below.

As pointed out previously the determination of  $E'_c$  depends on 1) age of concrete at loading and 2) duration of load.  $E'_c$  is independent of the level of stress in the concrete, which is reflected in  $sc$  ( $\mu$  in/in per 1 psi of stress).

ATTACHMENT 3 FOR ANSWER TO QUESTION 2.4(4) - CREEP (Cont'd)

Therefore, creep induced stress under either  $F_v$ ,  $F_H$ , or  $F_D$  will be reflected only in differences in  $E'_c$  for the various elements in the containment for each of these prestress loads. The total results would be obtained from the sum of the analyses shown below.



$A_{wv}$  = age of wall at time  $F_v$  is applied.

$A_{rgv}$  = age of ring girder at time  $F_v$  is applied.

$A_{dv}$  = age of dome at time  $F_v$  is applied.

Similar for  $A_{wH}$ ,  $A_{rgH}$ ,  $A_{dH}$  and  $A_{wD}$ ,  $A_{rgD}$ ,  $A_{dD}$ .

$D_v$  = duration of  $F_v$  from time of application to "present" or "40 yr" times.

similar for  $D_H$  and  $D_D$

Knowing the values of A and D permit calculation of  $E'_c$  for the three elements.

ATTACHMENT 3 FOR ANSWER TO QUESTION 2.4(4) - CREEP (Cont'd)

Values for  $E'_c$  were obtained based on average pour dates for the wall, ring girder, and dome and average stressing dates for the three tendon systems. This is presented below.

	<u>Wall</u>	<u>Ring Girder</u>	<u>Dome</u>
Average Pour Dates:	6-19-72	9-1-73	5-15-74
	<u>Vertical</u>	<u>Hoop</u>	<u>Dome</u>
Average Stressing Dates:	11-15-74	2-15-75	12-1-74

P/S System	Aw (da)	Arg (da)	Ad (da)	D (da)	"Present" Time			D (yrs)	"40 yr" Time		
					$E'_c$ (psi) x 10 <sup>6</sup>				$E'_c$ (psi) x 10 <sup>6</sup>		
					Wall	Ring Gir.	Dome		Wall	Ring Gir.	Dome
Vertical	880	425	180	545	3.13	2.89	2.63	41.5	2.08	1.96	1.75
Hoop	970	515	270	455	3.17	3.03	2.86	41.2	2.13	2.04	1.89
Dome	880	455	210	515	3.13	3.03	2.70*	41.4	2.08	2.04	1.80*

\* used in structural analysis of containment.

The differences between  $E'_c$  values for the wall, ring girder, and dome under a specific prestress condition is not enough to produce stresses significantly different from those reported.

SECTION 3.1

1. Discuss the reliability of direct tensile tests performed on cores. Since in the structure the radial tensile stress occurs simultaneously with two orthogonal compressions or with two orthogonal tensions, a more thorough investigation is required.

**Answer:** The direct tensile test was designed to identify the tensile capacity of the concrete in the structure in relation to its compressive strength. It was not intended to define the property of the concrete in a state of triaxial stresses, since the actual state of stress at points of stress concentration in the delaminated dome cannot be accurately defined.

The effect of the tensile stress in combination with two orthogonal compressions is discussed in Section 3.3.3 of the report. No further investigations are planned.

### SECTION 3.3

1. In the list of factors which may have contributed to the delamination problem, add: creep and stress concentrations (at tendons) inherent in this type of structure.

Answer: Creep in the membrane direction would not increase the radial stress. The effect of stress concentrations is discussed in section 3.3.2.

2. In Section 3.3.2 it is indicated that by using SAP IV computer program and the model shown in Fig. 3-16, the effects of material properties on radial tension stresses are evaluated. Identify in the model:

- (1) the steel elements, such as reinforcing steel, and tendon conduits,

Answer: There is no element representing reinforcing steel or tendon conduit. The effect of reinforcing steel is calculated as transformed concrete area and represented by effective Young's Modulus. Modeling of the tendon conduit is described in Section 3.3.2.

- (2) the manner in which the prestressing force is applied, indicating if the prestressing force component tangent to the dome curvature is considered.

Answer: Prestressing force is applied on three middle layers of the model in both the radial and the tangential directions of the dome.

3. Provide the hand calculation which you made to obtain the radial tension.

Answer: These calculations are included in attachment.

4. In Section 3.3.4, transient thermal gradients may generate shear stresses, and should be considered in the analysis. Similar effect exists for localized thermal gradients.

Answer: Since thermal restraint produces normal strain, but no shear strain, the thermal gradient causes shear stress; but only in the areas which are reinforced for shear (Chapter 14 of Reference 11).

5. The solution for stress concentrations as shown in Fig. 3-17 & 3-18 is incomplete. It should be noted that compression exists also in the direction parallel to the conduit ( $\sigma_1$ ). This stress generates additional stress concentration in the plane ( $\sigma_2$ ;  $\sigma_3$ ) orthogonal to the tendon, which should be added to the stresses shown in Fig. 3-18.

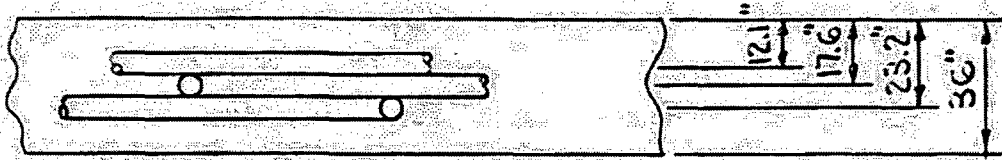
Answer: Assuming this question addresses the effect of Poisson's ratio, this effect was considered and is discussed in Section 3.3.2.

6. When the effect of tendon conduits is analyzed, it should be noted that this effect is different when evaluated in the direction parallel to the tendon and orthogonal to the tendon. In the direction parallel to the tendon a 1/4" thick pipe (5"Ø) approximately replaced the removed concrete. But in the direction perpendicular to the tendon, the pipe introduces a flexible link which modifies the average properties of the concrete section.

Answer: We have reviewed the effect of the conduit on stresses following a path parallel to the plane of the membrane and results are illustrated in the attached figure. The distribution shown in the attachment indicates that the effect will not be significant. However, the effect of conduits are conservatively represented by a concrete layer with equivalent Young's modulus calculated by the ratio of net concrete volume to gross concrete volume.

ATTACHMENT FOR ANSWER TO QUESTION 3.3(3)

The radial tension are hand-calculated as follows:



$$\text{Top Tendon } R_1 = 1343.9''$$

$$\text{Middle Tendon } R_2 = 1338.4''$$

$$\text{Bottom Tendon } R_3 = 1332.8''$$

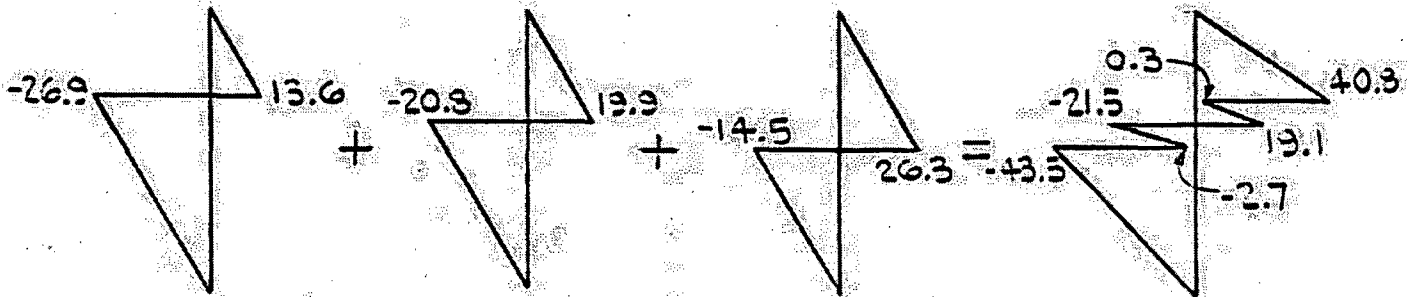
Tendon force at 0.7 ultimate = 1633<sup>k</sup> tendon spacing 30"

$$\text{Top Tendon } \sigma_1 = \frac{1633 \times 1000}{30 \times 1343.9} \times \frac{12.1}{36} = 40.5 \times \frac{12.1}{36} = 13.6 \text{ psi}$$

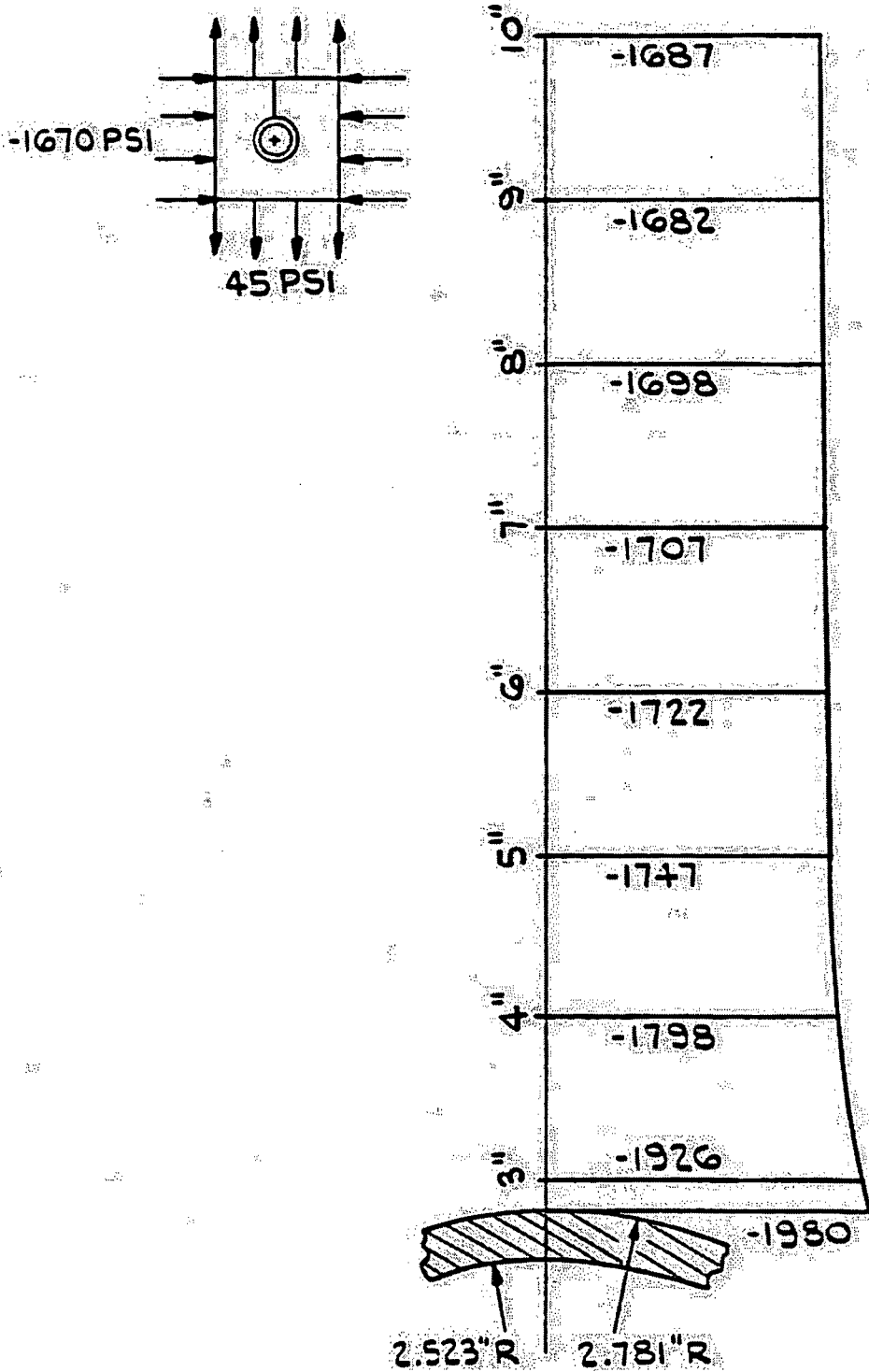
$$\text{Middle Tendon } \sigma_2 = \frac{1633 \times 1000}{30 \times 1338.4} \times \frac{17.6}{36} = 40.7 \times \frac{17.6}{36} = 19.9 \text{ psi}$$

$$\text{Bottom Tendon } \sigma_3 = \frac{1633 \times 1000}{30 \times 1332.8} \times \frac{23.2}{36} = 40.8 \times \frac{23.2}{36} = 26.3 \text{ psi}$$

The radial tension due to all three layers of tendon are superimposed as follows



ATTACHMENT FOR ANSWER TO QUESTION 3.3(6)



STRESS PROFILE PARALLEL TO MEMBRANE

SECTION 4.4

1. In Sections 4.4.1 and 4.4.2 you indicated that in order to consider the containment structure serviceable for the two loading conditions the shear capacity of the tendon conduit would have to be considered. Such consideration may not be possible, unless the bond stress between the conduit and concrete can be justified to be adequate.

Answer: The tendon conduit is not required and has not been considered as contributing to the shear capacity.

### SECTION 5.3

1. In releasing the prestressing force as a result of tendon detensioning, strain recovery will occur. However, most likely the strain recovery in concrete will be resisted by the steel reinforcing bars and steel liner, because of creep effects, and tension may result in the concrete. Provide an analysis to show that the resulting cracking in dome concrete will not jeopardize the structural integrity of the dome particularly in the region of the liner anchors.

Answer: Not applicable under new repair sequence.

2. The behavior of the detensioned dome is strongly influenced by the creep of the prestressed structure which has taken place after prestressing and up to this date. The detensioning of the dome will not return the structure to a previously unprestressed state, whatever the sequence of operations. It is therefore imperative to analyze the detensioned dome for the influence of creep. Present such an analysis and demonstrate that the integrity of the detensioned dome will not be impaired. The analysis should include the ring girder and the top of the cylindrical wall.

Answer: Not applicable under new repair sequence.

3. The figures 5-11 to 5-14 do not include a study on shears. Provide a detailed analysis of shear stresses in the detensioned dome and demonstrate that these shear stresses, acting simultaneously with normal stresses, do not endanger the stability of the dome. Special attention should be given to radial shears.

Answers: Not applicable under new repair sequence.

4. Either justify in detail the use of 24" for the dome thickness in the present analysis, or present a parametric study for different thicknesses; for instance 24"; 18"; 15".

Answer: The response of the structure to detensioning, and the parametric studies of section 3.0 indicate that the structure is responding as a 24" structure. The addition of epoxy grout, radial anchors and new reinforcing on the cap will assure its continued performance. Also see response to question 1.2.2

5. Demonstrate that the detensioned dome and the steel liner can take the load applied during the repair operations.

Answer: Not applicable under new repair sequence.

6. Present a detailed discussion of the provision made to monitor the behavior of the dome, the ring girder, and the top part of the cylindrical wall during repair operations. Indicate:

a. The acceptance criteria for safety in such operations, and

Answer: This information has been added to the report as Section 5.0 Corrective Action.

b. the provisions made to safely stop the repair procedures if the acceptance criteria for safety are not met.

Answer: All activities on the dome will be temporarily suspended and no personnel, except inspectors, will be allowed on the dome after a stop work signal until approval to proceed is obtained from the Engineer and the Owner.

The acceptance criteria shall be in accordance with the requirements noted for each measurement in Table 1. Work shall stop immediately when readings are outside the limits noted in Table 1 for displacements and liner strains and the Engineer shall be notified.

An unsatisfactory set of readings requiring immediate notification of the Engineer during detensioning shall be when one concrete strain or reinforcing bar gage reading exceeds the values specified in Table 1.

The top surface of the dome shall be visually inspected for cracks before commencement of detensioning and any findings recorded. During detensioning and retensioning operations, the inspection for cracking shall be made on a daily basis as a minimum. Observations shall be reported to the Engineer.

7. Describe in detail the methods, acceptance criteria and methods of inspection for the grouting of the cap on the dome, the radial anchors to be installed and the grouting of these anchors. Present the planned testing of these anchors.

Answer: Grouting of cap of dome is no longer part of the repair sequence. The procedure for sizing radial anchors is described in Section 5 of the report.

A test program is being conducted to choose the best set of anchoring devices among the following; a cone and expansion shell anchor system grouted with cement grout, a thread rod with nut bearing grouted with cement grout, a threaded anchor with nut bearing grouted with epoxy grout, and a deformed rod grouted with epoxy grout.

Three (3) types of anchors manufactured by Williams Form Engineering Company have been selected for testing.

1. Williams long cone and long expansion shell (LCS-200).
2. Williams standard cone and standard expansion shell (SCS-200).
3. Williams deformed anchor with and without an end nut. In addition a non-deformed anchor with nut bearing assembly will be tested.

Three (3) different grouts are being tested:

1. Masterflow 814 cement grout.
2. Masterflow 713 cement grout.
3. Sikadur Hi-Mod 370 epoxy.

Following series of tests are conducted to verify the anchor strength.

1. A shallow hole, 2" in diameter and 7 inches deep.
  - a. To verify that torquing of bolt will not cause damage or rupture to the nearby concrete.
  - b. To establish the failure mode of concrete for available minimum depth.
  - c. To establish the design load capacity of the anchor at the minimum available embedment depth.
2. A 2" diameter hole 10 inches deep.
  - a. To verify that torquing of bolt will not cause damage or rupture to the nearby concrete.
  - b. To establish the failure mode of concrete for this embedment.
  - c. To establish the load capacity of anchor for this embedment.
3. A 31 inch deep hole.
  - a. To develop and maintain the design preload in the bolt.
  - b. Upper and lower bound torque values requirements to develop the design preload.

- c. To verify strength of the anchor with respect to concrete capacity.
- 4. A 31 inch deep hole (epoxy grouted test block).
  - a. To investigate anchors capacity in epoxy grouted concrete.
  - b. To establish the failure mode of concrete.
  - c. To compare the anchor capacity with solid concrete block.

The most suitable anchor type will be established after testing is complete. Final anchor configuration and design basis for the anchor will be submitted as an addenda to the report.

- 8. Provide a commitment that sufficient strain instrumentation will be installed at the top and bottom of the dome to assure that during retensioning of tendons the upper portion of the dome (above the crack) will be participating in developing compressive stress at the same rate as the lower portion.

Answer: The instrumentation is described in Section 5.0. The gages which exist in the cap will be replaced with strain gages on embedded reinforcing bars and the radial anchors. Observation of this instrumentation during the retensioning and SIT should assure that the structure is responding as designed.

- 9. Indicate in more detail the planned method of waterproofing of the repaired dome and its protection against detrimental environmental conditions.

Answer: A detailed description will be provided later.

- 10. Describe the acceptance testing of the repaired dome and the inservice monitoring of the structure.

Answer: Acceptance of the repaired dome will be based on satisfactory completion of the SIT. After the SIT the currently accepted inservice inspection requirements will be performed.

- 11. Investigate the influence of possible cracking in the hoop direction on the dome tendon conduits.

Answer: Not applicable under new repair sequence.

TABLE 1 FOR ANSWER TO QUESTION 5.3(6b)

PREDICTED STRAINS AND DISPLACEMENTS  
15% PRESTRESS

<u>Gage No.</u>	<u>Type of Measurement</u>	<u>Predicted Measurement</u>	<u>Range</u>
E22	Liner Rad. Displace.	0.017 in	±0.004 in
E23	Liner Rad. Displace.	0.017 in	±0.004 in
E24	Liner Rad. Displace.	0.017 in	±0.004 in
E25	Liner Rad. Displace.	0.008 in	±0.002 in
E26	Liner Rad. Displace.	0.008 in	±0.002 in
E27	Liner Rad. Displace.	0.008 in	±0.002 in
E28AV	Liner Vert. Displace.	0.041 in	±0.01 in
E28BV	Liner Vert. Displace.	0.016 in	±0.004 in
E29AV	Liner Vert. Displace.	0.041 in	±0.01 in
E29BV	Liner Vert. Displace.	0.016 in	±0.004 in
E30AV	Liner Vert. Displace.	0.041 in	±0.01 in
E30BV	Liner Vert. Displace.	0.016 in	±0.004 in
	Apex Vert. Displace.	0.129 in	±0.032 in
	15' Radius Vert. Displace.	0.129 in	±0.032 in
	30' Radius Vert. Displace.	0.120 in	±0.03 in
	45' Radius Vert. Displace.	0.069 in	±0.017 in
R118M	Liner Merid. Strain	65 μ in/in	± 33 μ in/in
R118D	Liner Diag. Strain	-	-
R118H	Liner Hoop Strain	33 μ in/in	± 16 μ in/in
R119M	Liner Merid. Strain	65 μ in/in	± 32 μ in/in
R119D	Liner Diag. Strain	-	-
R119H	Liner Hoop Strain	67 μ in/in	± 33 μ in/in
R120M	Liner Merid. Strain	65 μ in/in	± 33 μ in/in
R120D	Liner Diag. Strain	-	-
R120H	Liner Hoop Strain	33 μ in/in	± 16 μ in/in
R121M	Liner Merid. Strain	65 μ in/in	± 32 μ in/in
R121D	Liner Diag. Strain	-	-
R121H	Liner Hoop Strain	67 μ in/in	± 33 μ in/in
R122M	Liner Merid. Strain	73 μ in/in	± 37 μ in/in
R122D	Liner Diag. Strain	-	-
R122H	Liner Hoop Strain	74 μ in/in	± 37 μ in/in
R123M	Liner Merid. Strain	65 μ in/in	± 33 μ in/in
R123D	Liner Diag. Strain	-	-
R123H	Liner Hoop Strain	33 μ in/in	± 16 μ in/in
R124M	Liner Merid. Strain	73 μ in/in	± 37 μ in/in
R124D	Liner Diag. Strain	-	-
R124H	Liner Hoop Strain	74 μ in/in	± 37 μ in/in
R125M	Liner Merid. Strain	65 μ in/in	± 33 μ in/in
R125D	Liner Diag. Strain	-	-
R125H	Liner Hoop Strain	33 μ in/in	± 16 μ in/in

SUPPLEMENT 2

RESPONSES TO  
STRUCTURAL ENGINEERING BRANCH  
COMMENTS AND REQUEST  
FOR

Amended 7/15/76 10-28-76

ADDITIONAL INFORMATION ON CRYSTAL RIVER UNIT NO. 3  
REACTOR BUILDING DOME DELAMINATION  
INTERIM REPORT AND SUPPLEMENT NO. 1

1. GENERAL COMMENTS.

In the report the applicant discussed all possible factors which could have caused the delamination of the dome. No single or overriding mechanism has been positively identified as the cause of the delamination. However, the following facts are significant.

1. The indication of a tension failure along the delaminated surface.
2. The complete fracture of the coarse aggregate on the delaminated surface.
3. Large variations in the strength values obtained from the direct tensile tests of the concrete.
4. The presence of cracks of various sizes and extents in the concrete below the delamination as indicated by core borings.

On the basis of these facts, the sequence of events that led to delamination could be surmised:

From the evidence indicated above, one could conclude that; (1) the characteristics of the dome concrete are such that it is crack-prone, and localized cracks may have existed even before the prestressing force was applied, and (2) the coarse aggregates are fragile, thus, instead of acting as crack arresters, they became the path of cracks.

With the existence of precracks and the presence of fragile coarse aggregates, the radial tension accumulated from all sources was so large that it overcame the very limited tensile strength of the concrete, resulting in the separation of the dome concrete.

It has been found by various investigators that cracking of concrete under compression is slight for loads below 30 to 50 percent of the ultimate. This is basically the reason why the allowable concrete compressive stress is limited to 45% of the ultimate. The cracks, if any, which initially may have developed in the dome concrete as a result of prestressing are unstable. They increase in length and width until either they eventually stabilize or ultimate failure occurs. The slow crack growth in concrete under sustained loading is most likely associated with creep.

The postulation of the delamination mechanism and the understanding of concrete crack initiation and propagation are essential for the establishment of the dome repair procedure and its evaluation. The following repair procedure is being pursued by the applicant:

1. Holes will be core-drilled into the lower concrete;
2. Top delaminated concrete will be removed;
3. Final inspection of 24" structure will be performed;
4. Lower level cracks will be grouted with epoxy;
5. Radial anchors will be set and the holes grouted;
6. New reinforcement and concrete will be added;
7. 18 tendons will be retensioned;\*
8. Structural Integrity Test will be performed.

\* The 18 tendons will be partially retensioned as described in Section 5.2.9, Page 5-6, September 22, 1976 revision to the report, "Reactor Building Dome Delamination."

On the basis of the postulation of the delamination mechanisms and understanding of concrete crack initiation and propagation as discussed above, the staff has reviewed and evaluated the repair procedure. However, before the staff can finalize its evaluation, the applicant should respond to the staff's concerns as indicated below:

II. DOME REPAIR.

1. An analysis of the repaired dome should be made for the following conditions:

(a) Before the hardening of the cap concrete.

Answer: Analysis of the repaired dome before the hardening of the cap concrete has been performed. The controlling stresses and deformations are reported in Appendix G, "COMPARISON OF DESIGNS," Pages G-7 through G-9, September 22, 1976 revision to Dome Delamination report. Refer to column headed "Dead Load Plus Prestress at Early Plant Life."

(b) After the hardening of the cap concrete, including all the loading conditions as described in the FSAR.

Answer: Controlling analytical results for the repaired structure with the new cap in place are summarized in Appendix C, "COMPARISON OF DESIGNS," Pages G-7 through G-9. Other FSAR load combinations have not been presented since they do not control any of the final dome design.

Indicate the stresses and strains in the mainly reinforced concrete cap portion and in the prestressed concrete lower portion.

Answer: Appendix G, "COMPARISON OF DESIGNS," includes the requested information.

2. Provide a description of the final design of the radial anchors and indicate how the combined action of the cap concrete and the lower dome concrete is ensured.

Answer: The final design of the radial reinforcement and the combined action of the cap with lower dome concrete are presented in Section 5.2.7 (Page 5-5, September 22, 1976 Revision). Specific reference is also made to figures 5-22 and 5-23, as well as Appendix I.

3. It was indicated that two layers of reinforcing steel will be provided in the cap. For the meridional reinforcing steel, if only one layer can be spliced to the existing meridional steel near the ring girder, indicate how the other layer can effectively carry the load if it is not spliced to the existing steel, noting that under internal pressure, dome concrete may crack in tension.

Answer: The #8 lower layer meridional reinforcement is provided for crack control only. Figure 5-20 illustrates meridional steel provided versus that required and does not include consideration of the #8 lower layer meridional steel shown in Figure 5-19. The lower layer of the meridional steel therefore is not assumed to "...effectively carry the load...". The top layer of meridional and both layers of hoop reinforcement in the new cap are considered to provide strength.

4. Since the repaired dome becomes a unique structural element of the containment structure, indicate any special considerations to meet the requirements of Regulatory Guide 1.18 in executing the structural integrity test of the containment.

Answer: Regulatory Guide 1.18 requires that displacement be measured at the apex and spring line of a containment dome. The instrumentation for the Crystal River Unit 3 Reactor Building has been considerably enhanced with regard to the dome. Refer to Section 5.2.1.c.

for detail on the dome instrumentation for the SIT. The additional measurements of dome displacement will be included in the SIT acceptance requirements. The predicted response data was supplied by letter of October 8, 1976 (Attachment 1).

5. The original dome design concrete strength,  $f'_c$  is based on 5000 psi; now a concrete strength of 6000 psi is used for evaluating the repaired dome. The basis for using 6000 psi is that the actual strength of the existing structure possesses that strength. It is a well-known fact that concrete strength increases with age beyond 28 days and stabilizes after a certain time. Generally, designers of concrete structures do not take such increases into consideration mainly to offset "ignorance factors" in areas of design and construction.

Provide a justification that such additional margins of safety are not required in the case of a concrete containment, noting that there is a reduction in dome concrete area due to the presence of cracks, sheathing ducts and other possible voids, and if such reduction of concrete area is disregarded in the stress computation, the computed membrane compressive stress may be less than the actual.

Answer: The in-place concrete strength is usually not taken into account in design of structural concrete. The reason for this practice is that the in-place strength is not known at the time the design is performed. However, it is also current practice to use a design strength ( $f'_c$ ) based on an age closer to the time of first service loads rather than based on an arbitrary age (e.g., 28 days).

For the Crystal River Unit 3 Reactor Building Dome, the in-place strength has been evaluated in accordance with the accepted practice of Chapter 4, Section 4.3.3 of ACI 318-71 and the compressive strength has been determined to be 6130 psi (See Table 3-2, Page 3-15, Dome Delamination Report.). Another calculation, using ACI 214 (Midcell Method) and ACI 318, Section 4.3.5.1, had given a compression strength of 6600 psi (See Page C-5, Dome Delamination Report.).

Therefore, there is sound technical basis for using a design in-place compressive strength of 6000 psi.

With regard to "...presence of cracks, sheathing ducts and other possible voids...":

1. The lower level cracks are parallel to the membrane and do not constitute a reduction in the concrete area available to carry membrane forces. They have been successfully grouted (see Attachment 2).
2. "Sheathing ducts" are 5" diameter Schedule 40 pipe and replace the displaced concrete. See Supplement 1, August 10, 1976 revision, page 5-8, Question 6 for additional detail.
3. We are not aware of "other possible voids." Considering the number of cores taken in the Crystal River Unit 3 dome (in excess of 2000), it is unlikely that any voids exist in the dome.

Considering the above 3 factors and the actual response of the structure to 15% detensioning program, "computed membrane compressive stress" should be quite close to actual stress seen by the structure under any load combination.

6. The cracks in the dome concrete as discussed in the general comments have reached stability. The Structural Integrity Test (SIT) will affect such stability. Provide an evaluation of SIT on the lower level cracks of concrete which may not be grouted with epoxy. Provide the data on the effectiveness of epoxy grout in controlling concrete cracks.

Answer: The current through-thickness stresses in the dome are compressive (see Figure 5-22, September 22, 1976 revision). The pressurization of the Reactor Building for the SIT will increase the existing radial compression through the entire thickness of the repaired dome. The added radial compression will vary from 63.3 psi on the inside surface to zero (0) on the outside surface. Since the through-thickness stresses will still be compressive, they will not disturb the stability of the lower level cracks. Although not essential to the structural behavior during the SIT, the epoxy grouting of lower level cracks has been accomplished (see response to Item II.5) and should enhance through-thickness stability.

### III. CAUSES OF DELAMINATION.

1. On Page C-3 in Appendix C under the subsection on "Direct Tensile Test Results" the applicant indicates that the range of direct tensile tests on 6 core samples was 230 psi to 505 psi with an average value of 420 psi. In view of these low results, the allowable membrane tensile stresses indicated in Table 2-2 appear high. Discuss the cause of these low tensile ultimate stresses, the reason for the wide scattering of the test results and the possibility that the delamination phenomena was caused by the poor quality of the aggregate, and the propagation of local cracks along the whole surface of the dome as surmised in the general comments above.

Answer: The variation of direct tensile test results is discussed in Appendix C of the report, "Reactor Building Dome Delamination." The Table on Page C-15 (Attachment D) presents direct tensile strength test results and describes in the remarks column the relative "hardness" of the coarse aggregate. A review of that table indicates tensile strength is related to "hardness" of coarse aggregate. Also, see Page C-6 for a discussion of direct tensile tests by Mr. Joseph F. Artuso.

With regard to the tensile load capability of the concrete, two types of tests were performed to measure the tensile capability of the "in-place" concrete; i.e., split tensile and direct tensile tests. Attachment B of Appendix C of the Dome Delamination Report indicated that the average value for split tensile test of the "in-place" concrete was 710 psi, with a minimum of 625 psi. Attachment C of Appendix C in the Report indicates that the average value for direct tensile tests of the "in-place" concrete was 420 psi, with two test values lower than the average; i.e., 360 and 230 psi.

As indicated on Table 2-2 of the Dome Delamination Report, in the original design criteria the allowable membrane tension stress for "factored" loads was 212 psi and zero for service loads. As indicated above, the lowest individual value for tensile strength obtained from either the split tensile or direct tensile tests was greater than the original design values for membrane tension for even the factored load condition.

The quality of the aggregate and the propagation of local cracks along the whole surface of the dome has been discussed in Sections 3.3.1c and 3.4 and Appendix F of the Reactor Building Dome Delamination Report as being a contributor to the delamination. However, Chapter 3 of the report discusses several additional factors which may have contributed to the delaminated condition of the dome.

The dome

(pours J through Q) did not contain radial reinforcement which would have prevented gross propagation of laminar cracking.

Radial ties have been incorporated into the repaired dome to resist predicted radial stresses (see Section 5.2.7).

2. The applicant presented in Fig. 3-22 the plane strain finite element model used to evaluate some stress concentrations at the tendon ducts.
  - a. Present a detailed description of boundary conditions (especially at the duct) and initial conditions introduced in the computer analysis for all cases of stress concentration.

Answer: The model shown in fig. 3-22 was used to calculate stresses in the concrete due to shrinkage effects. At the interface of concrete and duct, perfect bond was assumed because of compressive interface pressure. The outside boundary was assumed to be free. Rollers on the boundaries were used to simulate symmetry. The model was assumed to be stress-free prior to application of the shrinkage effects. The geometry and material behavior was assumed to be linear.

- b. Justify the use of plane strain to analyze what is essentially a three-dimensional problem.

Answer: The plane strain model is not intended to accurately describe the real situation (for example, 3 layers of conduit, double curvature and loads induced by the tendon in the conduit). It was, however, considered adequate to examine the replacement effect of the 5" Schedule 40 pipe.

INSTRUMENT LOCATION

The location of displacement measurements are as follows:

Cylinder Wall and Dome Junction Radial Displacements

<u>LP Gage Loc.</u>	<u>Elevation</u>	<u>Azimuth</u>	<u>Notes</u>
1, 2, 3	98'-0"	90°, 200°, 333°-55'	Radial Displacement
4, 5, 6	108'-0"	90°, 200°, 333°-55'	Radial Displacement
7, 8, 9	140'-0"	90°, 200°, 333°-55'	Radial Displacement
10, 11, 12	172'-0"	90°, 200°, 333°-55'	Radial Displacement
13, 14, 15	204'-0"	90°, 200°, 333°-55'	Radial Displacement
16, 17, 18	236'-0"	90°, 200°, 333°-55'	Radial Displacement
19, 20, 21	246'-0"	90°, 200°, 333°-55'	Radial Displacement
22, 23, 24	253'-0"	90°, 200°, 333°-55'	Radial Displacement
25, 26, 27	267'-0"	90°, 200°, 333°-55'	Radial Displacement
128, 129, 130	270'-8"	90°, 200°, 333°-55'	Radial Displacement

Ring Girder Vertical Displacement - LP

<u>LP Gage Loc.</u>	<u>Elevation</u>	<u>Azimuth</u>	<u>Notes</u>
28, 29, 30	267'-6"	90°, 200°, 333°-55'	Vertical Displacement

Dome Vertical Displacement - LP

<u>LP Gage Loc.</u>	<u>Elevation</u>	<u>Location</u>	<u>Notes</u>
34	282'-4 1/8"	Dome Apex	Vertical Displacement
128, 129, 130	49'-3" radius	90°, 200°, 333°-55'	Vertical Displacement
164, 165, 166	28'-8" radius	90°, 200°, 333°-55'	Vertical Displacement

Equipment Access Opening Displacement - LP

<u>LVDI Gage Loc.</u>	<u>Elevation</u>	<u>Notes</u>
35, 37, 38, 39 40, 41, 42	132'-0"	Radial Displacement
35, 37, 38, 39, 40, 41, 42	132'-0"	Vertical Displacement

Equipment Access Opening Displacement - LP (Cont.)

<u>LVDT Gage Loc.</u>	<u>Elevation</u>	<u>Notes</u>
36	120'-0"	Radial Displacement
36	120'-0"	Vertical Displacement
43	144'-0"	Radial Displacement
43	144'-0"	Vertical Displacement
44	147'-3"	Radial Displacement
44	147'-3"	Vertical Displacement
45	151'-6"	Radial Displacement
45	151'-6"	Vertical Displacement
46	155'-6"	Radial Displacement
46	155'-6"	Vertical Displacement
47	159'-6"	Radial Displacement
47	159'-6"	Vertical Displacement
48	163'-6"	Radial Displacement
48	163'-6"	Vertical Displacement

### Displacement Acceptance Criteria

Gage ID	Measurement	Theoretical Displacement (inches)	Limiting Displacement (inches)	Tolerance (inches)
1, 2, 3	Radial	0.010	0.020	0.010
4, 5, 6	Radial	0.090	0.115	0.025
7, 8, 9	Radial	0.205	0.260	0.055
10, 11, 12	Radial	0.200	0.250	0.050
13, 14, 15	Radial	0.205	0.260	0.055
16, 17, 18	Radial	0.160	0.205	0.045
19, 20, 21	Radial	0.060	0.080	0.020
22, 23, 24	Radial	-0.025	-0.040	0.015
25, 26, 27	Radial	-0.055	-0.070	0.015
28, 29, 30	Vertical	0.215	0.275	0.060
34	Vertical	0.905	1.135	0.230
35	Radial	0.10	0.130	0.030
35	Vertical	0.10	0.130	0.030
36	Radial	0.08	0.105	0.025
36	Vertical	0.10	0.130	0.030
37	Radial	0.12	0.155	0.035
37	Vertical	0.10	0.130	0.030
38	Radial	0.115	0.150	0.035
38	Vertical	0.10	0.130	0.030
39	Radial	0.115	0.150	0.035
39	Vertical	0.10	0.130	0.030

Displacement Acceptance Criteria (continued)

Cage ID	Measurement	Theoretical Displacement (inches)	Limiting Displacement (inches)	Tolerance (inches)
40	Radial	0.11	0.140	0.030
40	Vertical	0.10	0.130	0.030
41	Radial	0.11	0.140	0.030
41	Vertical	0.10	0.130	0.030
42	Radial	0.11	0.140	0.030
42	Vertical	0.10	0.130	0.030
43	Radial	0.090	0.120	0.030
43	Vertical	0.105	0.135	0.030
44	Radial	0.090	0.120	0.030
44	Vertical	0.105	0.135	0.030
45	Radial	0.095	0.125	0.030
45	Vertical	0.110	0.140	0.030
46	Radial	0.100	0.130	0.030
46	Vertical	0.11	0.140	0.030
47	Radial	0.105	0.135	0.030
47	Vertical	0.115	0.150	0.035
48	Radial	0.110	0.140	0.030
48	Vertical	0.120	0.155	0.035
128, 129, 130	Radial	0.015	0.025	0.010
128, 129, 130	Vertical	0.365	0.460	0.095
164, 165, 166	Vertical	0.900	1.130	0.230

JOHN C. KING, P.E.

CONSULTING ENGINEER

ATTACHMENT 2

101 East 57 Street / Cleveland, Ohio 44114  
(216) 711-0777

September 23, 1976

Dr. P. L. Koraadith  
Gilbert Associates, Inc.  
P.O. Box 1498  
Reading, Pa. 19603

F. L. Moresini

SEP 23 1976

Subject: CRJ Dome Repair  
Epoxy Grouting

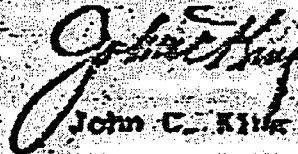
Dear Dr. Koraadith:

In my opinion the epoxy grouting of delamination and other cracks, if any, in the CRJ Dome has been a complete success. I estimate that between 90 and 100% of the cracks are filled with very strong epoxy bonded to both surfaces of the cracks.

The above conclusion is based on (1) my observation of the entire operation, (2) very few of quite a number of holes actually missed or presumably missed (for lack of logs showing that holes had been grouted) took any grout, and (3) a random selection of 10 holes that had been grouted and redrilled accepted no grout whatever at 200 psi.

Details of my observations are given in Field Notes on Epoxy Grouting of Cracks, copies of which have been sent to you by Mr. John Barr.

Sincerely,

  
John C. King